View metadata, citation and similar papers at core.ac.uk

brought to you by CORE

provided by University of Regensburg Publication Server

FRET Compatible Long-Wavelength Labels and Their Application in Immunoassays and Hybridization Assays

Dissertation zur Erlangung des

Doktorgrades der Naturwissenschaften

(Dr. rer. nat.)

der Fakultät Chemie und Pharmazie

der Universität Regensburg

vorgelegt von

Dipl. Chem. Michaela Gruber

aus Landshut

im August 2002

Danksagung

Diese Arbeit entstand zwischen April 2000 und September 2002
am Institut für Analytische Chemie, Chemo- und Biosensorik
an der Universität Regensburg.

In erster Linie gilt mein Dank
Herrn Prof. Dr. Otto S. Wolfbeis
für die Bereitstellung des interessanten Themas
und für die hervorragenden Arbeitsbedingungen am Lehrstuhl.

Für die gute Zusammenarbeit,
die zahlreichen Tips und Hilfestellungen gebührt mein besonderer Dank
Herrn Dr. Bernhard Oswald.

Ferner möchte ich mich bei meinen Kolleginnen und Kollegen,
Bianca Wetzl, Dr. Petra Bastian, und Dr. Axel Dürkop
für das gute Arbeitsklima bedanken,
sowie bei allen Mitarbeiterinnen und Mitarbeitern des Instituts,
die zum Gelingen dieser Arbeit beigetragen haben.

Mein größter Dank gebührt jedoch meinen Eltern
Martha und **Dieter Arbter,**
sowie meinem Gatten **Christian Gruber,**
die mich zu jeder Zeit und in jeder Hinsicht unterstützt haben.

Promotionsgesuch eingereicht am: 28.08.2002

Diese Arbeit wurde angeleitet von Prof. Dr. Wolfbeis.

Kolloquiumstermin: 31.10.2002

Prüfungsausschuß:

Vorsitzende:	Prof. Dr. Steinem
Erstgutachter:	Prof. Dr. Wolfbeis
Zweitgutachter:	Prof. Dr. Merz
Drittprüfer:	Prof. Dr. Liefländer

Table of Contents

1. Introduction 1

1.1. Long-Wavelength Fluorophores and Labels 1

1.1.1. Cyanine Dyes 2

1.1.2. Squarylium Dyes 5

1.1.3. Labels 6

1.2. Labeling 7

1.2.1. Labeling of Proteins 7

1.2.2. Labeling of DNA 9

1.2.3. Dyeing of Microparticles 10

1.3. Fluorescence Resonance Energy Transfer (FRET) 11

1.4. Immunoassays 12

1.4.1. The System HSA and Anti-HSA 12

1.4.2. FRET Immunoassays 14

1.5. Hybridization Assays 15

1.6. References 16

2. New Labels and Conjugates 19

2.1. Cyanines 19

2.1.1. FO544 19

2.1.2. FO545 20

2.1.3. FO546 22

2.1.4. FO548 25

2.1.5. FR642 27

2.1.6. FR646 31

2.2. Squarains 33

2.2.1. FR626 33

2.2.2. FR661 35

2.2.3. FR662 39
2.2.4. FR670 41
2.2.5. OB630 42
2.2.6. OG670 44
2.3. Non-covalent Protein Staining 44
2.4. Conclusions 45
2.5. References 50

3. Applications 52
3.1. Immunostudies 52
3.1.1. Binding Studies 52
3.1.2. Competitive Immunoassays 60
3.1.3. Cytometric Measurements 65
3.2. Hybridization Studies 67
3.2.1. Binding Studies 67
3.2.2. Competitive Hybridization Assays 73
3.2.3. Fluorescence in Situ Hybridization (FISH) 76
3.3. Conclusions 77
3.4. References 79

4. Experimental Part 80
4.1. Materials and Methods 80
4.1.1. Chemicals, Solvents, Proteins and Oligonucleotides 80
4.1.2. Chromatography 80
4.1.3. Melting Points 81
4.1.4. Spectra 81
4.2. Synthesis and Purification of the Dyes 81
4.2.1. FO544 81
4.2.1.1. 1-(3-Ethoxycarbonyl-propyl)-2,3,3-trimethyl-3*H*-indolium Bromide 81

4.2.1.2. 1-[2-(Diethoxyphosphoryl)-ethyl]-2,3,3-trimethyl-3*H*-indolium Bromide 82
4.2.1.3. FO544-Acid 83
4.2.1.4. FO544-OSI Ester 83
4.2.2. FO545 84
4.2.2.1. 1-(5-Carboxypentyl)-2,3,3-trimethyl-3*H*-indolium Bromide 83
4.2.2.2. FO545-Acid 85
4.2.2.3. FO545-OSI Ester 85
4.2.3. FO546 86
4.2.3.1. 1-(7-Carboxyheptyl)-2,3,3-trimethyl-3*H*-indolium Bromide 86
4.2.3.2. FO546-Acid 87
4.2.3.3. FO546-NHS Ester 87
4.2.4. FO548 88
4.2.4.1. 4-Hydrazino-benzenesulfonic acid 88
4.2.4.2. Potassium 2,3,3-Trimethyl-3*H*-indole-5-sulfonate 89
4.2.4.3. 1-(5-Carboxypentyl)-2,3,3-trimethyl-3*H*-5-indoliumsulfonate 89
4.2.4.4. FO548-Acid 90
4.2.4.5. FO548-OSI Ester 91
4.2.5. FO642 92
4.2.5.1. FR642-Acid 92
4.2.5.2. FR642-OSI Ester 92
4.2.6. FR646 93
4.2.6.1. FR646-Acid 93
4.2.6.2. FR646-OSI Ester 94
4.2.7. FR626 94
4.2.7.1. 1-Ethyl-2,3,3-trimethyl-3H-5-indoliumsulfonate 94
4.2.7.2. 3-Butoxy-4-(1-ethyl-3,3-dimethyl-1,3-dihydro-5-sulfonyl-indol-2-ylidenemethyl)-cyclobut-3-ene-1,2-dione 95
4.2.7.3. FR626-Acid 96
4.2.7.4. FR626-OSI Ester 96
4.2.8. FR661 97
4.2.7.1. 6-(4-Methyl-1-quinolinium)hexanoic acid bromide 97

4.2.8.2. 6-[4-(2-Butoxy-3,4-dioxo-cyclobut-1-enylmethylene)-4H-quinolin-1-yl]-hexanoic acid 97
4.2.8.3. FO661-Butylester 98
4.2.8.3. FO661-Acid 99
4.2.8.4. FO661-OSI Ester 99
4.2.9. FR662 100
4.2.9.1. 2-(2,3-Dibutoxy-4-oxo-2-cyclobutenyliden)malononitrile 100
4.2.9.2. {2-[2-(2-Butoxy-4-dicyanomethylene-3-oxo-cyclobut-1-enylmethylene)-3,3-dimethyl-2,3-dihydro-indol-1-yl]-ethyl}-phosphonic acid monoetyl ester 101
4.2.9.3. FR662-Butylester 101
4.2.9.4. FR662-Acid 102
4.2.9.5. *FR662-OSI Ester* 103
4.2.10. FR670 103
4.2.10.1. FR670-Acid 103
4.2.10.2. FR670-OSI Ester 104
4.2.11. OB630 105
4.2.11.1. 1-(6-Hydroxyhexyl)-2,3,3,-trimethyl-3*H*-indolium Bromide 105
4.2.11.2. 3-Butoxy-4-(1,3,3-trimethyl-1,3-dihydro-indol-2-ylidenemethyl)-cyclobut-3-ene-1,2-dione 105
4.2.11.3. 3-Hydroxy-4-(1,3,3-trimethyl-1,3-dihydro-indol-2-ylidenemethyl)-cyclobut-3-ene-1,2-dione 106
4.2.11.4. OB630-OH 107
4.2.11.5. OB630-PAM 107
4.2.12. OG670 108
4.2.12.1. 2-[3-Butoxy-4-oxo-2-(1,3,3-trimethyl-1,3-dihydro-indol-2-ylidenemethyl)-cyclobut-2-enyl]-malonitrile 108
4.2.12.2. OG670-OH 109
4.2.12.3. OG670-PAM 109
4.3. General Labeling Procedures 110
4.3.1. General Procedure for Labeling Proteins and Determination of Dye-to-Protein Ratios 110

4.3.2. General Procedure for Labeling Amino Acids 111
4.3.3. General Procedure for Labeling Oligonucleotides 111
4.3.4. General Procedure for Labeling dUTP 112
4.4. Determination of Quantum Yields 112
4.5. Determination of Dissociation Constants K_D^* 113
4.5. General Procedures for Energy Transfer Measurements 114
4.5.1. Immunostudies and Hybridization Studies 114
4.5.2. Competitive Assays 114
4.6. Flow-Cytometry 114
4.7. References 115

5. Summary 117

6. Acronyms, Definitions, and Nomenclature of the Dyes 118
6.1. Acronyms 118
6.2. Definitions 118
6.3. Nomenclature of the Dyes 118

7. Curriculum Vitae 120

8. List of Papers Posters and Presentations 121
8.1. Papers Published, Submitted, or in Preparation 121
8.2. Patent 121
8.2. Posters and Presentations 122

1. Introduction

Fluorescence spectroscopy and the closely related area of phosphorescence spectroscopy have become firmly established and widely employed techniques in analytical chemistry. Fluorimetry is now routinely used in the detection, quantitation, identification and characterization of structure and function of inorganic and organic compounds, and of biological structures and processes. Fluorescence spectroscopy is routinely applied and successfully to the monitoring of biospecific reactions like as in immunoassays and hybridization assays, and in the study of molecular interactions such as ligand-protein binding [1].

In most of these assays it is not the intrinsic fluorescence of the analyte that is measured. There are many cases where the molecule of interest is non-fluorescent (like DNA), or where the intrinsic fluorescence is not adequate for the desired experiment. Intrinsic protein fluorescence originates from the aromatic amino acids tryptophan, tyrosine, and phenylalanine. Their emission maxima are in the range of 280-350 nm. In the case of proteins it is frequently advantageous to label them with chromophores which have longer excitation and emission wavelengths than the aromatic amino acids. Then the labeled protein can be studied in the presence of unlabeled proteins [1, 2].

1.1. Long-Wavelength Fluorophores and Labels

Long-wavelength probes and labels are of current interest for several reasons. The sensitivity of fluorescence detection is often limited by the autofluorescence of biological samples like cells and tissue. It is well known that this autofluorescence decreases with increasing wavelength, and hence the detectability over background increases. Therefore the so-called optical window of blood and other biological material (see fig. 1.1) is in the range of 600-900 nm [2, 3].

In addition, light of longer wavelength penetrates tissue more easily due to the inverse relationship of the scatter of light to the fourth power of the wavelength (Tyndall) which makes longer wavelength excitation more attractive for in-vivo measurements, e.g., sensing applications through skin or in whole blood [4]. Besides, damage of biological matter is decreased at long-wave excitation. It is also advantageous that inexpensive light sources are available for excitation of long-wavelength fluorophores. Diode lasers provide convenient monochromatic intense excitation sources and are quite cheap in cost and operation [1, 2].

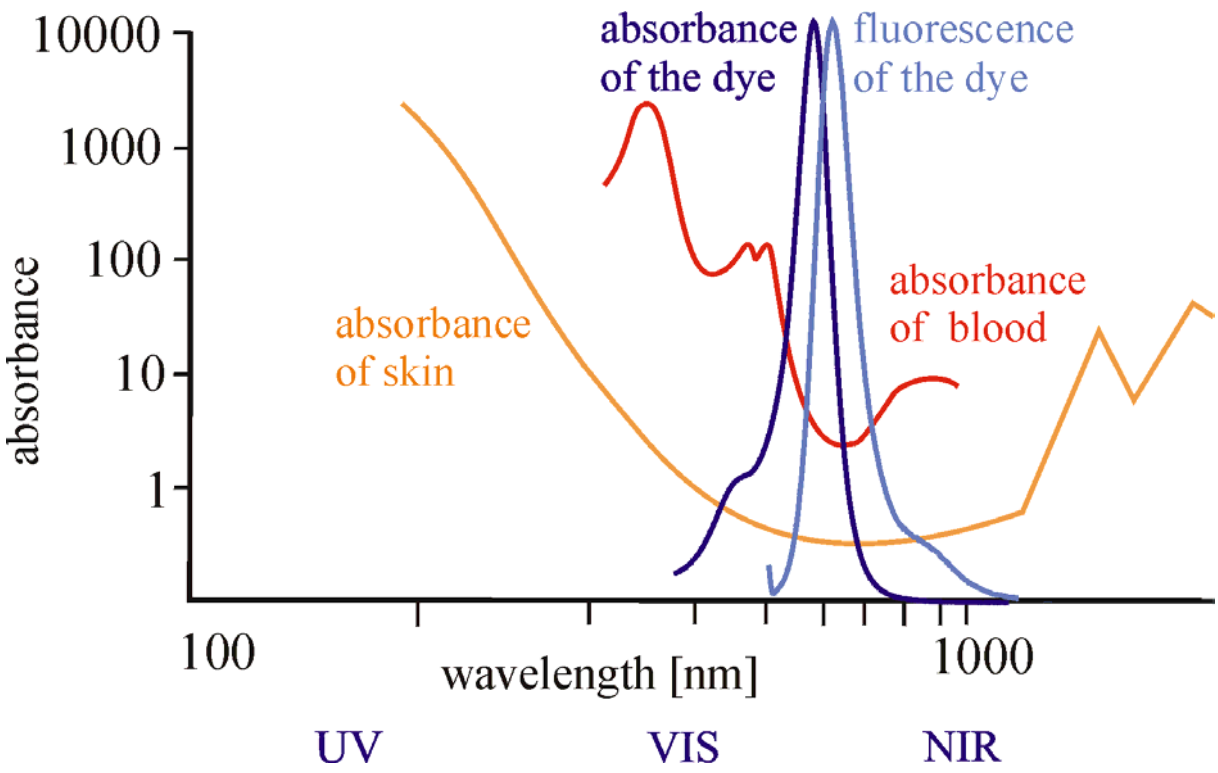

Figure 1.1. Absorption spectra of skin and blood with an optical window in the range of 600-750 nm, and absorption and emission spectra of a long-wavelength fluorophore.

In the following, the cyanine and the squaraine dyes are introduced as examples for long-wavelength fluorophores this work deals with.

1.1.1. Cyanine Dyes [5]

Cyanines are cationic polymethine dyes. They form a group of dyes that combine relatively long-wave absorption with comparatively small molecular size, a feature that is desirable for labels in order not to disturb the system to be probed. In addition, the color of the cyanine dye is fairly predictable from its molecular structure. The chemical structure of cyanine dyes can be represented in general form by structure **X(-CH=CH)$_n$-CH=Y**, where **X** and **Y** typically are nitrogen containing heterocycles like those shown in table 1.1. One of the two substitutents (here **X**) has to be present in quaternized (cationic) form (A to G in table 1.1).

Table 1.1. Typical substituents in cyanine dyes of the general structure **X(-CH=CH)$_n$-CH=Y**

X	**Y**
A 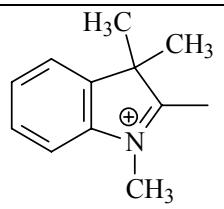	A' 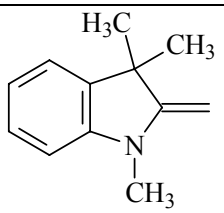
B 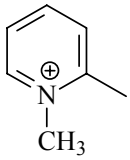	B' 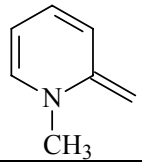
C 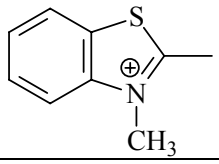	C' 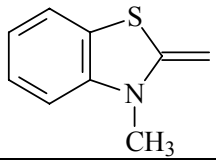
D 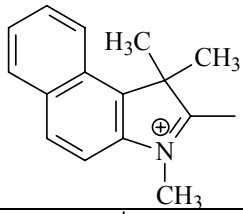	D' 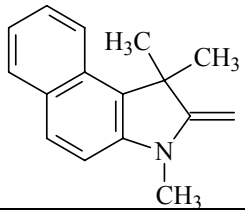
E 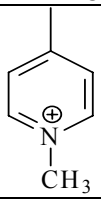	E' 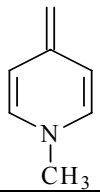
F 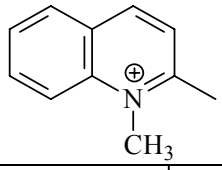	F' 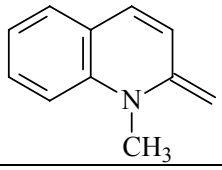
G 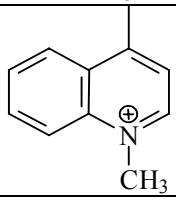	G' 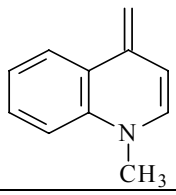

The parameter *n* in **X(-CH=CH)$_n$-CH=Y** has the largest effect on the absorption maximum (λ_{max}). The number of *n* typically varies from 0 to 3. It is known that the λ_{max} values of cyanines increase almost linearly by 100 nm with *n* (vinylene shift) [6]. Dyes with *n* = 0 are called monocyanines; if *n* = 1, 2, or 3, they are called tri-, penta- or heptacyanines, respectively [6, 7].

While the number for *n* exerts a massive effect on the absorption maxima, spectral fine-tuning can only be accomplished by variation of substitutents **X** and **Y** (see table 1). Symmetrical cyanines (i.e., those where heterocycle **X** is of the same type as is **Y**) have been

described rather often, and their absorption maxima have been measured [6-8]. The absorption wavelength of an unsymmetrical cyanine is usually shorter than the arithmetic mean of the wavelength of the corresponding two symmetrical dyes with identical end groups [9]. Table 1.2 displays compiled absorption maxima for some selected trimethine dyes.

Table 1.2. Calculated absorption maxima (in nm) of trimethine dyes of type **X-CH=CH-CH=Y**, showing that by proper variation of substituents (**A**–**G** and **A'-G'**, respectively; see table 1.1) the whole longwave part of the visible spectrum can be covered. Other substituents (e.g. benzo[c,d]indoles) are known as well. It should be mentioned that the absorption maximum and the shape of the absorption band is dependent on the solvent.

A	543						
B	547	552					
C	549	551	555				
D	565	567	572	590			
E	525	590	579	595	603		
F	551	578	577	598	597	610	
G	615	630	630	642	651	657	710
X / **Y**	**A'**	**B'**	**C'**	**D'**	**E'**	**F'**	**G'**

Based on the above logic, various functional dyes can be prepared [13]. They contain (a) a chromophore of predetermined color, (b) a functional group imparting water solubility, and (c) a spacer with a terminal functional group (such as COOH) to enable conjugation to biomolecules.

1.1.2. Squarylium Dyes

Squarylium dyes (squaraines) belong to the family of the cyanine dyes. In general, squarylium dyes are close in wavelength to the cationic pentacyanine dyes. They differ formally from them by substitution of H by O^- in the meso position of the chain and symmetrical bridging of the neighboring carbon atoms by a carbonyl group (fig. 1.2) [6].

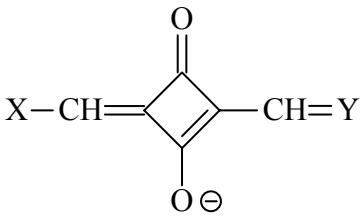

Figure 1.2. General structure of squarylium dyes (X, Y = heterocyclic end groups; see table 1.1).

Variation of the heterocyclic end groups X and Y and substitution of the oxygen e.g. by a dicyanomethylene group or by sulfur makes a large variety of absorption wavelengths accessible. Due to their electronic symmetry, squaraines exhibit a sharp absorption with high extinction coefficients in the red and near IR region (600-750 nm). The photostability of these dyes is very high [10, 11]. Squarylium dyes can be highly fluorescent because of their planarity and rigidity due to the bridged polymethine chain. Introduction of reactive groups which enable covalent attachment to biomolecules, and of sulfonic acid groups which enhance water solubility of the dyes makes the squaraines viable labels for the use in biological applications. In addition, the quantum yields of the free dyes generally rise upon binding to biomolecules. The high quantum yields combined with the high molar absorbances of the squaraines result in a high brightness and a low detection limits of the conjugates [3, 10-14]. Table 1.3 shows some selected squarylium dyes and their spectral properties.

Table 1.3. Some hydrophilic, reactive squarylium dyes, their absorption and emission maxima, molar absorbances (ε), and quantum yields (ϕ) in PBS [14, 15].

Structure	λ_{abs} [nm]	λ_{em} [nm]	ε [L/mol·cm]	ϕ
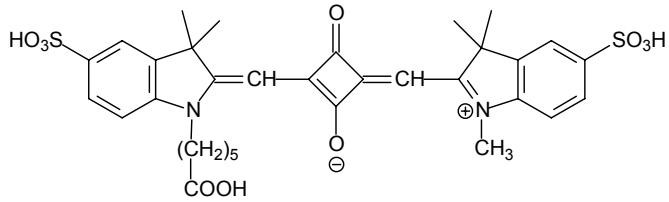	630	647	85,000	0.03
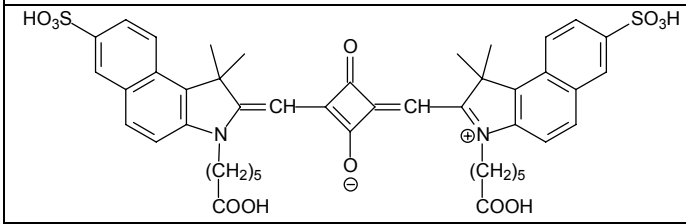	661	680	140,000	0.05
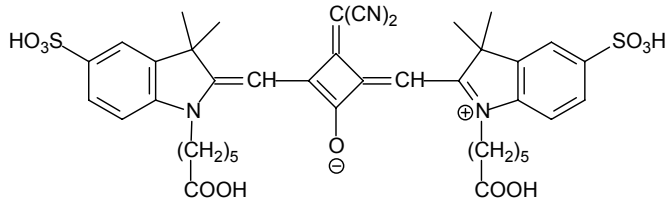	667	685	120,000	0.04
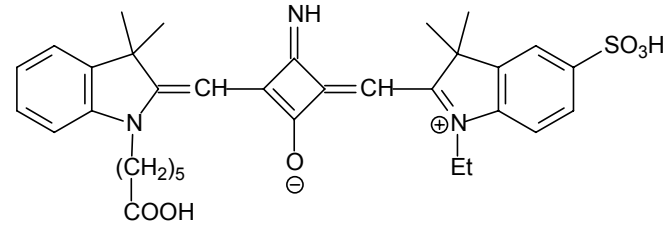	626	636	150,000	n.d.
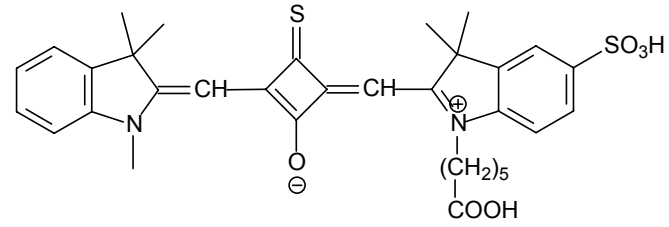	630	640	n.d.	n.d.
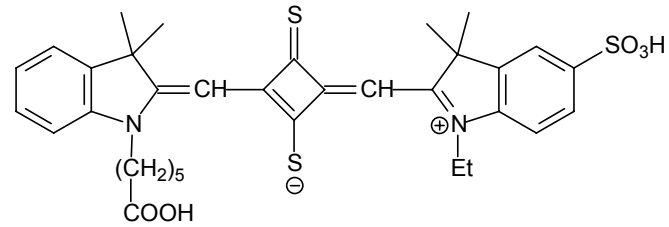	628	641	n.d.	n.d.

n.d.: not determined

1.1.3. Labels

There are several requirements for fluorescent biolabels. The fluorophore is expected to have a high molar absorbance and good solubility in water. Charged groups (usually anionic) are often introduced into the biolabel to avoid undesired electrostatic attraction to the

biomolecule. The fluorophore should be stable and soluble in organic solvents and in water. The fluorescence of the label should be weak in its unconjugated form and high if bound to the target. Fluorescence is expected to be pH-independent in the physiological range between pH 5 and 9. Besides, a high photostability and at least one reactive group for coupling to the target are required.

1.2. Labeling

The interest in bioanalysis focuses on analytes such as proteins and nucleic acids (DNA/RNA). In one of the actual bioanalytical indicator systems the molecule-specific probe is generated by coupling a detector molecule used for fluorescent signal generation. In order to obtain good signal-to-noise ratios, long-wave fluorophores are used because of reduced background fluorescence [16-18].

In the following some labeling methods for proteins and DNA are shown in brief. The use of labeled microparticles is not the main focus in this work, but must be mentioned for the sake of completeness.

1.2.1. Labeling of Proteins

Proteins and peptides are amino acid polymers containing a number of reactive side chains. Aliphatic ε-amino groups of the amino acid lysine and the α-amino groups of the N-terminal amino acids are the most common reactive groups of proteins. Reactive esters, especially oxysuccinimide (OSI) esters, are some of the most used reagents for amino group labeling. The labeling reaction competes favorably with hydrolysis of the active ester but the rates of both reactions depend on pH. Most labeling reactions with active esters are carried out between pH 8.5 and 9.5 over a period between 15 minutes and several hours (fig. 1.3 A). Isothiocyanates (fig. 1.3 B) are amine-modifying reagents of intermediate reactivity. They are somewhat more stable in water than OSI esters and react optimally with proteins at pH 9.0 – 9.5. Sulfonylchlorides are highly reactive labels. They are unstable in water but form extremely stable sulfonamide bonds which can survive even amino acid hydrolysis (fig. 1.3 C).

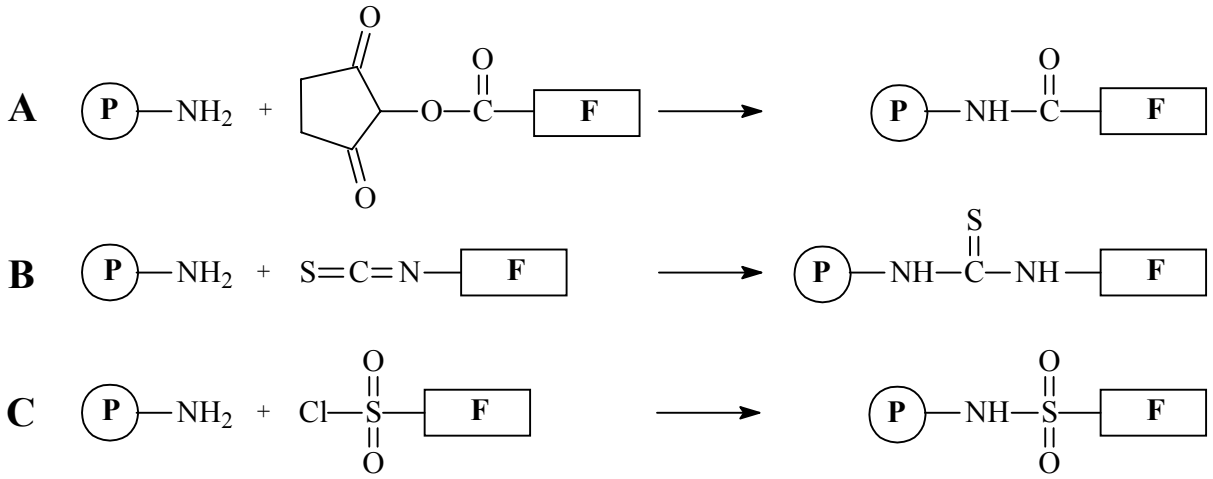

Figure 1.3. Common methods for labeling amino groups of proteins. A: the succinimidyl active ester method, B: the isothiocyanate method, C: the sulfonylchloride method. P denotes a protein, F a fluorophore.

Another common reactive group in proteins is the thiol group of the amino acid cystein. The iodoacetamide (fig. 1.4. A), the maleimide (fig. 1.4. B), and the disulfide exchange method (fig. 1.4. C) are the most frequently used methods for thiol labeling.

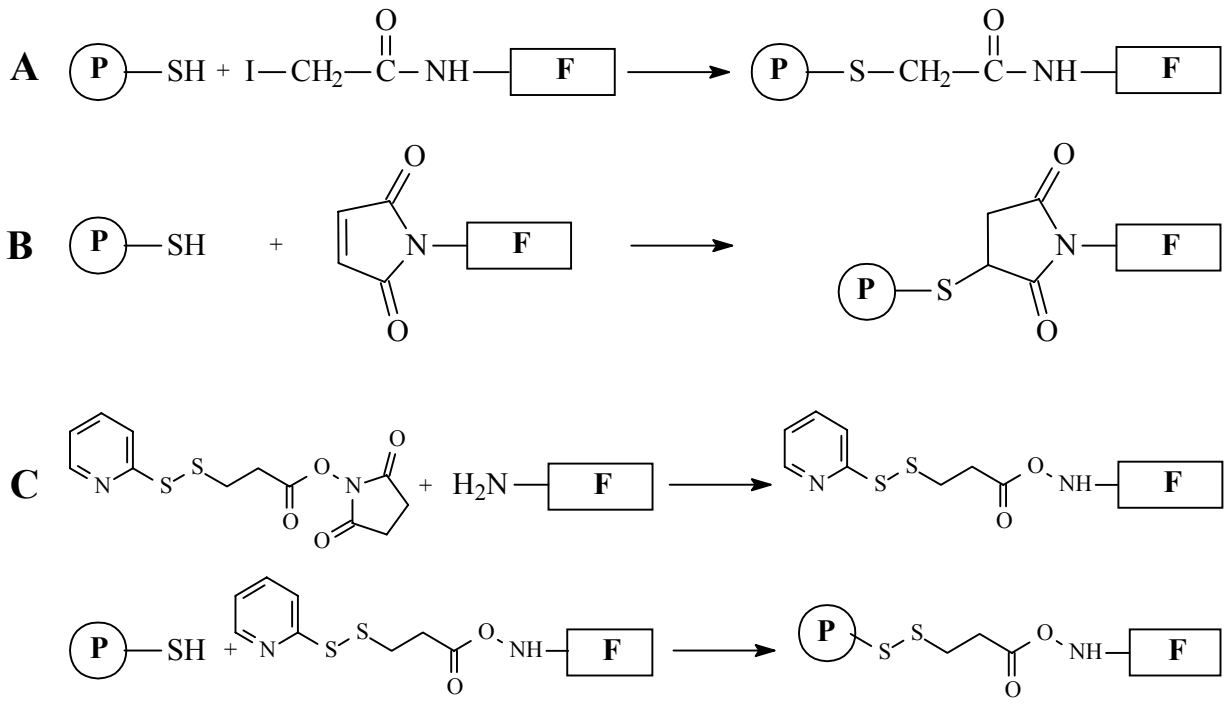

Figure 1.4. Common methods for thiol labeling. A: the iodoacetamide, B: the maleimide, and C the disulfide exchange method. P denotes a protein, F a fluorophore.

The carboxy acid groups of aspartic acid, glutamic acid and the C-terminal end of the peptide chain have only low activity in water and are therefore quite seldom used for labeling proteins [17, 19, 20].

1.2.2. Labeling of DNA

There is a great interest in labeling oligonucleotides with fluorophores, because the resulting fluorescent oligonucleotides are needed for DNA sequencing and DNA hybridization studies. Reactive groups like in proteins are usually absent or not abundant in natural nucleic acids. A common method is to introduce a reactive group into the oligonucleotide. An amino group may be incorporated into a synthetic oligonucleotide as the last step in the synthesis process. Then the label can be introduced into the oligonucleotide via a reactive group such as an OSI ester which binds to amino groups. Most amine-reactive labels contain spacer groups (C_4 – C_6) in order to reduce the interaction of the label with the oligonucleotide [5, 21, 22].

Although phosphate groups of nucleotides and oligonucleotides are not very reactive in aqueous solution, their terminal phosphate groups can react with carbodiimides and similar reagents in combination with nucleophiles to yield phosphodiesters, phosphoramidates and phosphorothioates. However, the most important tagging method for DNA is based on the use of a phosphoramidite derivative of a fluorophore. In order to obtain phosphoramidite labels, the hydroxylated fluorophore (F-OH) is reacted with a phosphine **I** to give the phosphoramidite label **II**. The dye activated in this way couples to the hydroxy group of the (desoxy)ribose unit of an oligonucleotide to give **III** which, on oxidation with iodine, yields the labeled nucleotide **IV** (fig. 1.5.) [5, 24, 25].

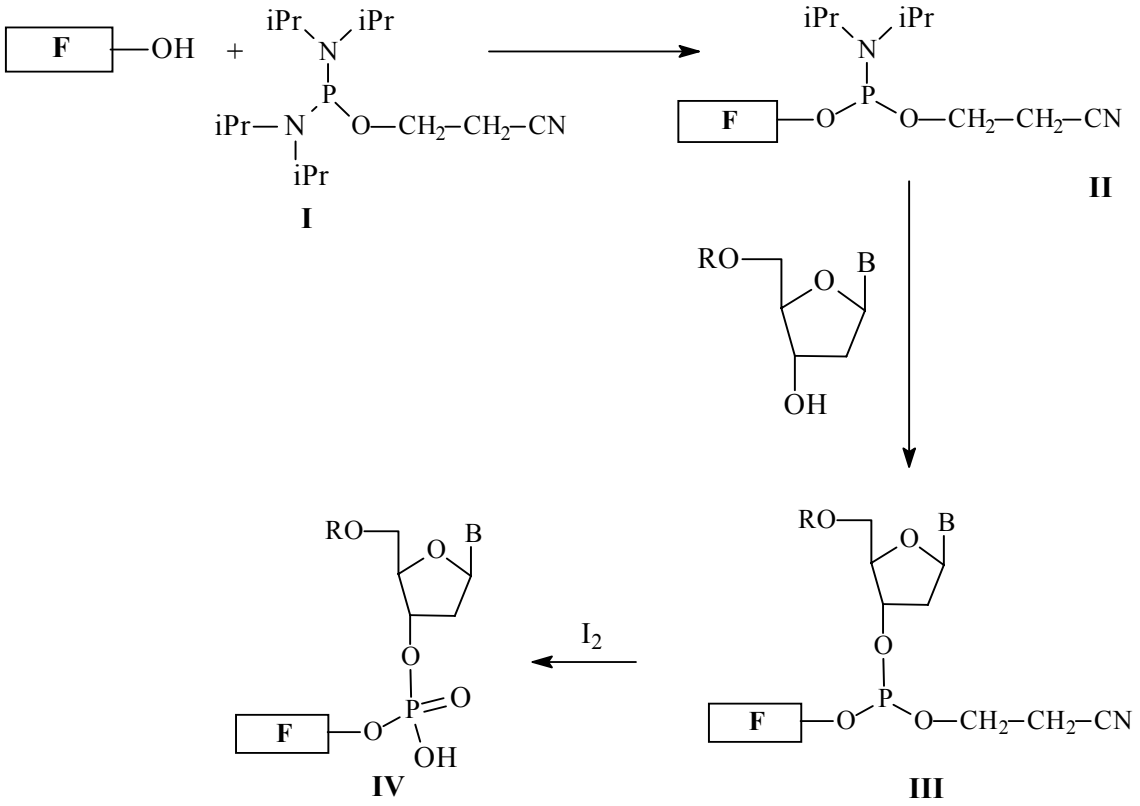

Figure 1.5. Scheme of the synthesis of fluorescently labeled nucleotides. F denotes a fluorophore, B a nucleobase.

1.2.3. Dyeing of Microparticles

Polystyrene beads (of 0.1-5 µm diameter) are widely used in immunoassays and in studies on receptor-ligand interactions, often in combination with flow cytometry. In recent years beads have been fluorescently dyed for purposes of encoding. The color of the fluorescence of the bead, the ratio of two fluorescence intensities of a bead, or the luminescence decay time of the fluorophore can serve for identification purposes [5].

It is possible to either covalently bind fluorescent dyes onto surface modified particles or to dissolve the dyes directly into the particles. For covalent coupling both the bead and the fluorophore need to possess functional groups for binding. In many cases the particles possess carboxy acid groups which are activated via the OSI ester method. Then amino-modified fluorophores can be attached to the surface.

Liopophilic fluorophores with long alkyl chains (C_{18}) are required for incorporating dyes inside beads. In most cases this method is preferred, because the interference of the dyes with the surface chemistry of the bead is reduced. Besides, there is more space available inside the particle than on its surface, so there is more incorporated fluorophore present which lowers the detection limit of the dyed bead [14].

1.3. Fluorescence Resonance Energy Transfer (FRET)

Fluorescence resonance energy transfer is transfer from the excited-state energy of the donor to an acceptor. Energy transfer occurs without the appearance of a photon. It is the result of long-range dipole-dipole interactions between donor and acceptor. The rate of energy transfer depends upon the extent of the spectral overlap of the emission spectrum of the donor with the absorption spectrum of the acceptor (see fig. 1.6.), the quantum yield of the donor, the relative orientation of the donor and acceptor transition dipoles, and the distance between donor and acceptor.

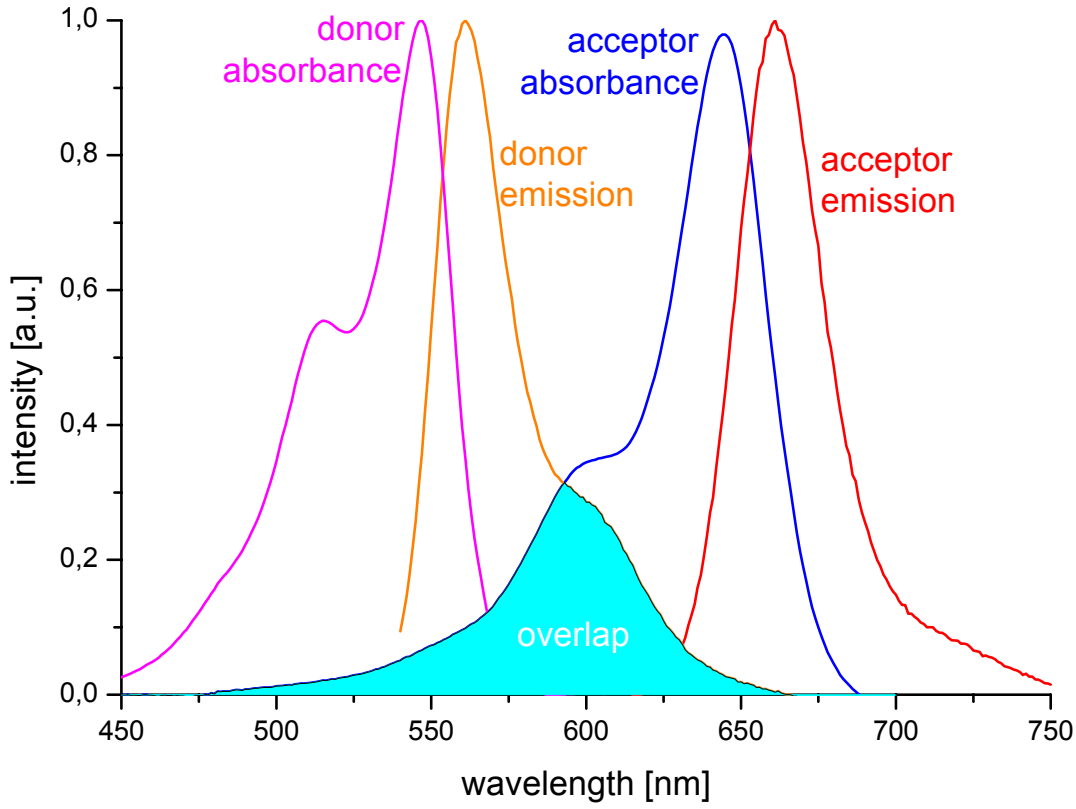

Figure 1.6. The spectral overlap of the emission spectrum of the donor and the absorption spectrum of the acceptor.

Energy transfer occurs over distances comparable to the dimensions of biological macromolecules. The distance at which FRET efficiency is 50% is called Förster distance (R_0). R_0 values are typically in the range of 2 - 6 nm. The rate of energy transfer (k_T) from a donor to an acceptor is given by the following formula

$$k_T = \frac{1}{\tau_D}\left(\frac{R_0}{r}\right)^6, \qquad (1.1)$$

where τ_D is the decay time of the donor in absence of the acceptor, R_0 is the Förster distance and r is the donor-to-acceptor distance. The rate of energy transfer strongly depends on the donor-to-acceptor distance being inversely proportional to r^6 [2].

The Förster radius R_0 was calculated by the standard formula

$$R_0^6 = \frac{9\kappa^2}{8\pi(2\pi)^4 n^4}\phi_d \frac{\int d\lambda F_d(\lambda)\sigma(\lambda)\lambda^4}{\int d\lambda F_d(\lambda)}, \qquad (1.2)$$

where κ^2 is a factor accounting for the relative orientation of the emission and absorption dipoles of donor and acceptor, respectively; n is the refractive index of the solvent; $F_d(\lambda)$ is the emission spectrum of the donor (in arbitrary units) at wavelength λ; and $\sigma(\lambda)$ is the absorption cross section of the acceptor which can be found from its extinction $\varepsilon(\lambda)$ by

$$\sigma(\lambda) = \frac{10^3 \cdot \ln 10 \cdot \varepsilon(\lambda)}{N_A} \approx \frac{2303}{N_A}\varepsilon(\lambda), \qquad (1.3)$$

where N_A is the Avogadro-Loschmidt number. In the calculations, freely rotating donors and acceptors are assumed, so that for κ^2 the standard value of $2/3$ can be adopted. The donor-acceptor distance (r) can easily be calculated according to the following two formulae:

$$E = \frac{{R_0}^6}{{R_0}^6 + r^6} \qquad (1.4)$$

and

$$E = 1 - \frac{F_{DA}}{F_D}, \qquad (1.5.)$$

where E is the efficiency of energy transfer, R_0 is the Förster distance and F_D and F_{DA} are the relative fluorescence intensities of the donor in absence and in presence of the acceptor, respectively. [2]

1.4. Immunoassays

In this work, immunoassays were performed on the system HSA/anti-HSA which is described briefly in the following.

1.4.1. The System HSA and Anti-HSA

Human serum albumin (HSA) is an extremely abundant blood protein, forming about 50% of the total plasma protein in humans. HSA is composed of a single polypeptide chain and consists of 585 amino acids. It is 67% alpha-helical and does not contain any beta-sheet

structure. The protein has a molecular mass of 65,000 Dalton and contains 17 disulfide bridges. The primary function of HSA is to transport fatty acid molecules, but it also binds various metals, hormones, and a wide variety of drugs [26, 27].

The role of HSA molecules which are present in blood plasma at about 0.6 mM is to increase the capacity of the circulatory system to carry fatty acids. Figure 1.7 shows an HSA molecule in its free form and complexed with fatty acid. The protein binds at least five fatty acid molecules which are only sparingly soluble in water because of their hydrophobic tails. The surface of HSA is very hydrophilic. This makes the protein very soluble in water [26].

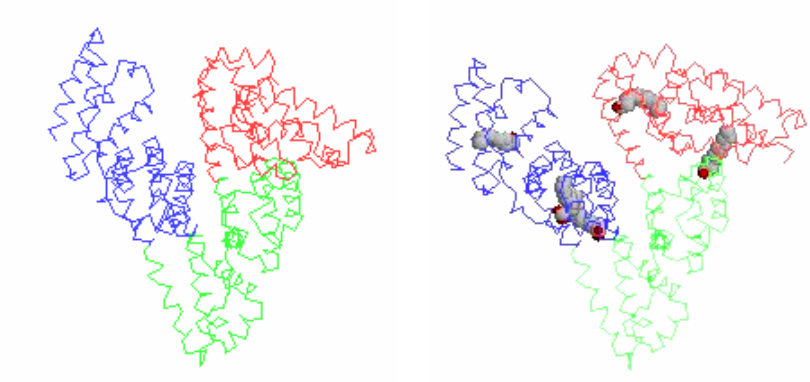

Figure 1.7. The structure of HSA in its free form and complexed with myristic acid (C14 fatty acid) [26].

The antibody to HSA, anti-HSA, is an immunoglobulin G (IgG), also known as γ-globulin. It is developed in animal (e.g. rabbit, mouse, goat) using purified human albumin as the immunogen. Figure 1.8 shows the "Y"-shaped protein, composed of three fragments, two Fab fragments (the "arms" of the Y), and one Fc fragment (the "stem" of the Y) [28]. Each antibody has a molecular weight of approximately 150,000 Daltons and is composed of two identical heavy (dark and light blue) and two identical light chains (green and orange), all held together by disulfide bonds. In each chain there are constant domains and a variable domain. The four variable domains are positioned at the ends of the Y-like fork of the molecule where they form two binding sites for antigenic determinants. The carbohydrate (red) attached to the heavy chains aids in determining the destination of antibodies in tissues [27, 29, 30].

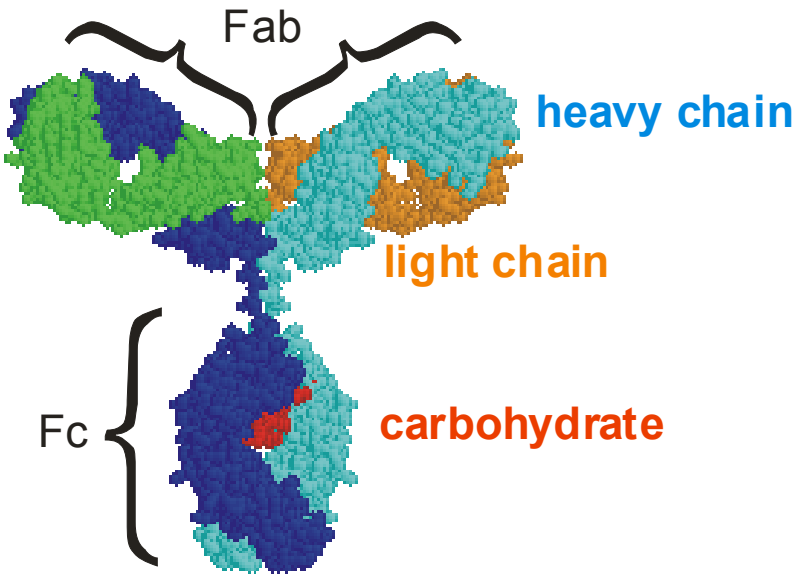

Figure 1.8. The "Y"-structure of an IgG antibody [31].

In this work HSA/anti-HSA was chosen as the model system for immunoassays because serum albumin has long been used as a model protein and served for numerous applications in both industrial processes and academic research areas [32-34]. Anti-HSA is a quite stable antibody and can be stored at 2-8 °C for at least one month. Last but not least, HSA and anti-HSA are relatively inexpensive.

1.4.2. FRET Immunoassays

Immunoassays constitute a large and diverse family of assays. At present, they are mainly based on fluorescence detection. Perhaps the most commonly used immunoassay format is the enzyme-linked immunosorbent assay (ELISA) owing to its high sensitivity and applicability to a wide range of antigens. ELISA is described as a heterogeneous assay. Antibodies are bound to a surface and separation steps are required. A major advantage is the use of homogenous assays, like FRET immunoassays. In this case separation steps are not required and sample handling is minimized. Such an assay is typically performed in a competitive format [2]. This means that for example the antigen is labeled with a fluorescent donor dye and the corresponding antibody is labeled with an acceptor dye. If non-labeled antigen is added, the donor labeled antigen is displaced and energy transfer efficiency is reduced. The acceptor dye can either be a quencher or, preferably, a fluorescent dye. If both donor and acceptor are fluorescent, ratiometric (2-wavelength) data evaluation is possible.

1.5. Hybridization Assays

Detection of DNA hybridization is often required in molecular biology, genetics, and forensics. A variety of methods has been used to detect DNA hybridization by fluorescence. Most of them rely on energy transfer between donor and acceptor labeled DNA. The presence of complementary DNA sequences can be detected by increased energy transfer when these sequences are brought into proximity by hybridization (fig. 1.9 A_1 and A_2). Competitive hybridization (fig. 1.9 B) in which increased amounts of non-labeled target DNA competes with the formation of donor-acceptor pairs can also be performed [2, 5]. "Molecular Beacons" (fig. 1.9 C) are not only of scientific interest, but can also be used to record hybridization of nucleic acids in homogeneous assays [35].

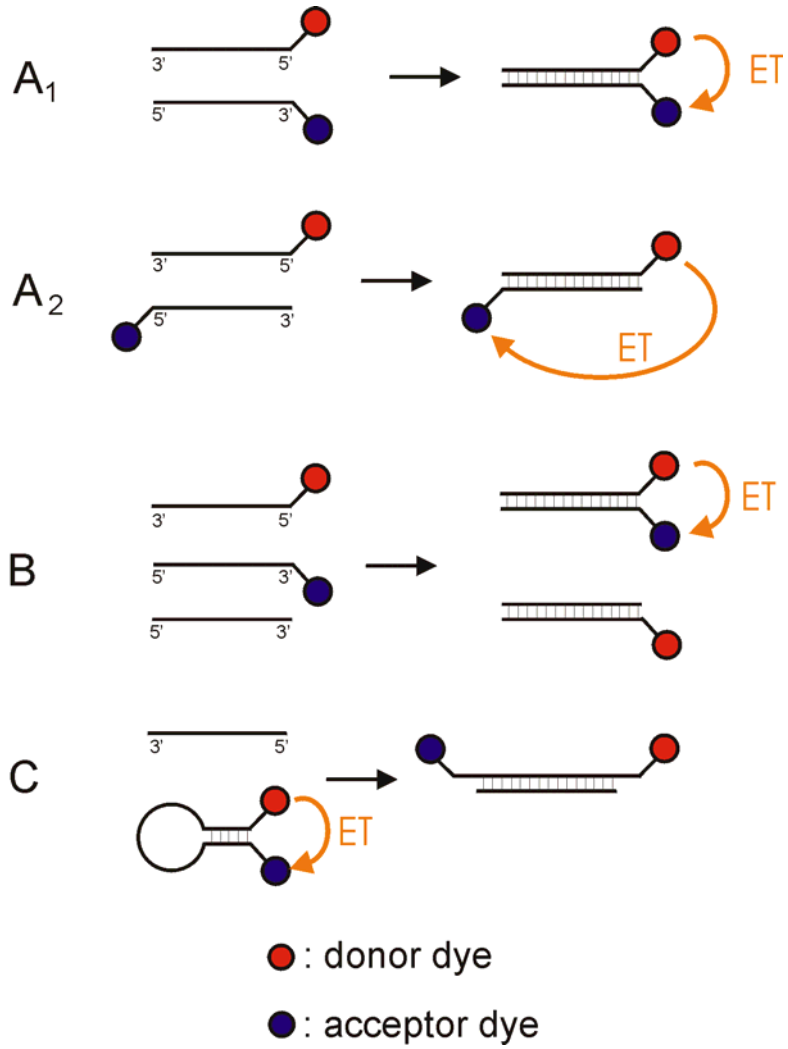

Figure 1.9. Some methods for studying the hybridization of oligonucleotides via FRET: binding studies (A_1 and A_2), competitive hybridization assays (B), and molecular beacons (C).

1.6. References

[1] O. S. Wolfbeis (Ed.) (1993) Fluorescence Spectroscopy: New Methods and Applications, Springer Verlag, Berlin.

[2] J. R. Lakowicz (1999) Principles of Fluorescence Spectroscopy (2nd edition), Kluwer Academic/Plenum Publishers, New York.

[3] B. Oswald, L. Patsenker, J. Duschl, H. Szmacinski, O. S. Wolfbeis, and E. Terpetschnig (1999) Synthesis, Spectral Properties, and Detection Limits of Reactive Squaraine Dyes, a New Class of Diode Laser Compatible Fluorescent Protein Labels. *Bioconjugate Chem.* **10**, 925-931.

[4] E. Terpetschnig and O. S. Wolfbeis (1998) Luminescent Probes for NIR Sensing Applications *in* Near-Infrared Dyes for High Technology Applications, (S. Daehne, Resch-Genger and O. S. Wolfbeis, Eds.), NATO ASI Ser.3 (High Technology), **53**, Kluwer Acad. Publ., Dortrecht (NL).

[5] O. S. Wolfbeis, M. Böhmer, A. Dürkop, J. Enderlein, M. Gruber, I. Klimant, C. Krause, J. Kürner, G. Liebsch, Z. Lin, B. Oswald, and M. Wu (2002) Advanced Luminescent Labels, Probes, and Beads, and Their Application to Luminescence Bioassay, and Imaging *in* Springer Series in Fluorescence, (Kraayenhof, R., Ed.), Springer Verlag, Berlin-Heidelberg.

[6] J. Fabian, N. Nakazami, M. Matsuoka (1992) Near Infrared-Absorbing Dyes. *Chem. Rev.* **92**, 1197-1226.

[7] M. Matsuoka (Ed.) (1990) Infrared Absorbing Dyes. Plenum Press. New York.

[8] R. B. Mujumdar, L. A. Ernst, S. R. Mujumdar, C. J. Lewis, A. S. Waggoner (1993) Cyanine dye labeling reagents: sulfoindocyanine succinimidyl esters. *Bioconjugate Chem.* **4,** 105-111.

[9] J. Fabian, H. Hartmann (1980) Light Absorption of Organic Colorants, Springer-Verlag, Berlin, Heidelberg.

[10] E. Terpetschnig and J. R. Lakowicz (1993) Synthesis and Characterization of Unsymmetrical Squaraines: A New Class of Cyanine Dyes. *Dyes and Pigments* **21**, 227-234.

[11] E. Terpetschnig, H. Szmacinski, and J. R. Lakowicz (1993) Synthesis, Spectral Properties and Photostabilities of Unsymmetrical Squaraines; A New Class of Fluorophores with Long-Wavelength Excitation and Emission. *Anal. Chim. Acta* **282**, 633-641.

[12] B. Oswald, F. Lehmann, L. Simon, E. Terpetschnig, and O. S. Wolfbeis (2000) Red Laser-Induced Fluorescence Energy Transfer in an Immunosystem. *Anal. Biochem.* **280**, 272-277.

[13] B. Oswald, M. Gruber, M. Böhmer, F. Lehmann, M. Probst, and O. S. Wolfbeis (2001) Novel Diode Laser-compatible Fluorophores and Their Application to Single Molecule Detection, Protein Labeling and Fluorescence Resonance Energy Transfer Immunoassay. *Photochem. Photobiol.* **74(2)**, 237-245.

[14] B. Oswald (2000) New Long-Wavelength Fluorescent Labels for Bioassays, *Dissertation*, University of Regensburg (Germany).

[15] B. Wetzl (2002) New Rhodamines and Squarylium Dyes for Biological Applications, *Diploma Thesis,* University of Regensburg (Germany).

[16] C. Kessler (1994) Non-radioactive analyses of biomolecules. *J. Biotech.* **35**, 165-189.

[17] A. Waggoner (1995) Covalent Labeling of Proteins and Nucleic Acids with Fluorophores. *Methods Enzymol.* **246**, 362-373.

[18] D. B. Shealy, R. Lohrmann, J. R. Ruth, N. Narayanan, S. L. Sutter, G. A. Casay, L. Evans III, G. Patonay (1995) Spectral Characterization and Evaluation of Modified Near-Infrared Laser Dyes for DNA Sequencing. *Applied Spectroscopy,* **49**, 1815-1820.

[19] M. Brinkley (1993) A Brief Survey of Methods for Preparing Protein Conjugates with Dyes, Haptens, and Cross-Linking Reagents. *Bioconjugate Chem.* **3**, 2-13.

[20] G. E. Means, R. E. Feeney (1990) Chemical Modifications of Proteins: History and Applications, *Bioconjugate Chem.* **1**, 2-12.

[22] R. P. Haugland (2001) Handbook of Fluorescent Probes and Research Chemicals, 8th ed, see: www.probes.com; Molecular Probes, Oregon.

[23] H. M. Lyttle, C. G. Carter, D. J. Dick, R. M. Cook (2000) A tetramethyl rhodamine (Tamra) phosphoramidite facilitates solid-phase-supported synthesis of 5'-Tamra DNA. *J. Org. Chem.* **65**, 9033-9038.

[24] W. Bannwarth (1988) Solid-Phase Synthesis of Oligodeoxynucleotides Containing Phosphoramidate Internucleotide Linkages and their Specific Chemical Cleavage. *Helv. Chim. Acta*, **71**, 1517-1527.

[25] S. L. Beaucage, and R. P. Iyer (1992) Advances in the Syntheses of Oligonucleotides by the Phosphoramidite Approach. *Tetrahedron* **48**, 2223-2311.

[26] http://www.bio.ph.ic.ac.uk.

[27] C. K. Mathews and K. E. van Holde (1996) Biochemistry (2nd edition), The Benjamin/Cummings Publishing Company, Menlo Park, California.

[28] http://merlin.mbcr.bcm.tmc.edu:8001/bcd/ForAll/Introd/antibody.html.

[29] http://www.path.cam.ac.uk/~mrc7/movies/igg1y.html.

[30] http://microvet.arizona.edu/Courses/MIC419/SystemModules/antibody.html.

[31] http://www.umass.edu/microbio/rasmol/workshop.htm.

[32] L. Stryer (1995) Biochemistry (4th edition), W. H. Freeman and Company, New York.

[33] D. H. Bing (1979) The Chemistry and Physiology of the Human Plasma Proteins, Pergamon Press, New York.

[34] F. Haurowitz (1950) The Chemistry and Function of Proteins (2nd edition), Academic Press, New York and London.

[35] Tyagi, S. (2000) Wavelength-shifting molecular beacons. *Nature Biotech.* (**18**) 1191-1196.

2. New Labels and Conjugates

In this chapter, new long-wavelength excitable fluorescent labels and their conjugates are presented. The dyes belong to either the group of the cyanines or the squaraines. All dyes contain only one reactive group which avoids crosslinking. For the syntheses of amine-reactive labels the NHS/DCC method was used, because the mild reaction conditions do not lead to decomposition of the dye and high yields (up to 70%) can be achieved. Furthermore, saccharide-reactive phosphoramidites (PAM) were synthesized which bind to the 5'-hydroxy group of the desoxyribose of oligonucleotides. The syntheses and the spectral properties of the dyes and their conjugates are described in the following.

2.1. Cyanines

In this work unsymmetrical cyanine labels have been developed. They contain one reactive oxysuccinimide (OSI) ester group which enables coupling to amino groups of biomolecules. All dyes also contain phosphonic acid groups and sometimes additional sulfo groups (FO548 and FR646) to enhance their water solubility. This is important, because the labeling reaction of the OSI esters to the biomolecules is carried out in aqueous solution and measurements are performed in aqueous buffers. The dyes FO544, FO545, FO546, and FO548 are trimethine dyes. Their solutions are intensely pink colored. The acronym FO stands for "fluorescent orange", because the fluorescence of these labels is orange. FR642 and FR646 are pentamethines with blue color. They have red fluorescence which is considered by the acronym FR.

2.1.1. FO544

Synthesis

The unsymmetrical monoreactive label FO544 can be synthesized via a four step reaction (fig. 2.1). The first step is to quaternize 2,3,3-trimethyl-3*H*-indole (**I**) on the one hand with diethyl(2-bromoethyl)phosphonate [1], and on the other hand with ethyl-4-bromobutyrate to achieve the quaternized indoles **II** and **III**, respectively. Equimolar amounts of **II** and **III** are reacted with excess 1,1,1-trimethoxymethane in pyridine [2] to get the dye ethyl ester which is cleaved with K_2CO_3 in a methanol/water mixture to get the free acid of FO544. FO544-acid (**IV**) is separated from its byproducts (i.e. symmetrical dyes) by column chromatography. The reactive dye (**V**) is prepared by reacting the acid (**IV**) with NHS and DCC in dry acetonitrile [3].

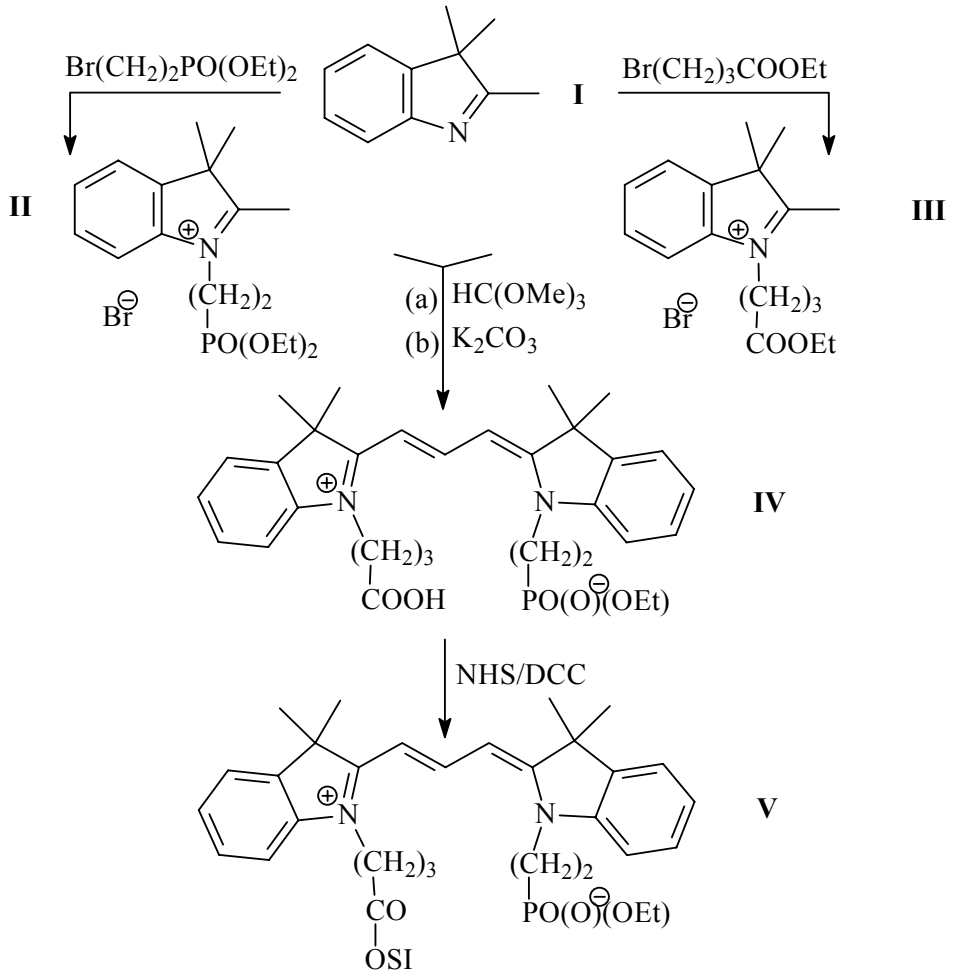

Figure 2.1. Synthesis of FO544 (V).

Spectral Properties and Stability

FO544 has an absorption maximum at 545 nm in PBS. The emission maximum is at 562 nm. It was found out that the OSI ester of the dye is very unstable in that the reactive dye is completely hydrolyzed in aqueous solution within approximately two hours. In methanol the dye is hydrolyzed, too, and the methyl ester is formed, a phenomenon which does not appear with the OSI esters of the other dyes. Even in solid form the OSI ester seems to decompose within a couple of days.

2.1.2. FO545

FO545 is an unsymmetrical monoreactive label. It has a very similar chemical structure to FO544, with the only difference that the spacer between the chromophore and the reactive group is prolonged by two methylene groups to examine if the stability of the OSI ester can be enhanced by changing the length of the spacer.

Synthesis

FO545 can be synthesized by analogy to FO544 as described above. The only difference is to use 6-bromohexanoic acid instead of ethyl-4-bromobutyrate for the quaternization of the indole. In this case, of course, an ester hydrolysis with K_2CO_3 is not required.

Spectral Properties of FO545 and its HSA Conjugates

FO545 has an absorption maximum at 545 nm in PBS. The emission maximum is at 562 nm in PBS. The following molar absorbances were determined: $\varepsilon_{545\ nm}$ (PBS) = 110,000 L/(mol · cm), $\varepsilon_{280\ nm}$ (PBS) = 11,000 L/(mol · cm), and $\varepsilon_{260\ nm}$ (PBS) = 7,000 L/(mol · cm).

The absorption maximum shifts bathochromically to 553 nm and the emission maximum shifts to 573 nm upon covalent linkage to HSA. The quantum yield of the free dye in PBS is 0.03 and rises to 0.43 (DPR = 0.2) upon binding to HSA. DPR is the acronym for dye-to-protein ratio which is defined as the number of dye molecules per protein molecul.

Several FO545/HSA conjugates with various DPRs (0.2 - 4.2) were prepared to monitor the effect of the DPR on the fluorescence intensities and on the quantum yields. Two different types of measurements were performed either with constant dye concentration or with constant protein concentration. The fluorescence intensities of solutions with a constant dye concentration ([FO545] = $9.3 \cdot 10^{-7}$ mol/L) were measured. Figure 2.2 shows the plot of the fluorescence intensities at the emission maximum versus the DPR. It is clearly visible that the fluorescence intensity decreases rapidly with increasing DPR. The quantum yield decreases from 0.43 at a DPR of 0.2 to 0.04 at a DPR of 3.3.

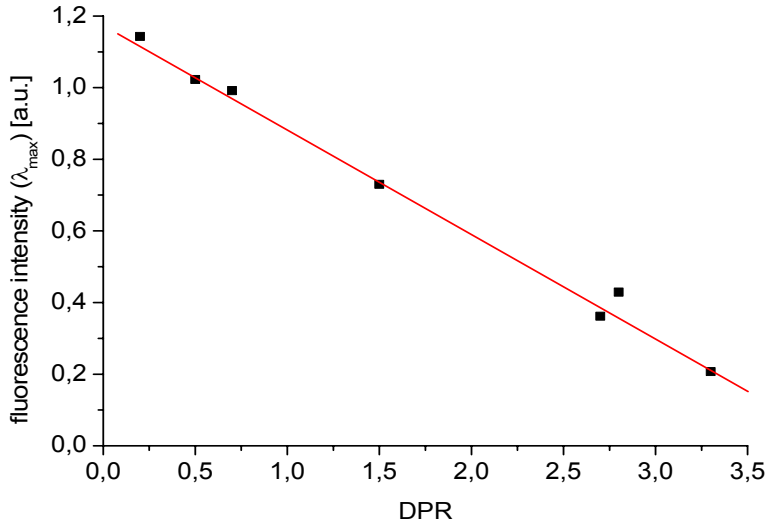

Figure 2.2. Plot of the fluorescence intensities of FO545/HSA conjugates at the emission maximum versus the DPR. [FO545] = $9.3 \cdot 10^{-7}$ mol/L.

If the same measurement is carried out with a constant protein concentration ([HSA] = $1.4 \cdot 10^{-6}$ mol/L) the plot (fig. 2.3) looks totally different compared to that with constant dye concentration (fig. 2.2). It can be seen that saturation is reached at a DPR of 2. This means if more than two dye molecules are bound to one protein molecule the dye undergoes self-quenching.

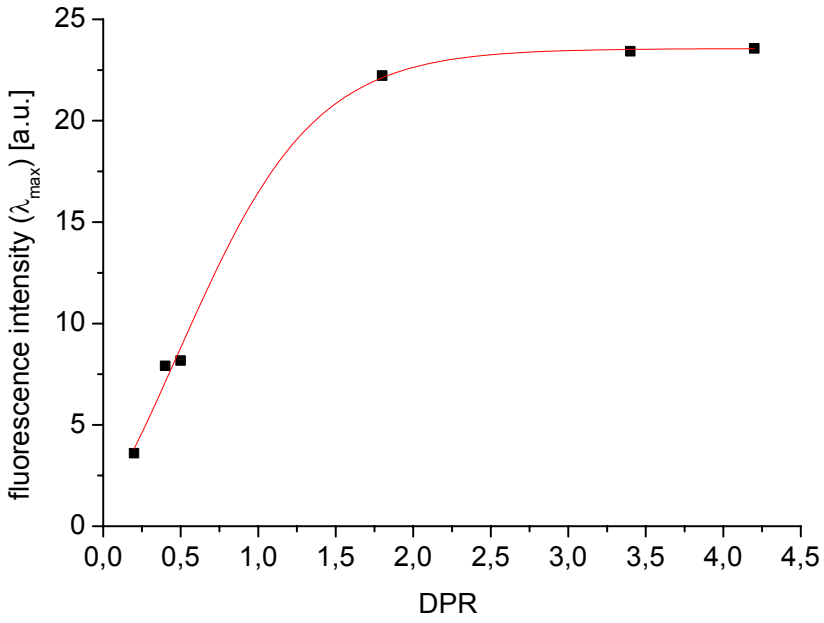

Figure 2.3. Plot of the fluorescence intensities of FO545/HSA conjugates at the emission maximum versus the DPR. [HSA] = $1.4 \cdot 10^{-6}$ mol/L.

Stability

The OSI ester of FO545 is much more stable than that of FO544. The reactive dye was dissolved in a methanol/water mixture and allowed to stand for 24 h at room temperature to prove the stability of the OSI ester. About 60% of the reactive dye were hydrolyzed within this time. In solid form the OSI ester is stable for a few weeks.

2.1.3. FO546

The chromophore of FO546 has the same structure as the chromophores of FO544 and FO545. The linker was prolonged by two methylene groups intending to further enhance the stability of the OSI ester.

Synthesis

FO546 can be synthesized by analogy to FO544 as described above. 8-Bromooctanoic acid is used instead of ethyl-4-bromobutyrate for quaternization of the indole.

Spectral Properties of FO546 and its Conjugates

FO546 has an absorption maximum at 545 nm in PBS and an emission maximum at 560 nm. The following molar absorbances were determined: $\varepsilon_{545\ nm}$ (PBS) = 86,000 L/(mol · cm), $\varepsilon_{280\ nm}$ (PBS) = 7,000 L/(mol · cm), and $\varepsilon_{260\ nm}$ (PBS) = 3,500 L/(mol · cm).

A solution of non-reactive FO546-acid ([FO546] = $6.3 \cdot 10^{-7}$ mol/L) was titrated with various amounts of HSA (0-1000 mg/L) in order to find out if non-covalently conjugated HSA affects the fluorescence of FO546. Addition of 1000 mg/L HSA caused a two fold enhancement of the fluorescence intensity (fig. 2.4). The position of the fluorescence maximum is shifted by 3 nm to longer wavelengths. This effect is probably due to the fact that the dye interacts with the protein. It is possible that the dye moves into the hydrophobic domains of the protein. Then, the fluorophore is better shielded from the water molecules which are known to quench fluorescence, and on the other hand the dye is rigidized upon non-covalent interaction with the protein. As a result, fluorescence intensity is enhanced.

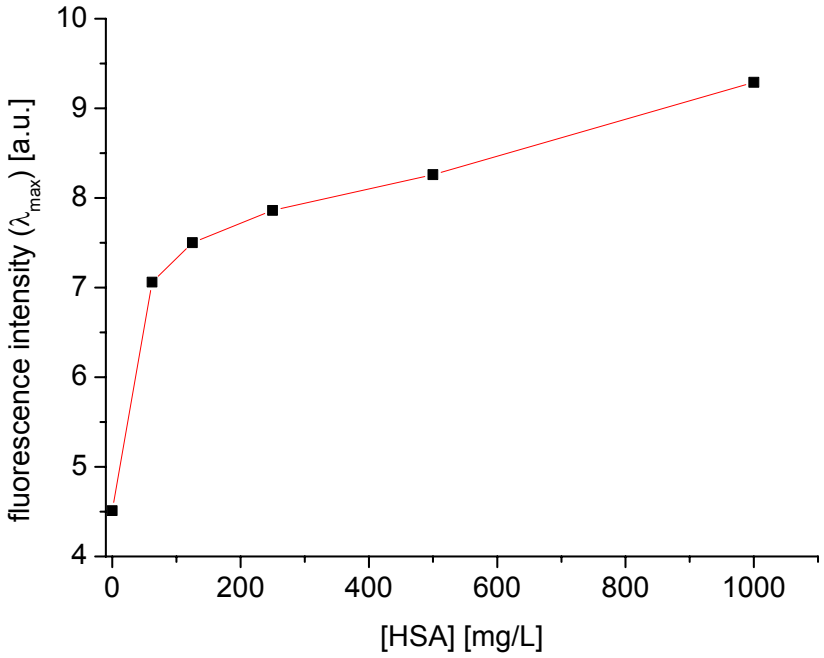

Figure 2.4. Plot of the fluorescence intensities of FO546 at the emission maximum versus the concentration of the added HSA. [FO546] = $6.3 \cdot 10^{-7}$ mol/L. λ_{exc} = 500 nm.

The absorption maximum shifts bathochromically to 553 nm and the emission maximum shifts to 564 nm upon covalent linkage to HSA. The quantum yield of the free dye in PBS is 0.04 and rises to 0.08 when the dye is labeled to HSA with a DPR of 1.7. The absorption maximum shifts to 548 nm, and the emission maximum to 570 nm when the dye is covalently bound to anti-HSA. The quantum yield is 0.09 if FO546 is covalently bound to anti-HSA with DPR = 6.0.

The highest quantum yield measured (0.31) is reached by attaching FO546 covalently to an amino modified 15-mer oligonucleotide of sequence amino-5'-CCG GCA GCA AAA TGT-3'. The labeling conditions are similar to those when labeling HSA (see Exptl. Part, chapter 4.3.3.). The absorption maximum of the FO546/oligonucleotide conjugate is at 550 nm, the emission maximum at 565 nm. The emission spectra of FO546 in its free form and some of its conjugates are shown in figure 2.5. Finally FO546 was covalently linked to the amino groups of the amino acids valin and aspartic acid. Not unexpectedly this did not lead to any changes in absorption and emission spectra.

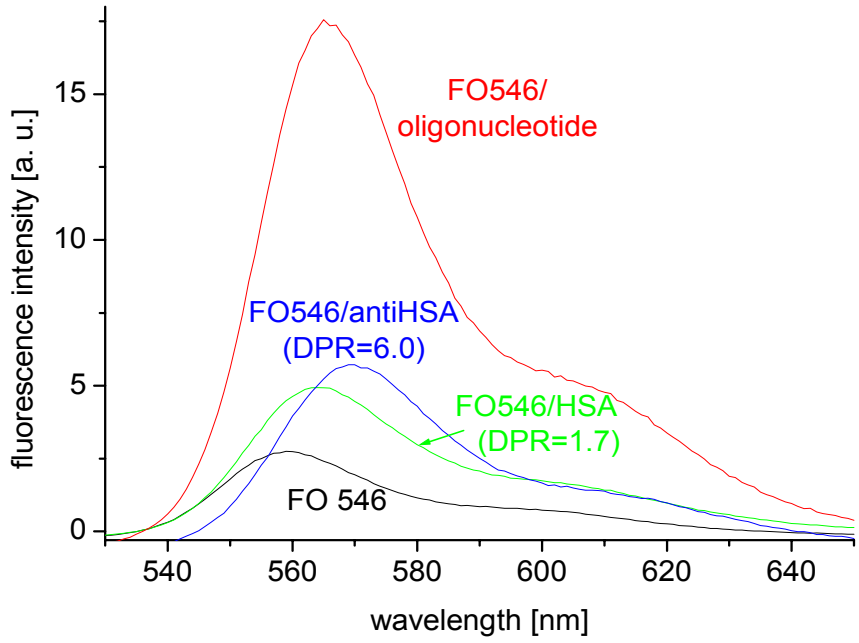

Figure 2.5. Fluorescence spectra of FO546, FO546/HSA (DPR = 1.7), FO546/anti-HSA (DPR = 6.0), and FO546/oligonucleotide. λ_{exc} = 500 nm.

Stability

The stability of the FO546-OSI ester is very high. The reactive dye was dissolved in a methanol/water mixture and allowed to stand for 24 h at room temperature to prove the

stability of the OSI ester. Only 3% of the reactive dye were hydrolyzed within this time. In solid form the OSI ester seems to be stable at least for several months.

2.1.4. FO548

FO548 is an analogon to FO545 containing a sulfonic acid group attached to the benzene ring of the indole. This sulfo group is supposed to enhance the water solubility and to reduce non-covalent binding of the fluorophore to protein.

Synthesis

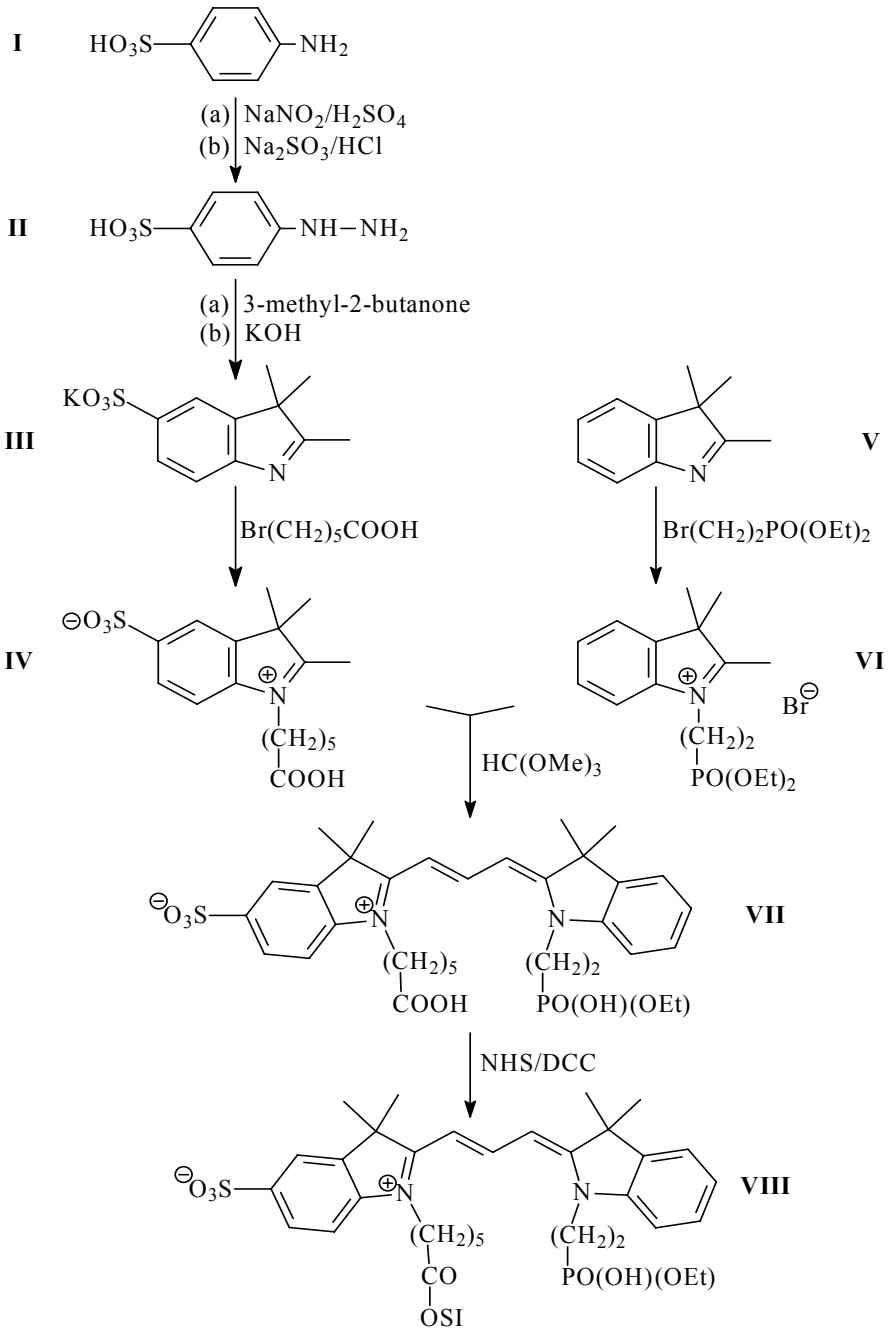

Figure 2.6. Synthesis of FO548 (VIII).

FO548 is synthesized in a six step reaction (see fig. 2.6) starting from 4-aminobenzene sulfonic acid (**I**) which is converted to the corresponding hydrazine derivative (**II**) via the diazo compound as an intermediate [4]. The 4-hydrazinobenzene sulfonic acid reacts to the corresponding indole (**III**) by a standard Fischer indole synthesis. The sulfonic acid group is then transformed into the potassium salt which is easier to purify. The next step is the alkylation of the indole with 6-bromohexanoic acid to introduce a carboxy acid as the reactive center (**IV**) [5]. 2,3,3-Trimethyl-3*H*-indole (**V**) is quaternized with diethyl(2-bromoethyl)phosphonate to obtain the indole containing the phosphonic acid group (**VI**) [1]. Equimolar amounts of the indoles **IV** and **VI** are reacted with excess 1,1,1-trimethoxymethane in pyridine to give FO548-acid (**VII**) [2] which is purified by column chromatography and then activated with NHS and DCC in dry DMSO to give the label **VIII** [3].

Spectral Properties of FO548 and its Conjugates

FO548 has an absorption maximum at 548 nm and an emission maximum at 562 nm in PBS. The quantum yield of the free dye in PBS is 0.05. The following molar absorbances were determined: $\varepsilon_{548\ nm}$ (PBS) = 155,000 L/(mol · cm), $\varepsilon_{280\ nm}$ (PBS) = 21,000 L/(mol · cm), and $\varepsilon_{260\ nm}$ (PBS) = 20,000 L/(mol · cm).

A solution of non-reactive FO548-acid ([FO548] = $1.4 \cdot 10^{-6}$ mol/L) was titrated with various amounts of HSA (0-1000 mg/L) in order to find out if non-covalently conjugated HSA affects the fluorescence of FO548. Addition of HSA affected neither the fluorescence intensity nor the position of the fluorescence maximum. This effect can be attributed to the sulfo group in the molecule. At neutral pH FO548 carries three negative charges, one at the sulfo group, a second one at the phosphonic acid group, and a third one at the carboxy acid group. This results in an electronic repulsion of the anionic dye and the protein which also carries several negative charges at neutral pH. Therefore the influence of the protein on the fluorescence intensity of FR548 is not only reduced but even eliminated.

Covalent linkage to HSA does affect fluorescence intensities as well as the quantum yields and the positions of the absorption and emission maxima. The absorption maximum of the dye shifts to 556 nm, the emission maximum to 571 nm upon labeling to HSA (see fig. 2.7). At low DPRs the quantum yields are high. At a DPR of 0.4 the quantum yield is 0.41 and it decreases to 0.11 at a DPR of 7.2.

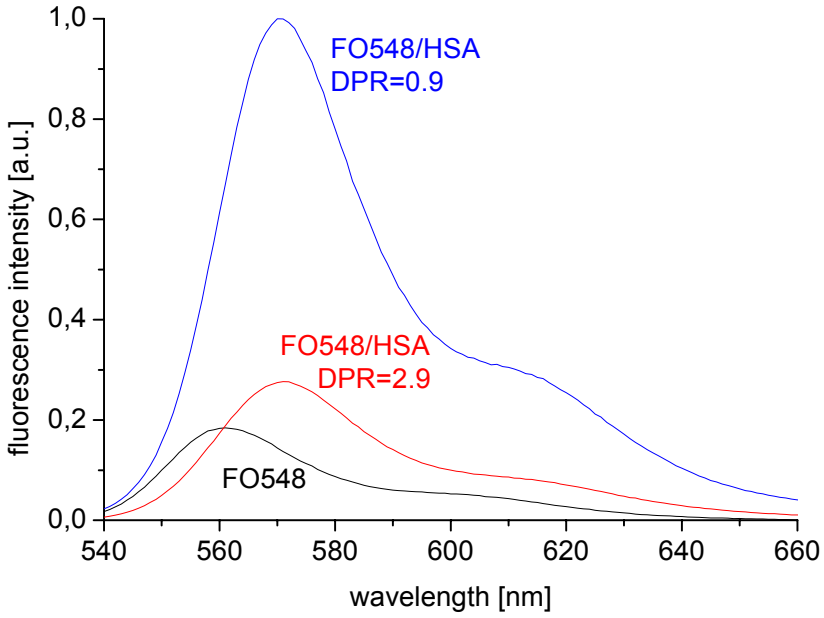

Figure 2.8. Fluorescence spectra of FO548 and FO548/HSA (DPR = 0.9 and 2.9). λ_{exc} = 520 nm.

FO548 was also covalently attached to a 15-mer oligonucleotide of sequence amino-5'-CCG GCA GCA AAA TGT-3'. The absorption maximum of the FO548/oligonucleotide conjugate is at 545 nm, the emission maximum at 569 nm. The quantum yield of the dye rises to 0.28 upon binding to the oligonucleotide.

2.1.5. FR642

FR642 is an unsymmetrical pentamethine dye. It has a very similar structure to FO545 but the polymethine chain is prolonged by a vinyl group.

Synthesis

The unsymmetrical monoreactive label FR642 can be synthesized via a four step reaction (fig. 2.8). The first step is to quaternize 2,3,3-trimethyl-3*H*-indole (**I**) on the one hand with diethyl(2-bromoethyl)phosphonate, and on the other hand with 6-bromohexanoic acid to achieve the quatenized indoles **II** and **III**, respectively. Equimolar amounts of **II** and **III** are reacted with excess 1,1,3,3-tetramethoxypropane in pyridine [2] to give FR642-acid (**IV**) which is separated from its byproducts (i.e. symmetrical dyes) by column chromatography. The reactive dye (**V**) is obtained by reacting the acid (**IV**) with NHS and DCC in dry DMSO [3].

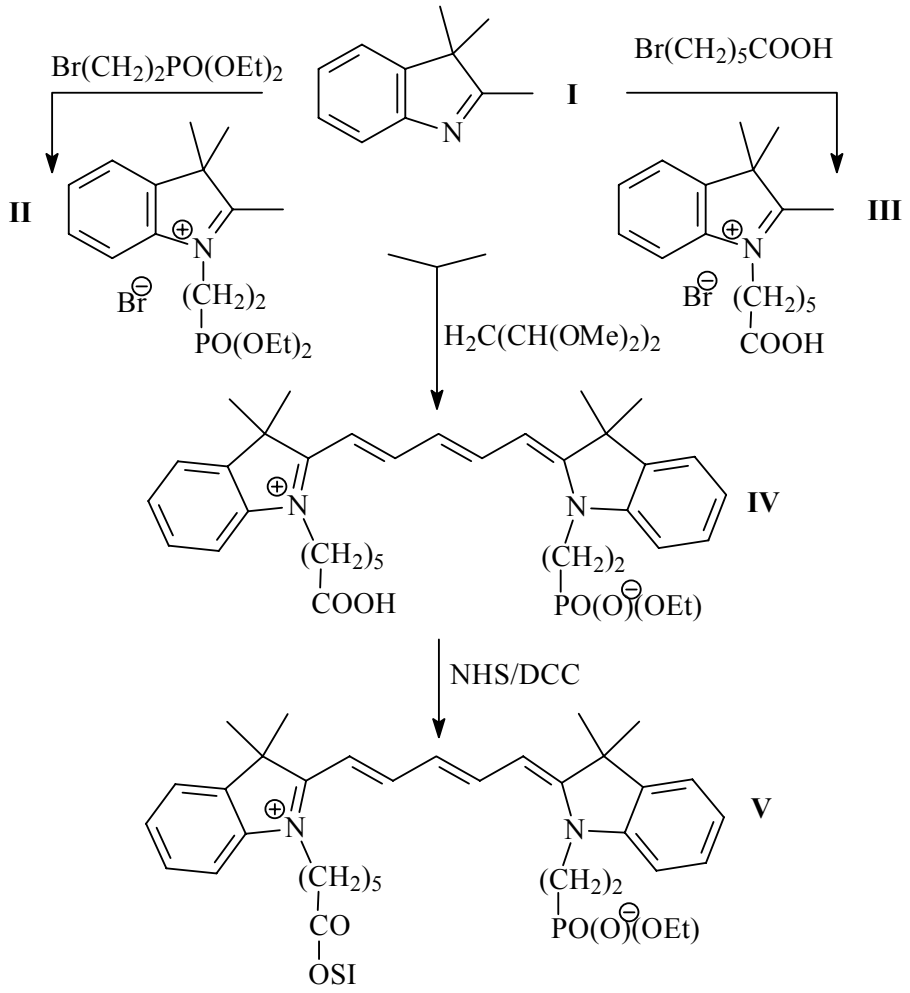

Figure 2.8. Synthesis of FR642 (V).

Spectral Properties of FR642 and its Conjugates

FR642 has an absorption maximum at 642 nm and an emission maximum at 660 nm in PBS. The quantum yield of the free dye in PBS is 0.17. The following molar absorbances were determined: $\varepsilon_{642\ nm}$ (PBS) = 170,000 L/(mol·cm), $\varepsilon_{280\ nm}$ (PBS) = 7,000 L/(mol·cm), and $\varepsilon_{260\ nm}$ (PBS) = 8,000 L/(mol·cm).

A solution of the non-reactive FR642-acid ([FR642] = $3.6 \cdot 10^{-7}$ mol/L) was titrated with various amounts of HSA (0-1000 mg/L) in order to find out whether non-covalently conjugated HSA affects the fluorescence of FR642. Addition of 1000 mg/L HSA raised the fluorescence intensity about three-fold (fig. 2.9). The position of the fluorescence maximum is shifted by 7 nm to longer wavelengths. The enhancement of the fluorescence intensity allows the speculation that FR642 may interact with HSA and move into the hydrophobic domains of the protein. There it is rigidized and shielded from the solvent molecules which might be the reason for the enhancement of the fluorescence intensity.

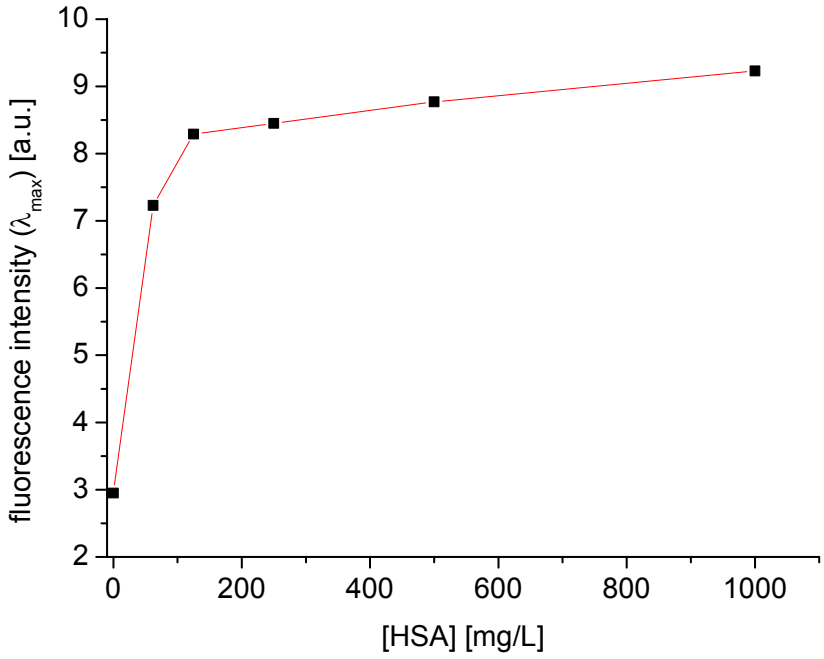

Figure 2.9. Plot of the fluorescence intensities of FR642 (free dye) at the emission maximum versus the concentration of the added HSA. [FR642] = $3.6 \cdot 10^{-7}$ mol/L. λ_{exc} = 620 nm.

The absorption maximum shifts bathochromically to 648 nm and the emission maximum shifts to 666 nm upon covalent linkage to HSA. FR642/HSA conjugates with various DPR (0.6 - 5.4) were prepared to show the influence of the DPR on the fluorescence intensity. Two different types of measurements were performed either with constant dye concentration or with constant protein concentration. Fluorescence intensities of solutions with a constant dye concentration ([FR642] = $5.9 \cdot 10^{-7}$ mol/L) were measured. Figure 2.10 shows the plot of the fluorescence intensities at the emission maximum versus the DPR. It is clearly visible that fluorescence intensity decreases rapidly with increasing DPR.

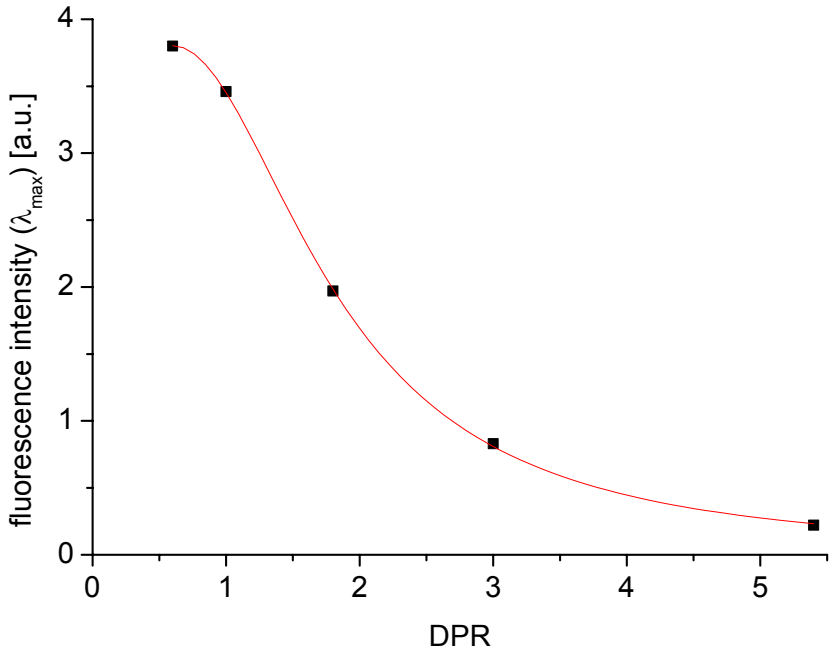

Figure 2.10. Plot of the fluorescence intensities of FR642/HSA conjugates at the emission maximum versus the DPR. [FR642] = $5.9 \cdot 10^{-7}$ mol/L.

If the same measurement is carried out at a constant protein concentration ([HSA] = $1.7 \cdot 10^{-6}$ mol/L), the plot (fig. 2.11) looks totally different compared to that with constant dye concentration (fig. 2.10). It can be seen that at a DPR of about 1 the maximal intensity is reached. This demonstrates that binding of more than one dye molecule to one protein molecule leads to self-quenching.

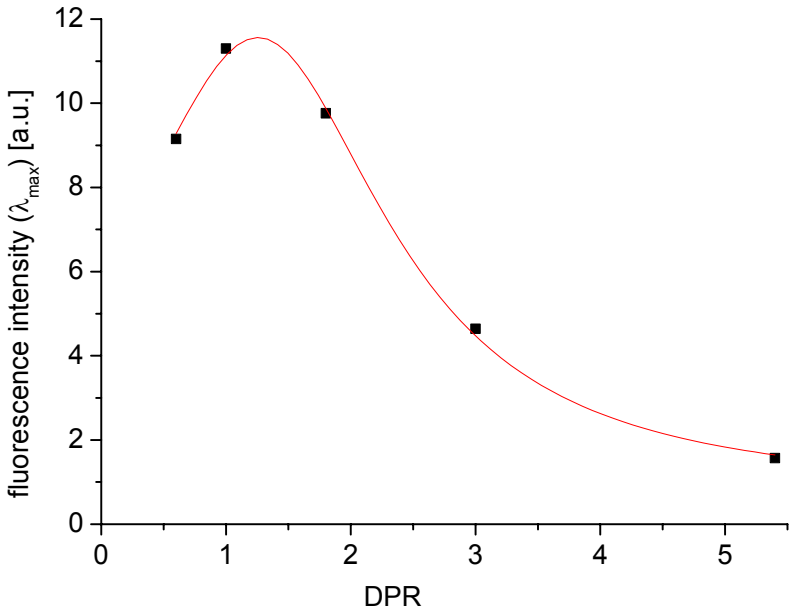

Figure 2.11. Plot of the fluorescence intensities of FR642/HSA conjugates at the emission maximum versus the DPR. [HSA] = $1.7 \cdot 10^{-6}$ mol/L.

The absorption maximum shifts to 646 nm and the emission maximum to 665 nm if FR642 is labeled to anti-HSA. The quantum yield is 0.32 at a DPR of 0.7, 0.30 at a DPR of 1.3, and 0.17 at a DPR of 5.9.

FR642 was also covalently attached to a 15-mer oligonucleotide. The quantum yield of FR642 rises to 0.22 upon covalent binding to the oligonucleotide. In this case the absorption maximum shifts to 647 nm, the emission maximum to 666 nm. Finally FR642 was covalently linked to the amino groups of the amino acids valin and aspartic acid. Not unexpectedly this did not lead to any changes in absorption and emission spectra.

2.1.6. FR646

FR646 is an analogon to FR642 containing a sulfonic acid group attached to the benzene ring of the indole [6]. This sulfo group is supposed to enhance the water solubility and to reduce non-covalent binding of the fluorophore to the protein.

Synthesis

The unsymetrical monoreactive label FR646 is synthesized in analogy to FR642 using 1-(5-carboxypentyl)-2,3,3-trimethyl-3*H*-5-indoliumsulfonate instead of 1-(5-carboxypentyl)-2,3,3-trimethyl-3*H*-indolium bromide.

Spectral Properties of FR646 and its Conjugates

FR646 has an absorption maximum at 645 nm and an emission maximum at 664 nm in PBS. The quantum yield of the free dye in PBS is 0.20. The following molar absorbances were determined: $\varepsilon_{646\ nm}$ (PBS) = 220,000 L/(mol·cm), $\varepsilon_{280\ nm}$ (PBS) = 20,000 L/(mol·cm), and $\varepsilon_{260\ nm}$ (PBS) = 24,000 L/(mol·cm).

A solution of non-reactive FR646-acid ([FR646] = $1.7 \cdot 10^{-6}$ mol/L) was titrated with various amounts of HSA (0-1000 mg/L) in order to find out whether non-covalently conjugated HSA affects the fluorescence of FR646. Addition of HSA decreases the value of the fluorescence intensity to 80% (fig. 2.12). The position of the fluorescence maximum is shifted by 9 nm to longer wavelengths. This decrease in the quantum yield is in contrast to the behavior of all other dyes described in this work.

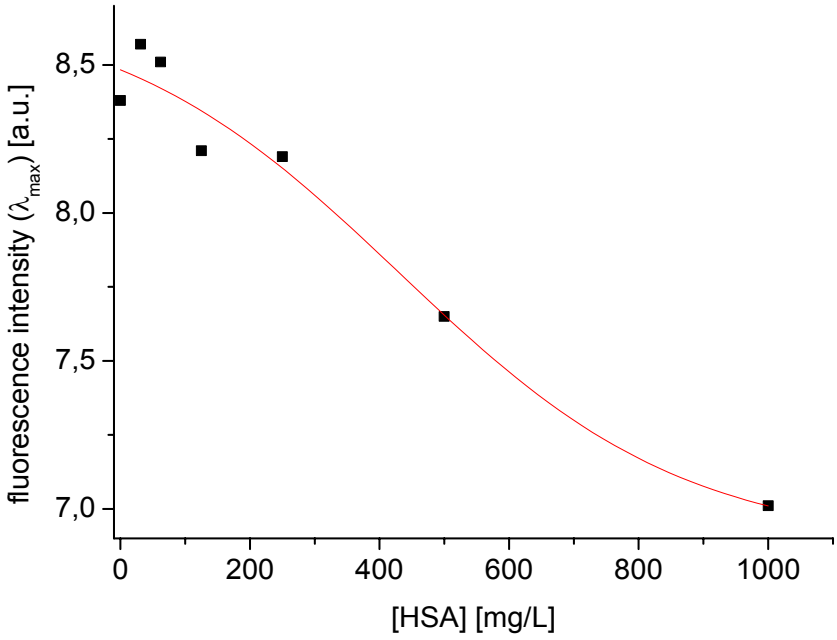

Figure 2.12. Plot of the fluorescence intensities of FR646 (free acid) at the emission maximum versus the concentration of the added HSA. [FR646] = $1.7 \cdot 10^{-6}$ mol/L. λ_{exc} = 600 nm.

The absorption maximum of FR646 shifts bathochromically to 646 nm and the emission maximum shifts to 664 nm upon covalent linkage to anti-HSA. The fluorescence intensities of the anti-HSA conjugates increase at a low DPR. Figure 2.13 shows a 1.9-fold increase of the fluorescence intensity at a DPR of 0.6 and a 1.7-fold increase at a DPR of 1.8. At a higher DPR (7.1) the fluorescence intensity even decreases slightly. The quantum yields decrease from 0.39 at a DPR of 0.6 to 0.20 at a DPR of 7.1.

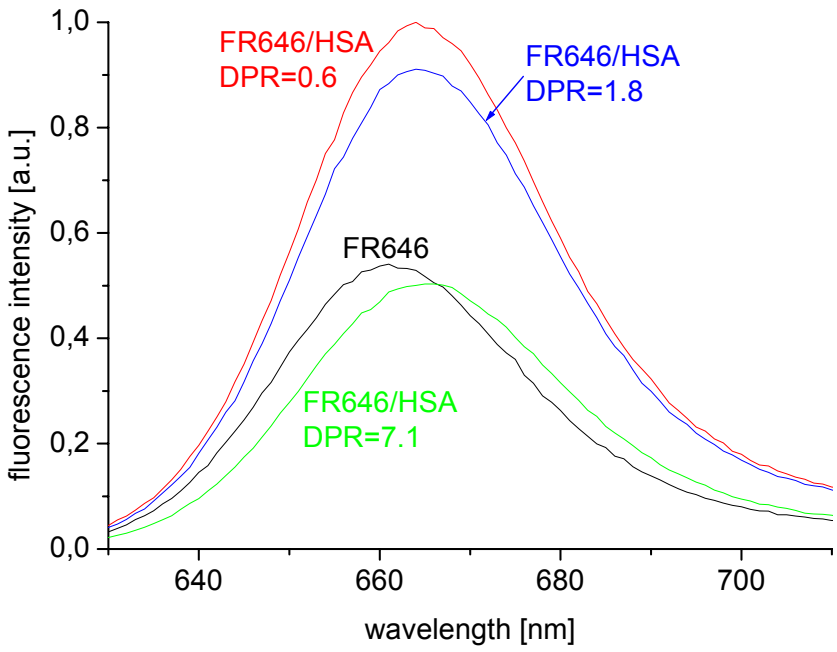

Figure 2.13. Fluorescence spectra of FR646 and FR646/HSA (DPR = 0.6, 1.8, and 7.1). λ_{exc} = 600 nm.

Covalent coupling of FR646 to a 15-mer oligonucleotide shifts both the absorption maximum and the emission maximum 3 nm to longer wavelengths.

2.2. Squaraines

In additon to the cyanine labels described in 2.1, unsymmetrical squaraine labels have been developed. Both amine-reactive OSI esters and saccharide-reactive phosphoramidites have been synthesized. The squaraine labels like the cyanine labels contain only one reactive group to avoid crosslinking. The OSI esters (FR626, FR661, FR662, and FR670) are well soluble in aqueous solution and the PAM dyes (OB630 and OG670) are well soluble in chloroform which is important for labeling oligonucleotides in the last step of the automated synthesis process. The dyes FR626, FR661, and OB630 are conventional squarylium dyes, whereas FR662, FR670, and OG670 are derivatives of squaraines in which one oxygen atom of the squaric acid moiety is substituted by a dicyanomethylene group.

2.2.1. FR626

FR626 is an amine-reactive unsymmetrical squarylium dye. It contains a sulfo group to enhance water solubility.

Synthesis[*]

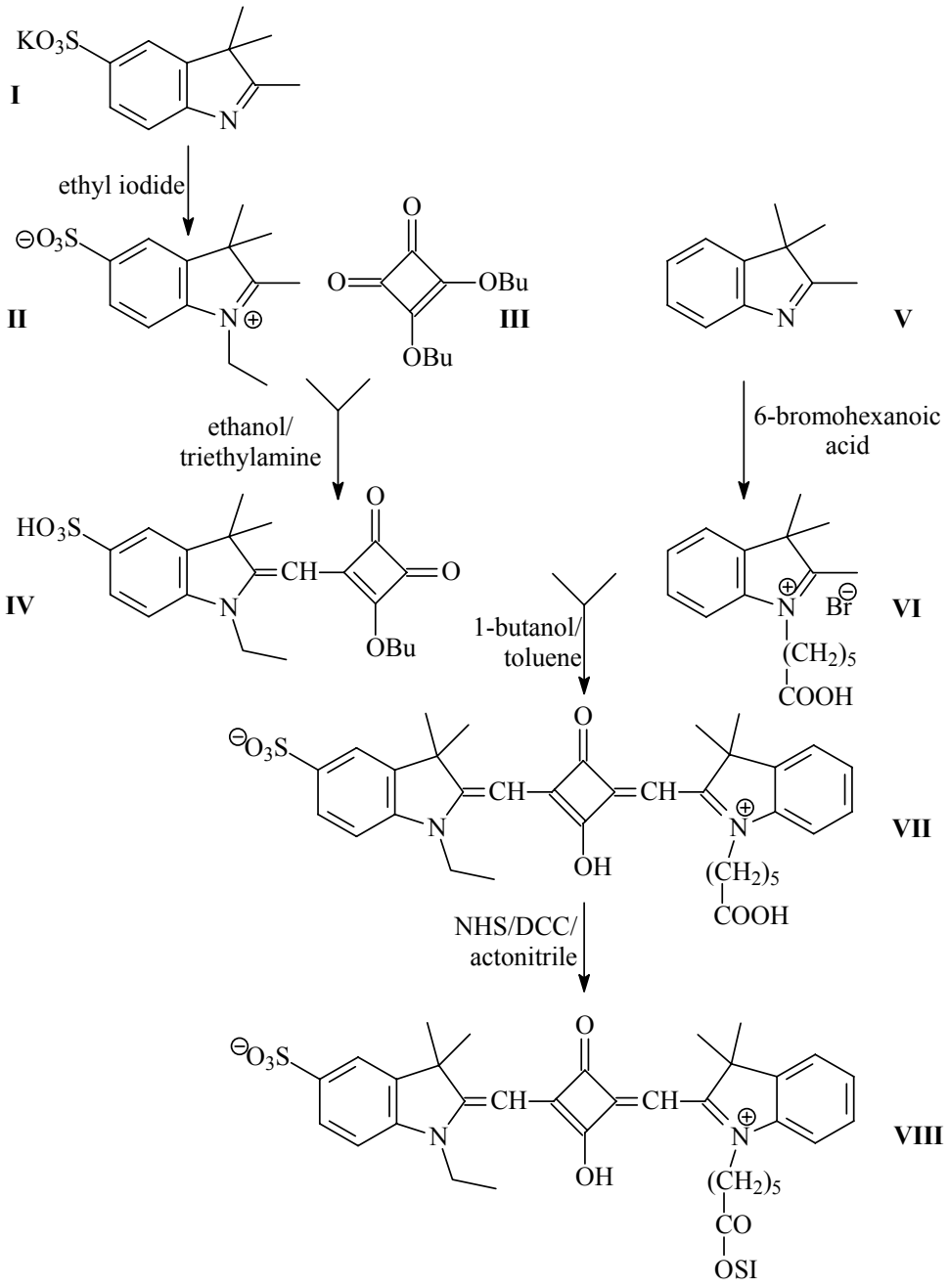

Figure 2.14. Synthesis of FR626 (VIII).

FR626 can be synthesized via a five step reaction [7]. First, potassium 2,3,3-trimethyl-3*H*-5-indolesulfonate (**I**) is quaternized with ethyliodide. The sulfonated indolium derivative (**II**) and 3,4-dibutoxy-3-cyclobutene-1,2-dione (**III**) react in ethanol when catalytic amounts of triethylamine are present. The semi-substituted squaric acid derivative (**IV**) reacts with 1-(5-

[*] FR626 was synthesized by Bianca Wetzl, Institute of Analytical Chemistry, Chemo- and Biosensors, University of Regensburg, Germany.

carboxypentyl)-2,3,3-trimethyl-3*H*-indolium bromide (**VI**) which was synthesized by quaternation of 2,3,3-trimethyl-3*H*-indole (**V**) with 6-bromohexanoic acid to give FR626-acid (**VII**) which is purified by column chromatography. The OSI ester of the dye (**VIII**) is synthesized by activating the acid (**VII**) with NHS and DCC in acetonitrile.

Spectral Properties of FR626 and its Conjugates

FR626 has an absorption maximum at 626 nm and an emission maximum at 637 nm in PBS. The molar absorbance at the absorption maximum is 113,000 L/(mol·cm) and 15,000 L/(mol·cm) at 280 nm. The quantum yield of the free dye in PBS is 0.02 and rises to 0.17 if the dye is covalently attached to HSA at a DPR of 2.0.

2.2.2. FR661

FR661 is an unsymmetrical squaraine label which can be attached to amino groups. It contains an indolium and a quinolinium heterocycle. The presence of a lepidine (4-methylquinoline) moiety causes a bathochromic shift of the absorption maximum of about 35 nm compared to a squaraine containing two indolium heterocycles.

Synthesis

FR661 can be synthesized in a five step reaction. Lepidine (**I**) is quaternized with 6-bromohexanoic acid in 1,2-dichlorobenzene. The quaternized lepidine (**II**) and 3,4-dibutoxy-3-cyclobutene-1,2-dione react in ethanol containing catalytic amounts of triethylamine [in analogy to 8, 9, 10] to the semi-substituted squaric acid derivative (**III**). This reacts with 1-[2-(diethoxyphosphoryl)ethyl]-2,3,3-trimethyl-3*H*-indolium bromide (**V**) which was synthesized by quaternization of 2,3,3-trimethyl-3*H*-indole (**IV**) with diethyl(2-bromoethyl)phosphonate [1] to give FR661-acid (**VI**) which is purified by column chromatography. The OSI ester of the dye (**VII**) is synthesized by activating the acid (**VI**) with NHS and DCC in an acetonitrile/DMF mixture.

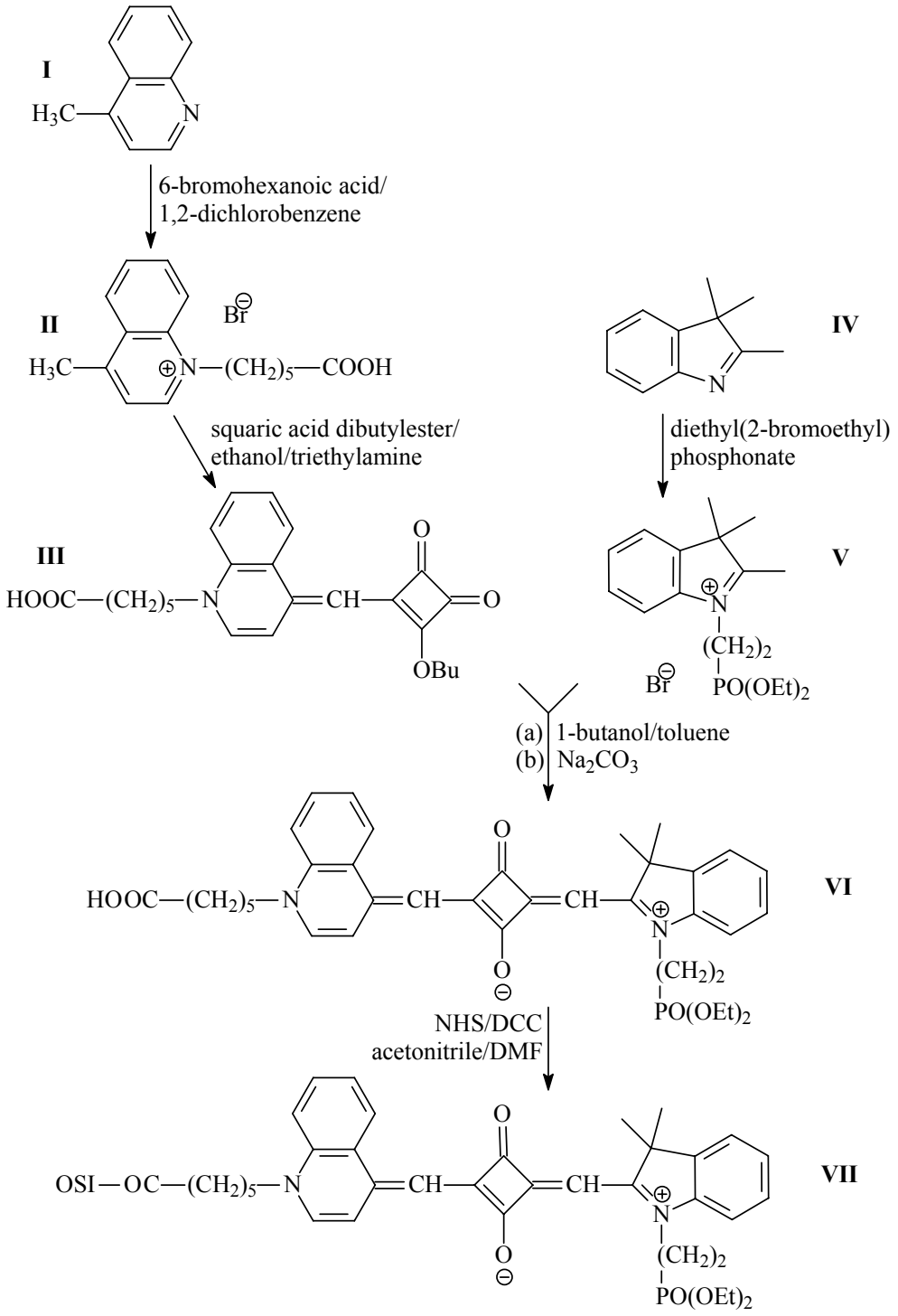

Figure 2.15. Synthesis of FR661 (VII).

Spectral Properties of FR661 and its Conjugates

FR661 has an absorption maximum at 661 nm and an emission maximum at 725 nm in PBS. The Stokes' shift of 64 nm is remarkably large compared to those of the other squaraine and cyanine dyes presented in this work. Those dyes have Stokes' shifts of only 10-20 nm. It is known that dyes containing quinoline entities display comparably larger Stokes' shifts. The

molar absorbance of FR661 at the absorption maximum is 120,000 L/(mol·cm) and 20,000 L/(mol·cm) at 280 nm.

The fluorescence of the free dye is very weak but rises upon addition of HSA. Figure 2.16 shows the enhancement of the fluorescence intensity of FR661 upon addition of increasing amounts (0-4000 mg/L) of HSA. Addition of 4000 mg/L HSA to the dye solution causes a 13-fold increase compared to the fluorescence intensity of FR661 in PBS.

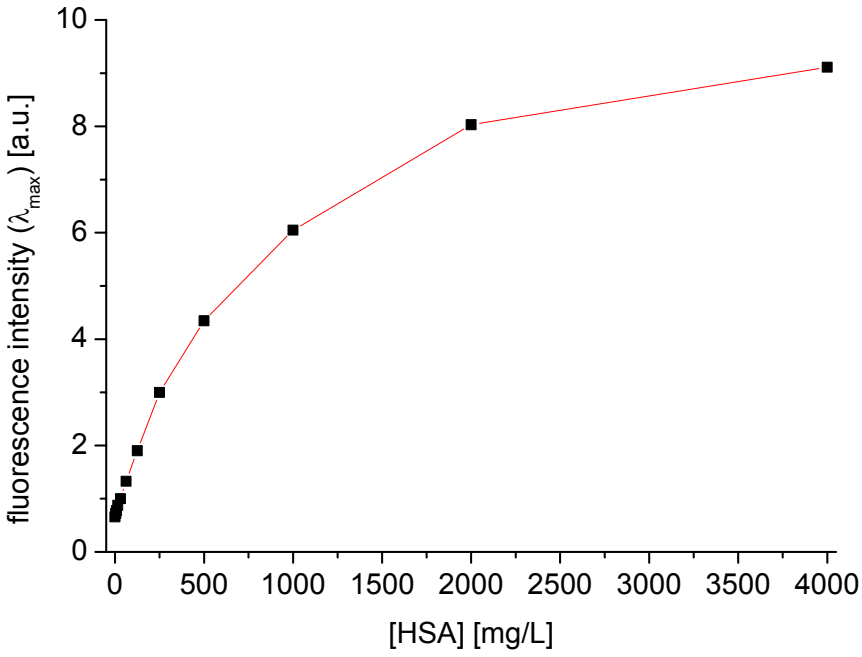

Figure 2.16. Plot of the fluorescence intensities of FR661 (free dye) at the emission maximum versus the concentration of the added HSA. λ_{exc}=660 nm.

The fluorescence of FR661 is quenched almost completely (see figure 2.17) upon covalent attachment to HSA at a DPR of 1.9 Therefore, the dye is not suitable for labeling HSA and for the use in FRET studies.

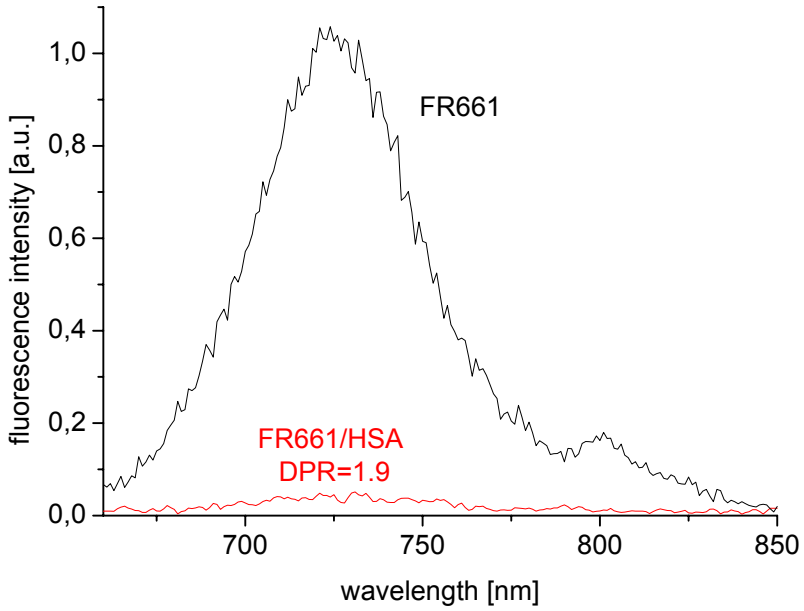

Figure 2.17. Fluorescence spectra of FR661 and FR661/HSA (DPR=1.9). λ_{exc}=650 nm.

Covalent attachment to aminoallyl-dUTP shifts the absorption maximum to 675 nm, the emission maximum to 729 nm. Figure 2.18 shows the excitation and emission spectra of FR661 and FR661/dUTP. The fluorescence intensity of FR661 increases more than three-fold upon labeling to dUTP but the quantum yields are still very low.

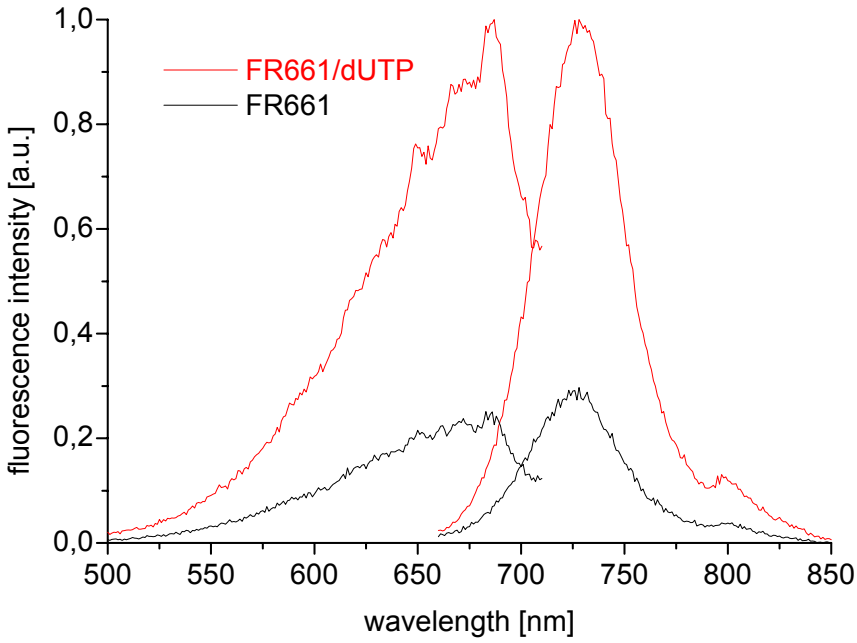

Figure 2.18. Excitation and emission spectra of FR661 and FR661/dUTP. λ_{exc}=650 nm.

2.2.3. FR662

FR662 is a squarylium dye derivative in which one oxygen atom at the squaric acid moiety is substituted by a dicyanomethylene group [6, 11]. The dicyanomethylene group causes a bathochromic shift of the absorption maximum of about 35 nm. The label is amine-reactive and contains both a sulfo group and a phosphonic acid group which enhance the solubility of the fluorophore in aqueous media.

Synthesis

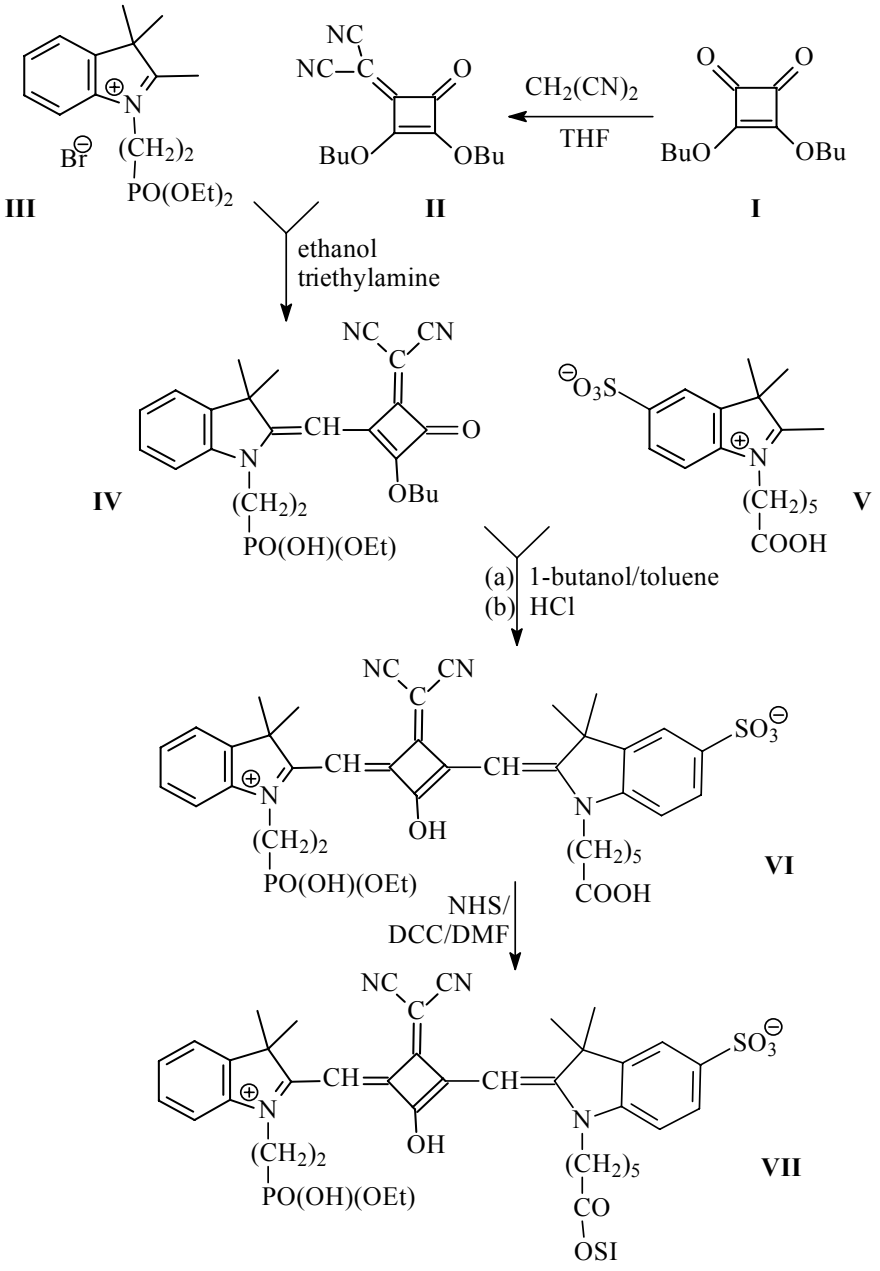

Figure 2.19. Synthesis of FR662 (VII).

Figure 2.19 shows the synthesis of FR662. First, one oxygen of squaric acid dibutylester (**I**) is subsituted by the reaction with malonodinitrile in THF. 2-(2,3-dibutoxy-4-oxo-2-cyclobutenyliden)malonodinitrile (**II**) and the quaternized indole (**III**) react in ethanol containing catalytic amounts of triethylamine to the semi-substituted squaric acid derivative (**IV**). This reacts with the indole (**V**) to give FR662-butyl ester. The butyl ester is cleaved with HCl and the free acid (**VI**) is obtained. Activation to the reactive label (**VII**) is carried out in DMF using NHS and DCC.

Spectral Properties of FR662 and its Conjugates

FR662 has an absorption maximum at 662 nm and an emission maximum at 682 nm in PBS. The following molar absorbances were determined: $\varepsilon_{662\ nm}$ (PBS) = 130,000 L/(mol · cm), $\varepsilon_{280\ nm}$ (PBS) = 8,000 L/(mol · cm), and $\varepsilon_{260\ nm}$ (PBS) = 7,000 L/(mol · cm). The quantum yield of the free dye in PBS is 0.02.

A solution of non-reactive FR662-acid ([FR642] = $6.8 \cdot 10^{-7}$ mol/L) was titrated with various amounts of HSA (0-1000 mg/L) in order to find out whether non-covalently conjugated HSA affects the fluorescence of FR662. Addition of 1000 mg/L HSA raised the fluorescence intensity about 8-fold (fig. 2.20). The position of the fluorescence maximum is shifted to 696 nm. Since FR662 contains both a sulfo group and a phosphonic acid group the dye carries several negative charges at neutral pH and is expected to be repulsed from the negatively charged protein. The dependence of the fluorescence intensity of the dye on the concentration of added HSA is surprisingly high, thus demonstrating that the dye interacts with HSA although both are negatively charged.

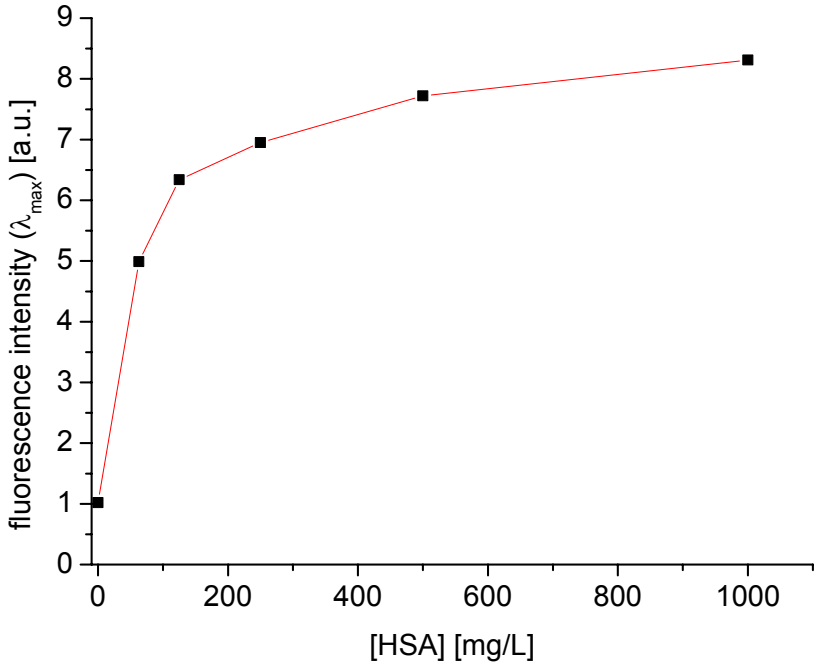

Figure 2.20. Plot of the fluorescence intensities of FR662 (free dye) at the emission maximum versus the concentration of added HSA. [FR662] = $6.8 \cdot 10^{-7}$ mol/L. λ_{exc} = 640 nm.

2.2.4. FR670

FR670 is a monoreactive amino label. The structure of the chromophore is the same like that of FR662. FR670 contains one sulfo group to enhance water solubility.

Synthesis

FR670 can be synthesized in analogy to FR662 [6, 11]. The quaternized indole 1-ethyl-2,3,3-trimethyl-*3H*-5-indoliumsulfonate is reacted with 2-(2,3-dibutoxy-4-oxo-2-cyclobutenyliden) malonodinitrile in ethanol containing catalytic amounts of triethylamine to give the semi-substituted squaric acid derivative which is used without further purification. It reacts with 1-(3-ethoxycarbonyl-propyl)-2,3,3-trimethyl-3*H*-indolium bromide to give FR670-butyl ester which is cleaved with NaOH. The free acid is activated in acetonitrile using NHS and DCC.

Spectral Properties of FR670 and its Conjugates

FR670 has an absorption maximum at 658 nm and an emission maximum at 676 nm in PBS. The quantum yield of the free dye in PBS is 0.03. The following molar absorbances were

determined: $\varepsilon_{658\ nm}$ (PBS) = 145,000 L/(mol·cm), $\varepsilon_{280\ nm}$ (PBS) = 15,000 L/(mol·cm), $\varepsilon_{260\ nm}$ (PBS) = 14,000 L/(mol·cm).

A solution of non-reactive FR670-acid ([FR670] = $3.8 \cdot 10^{-7}$ mol/L) was titrated with various amounts of HSA (0-1000 mg/L) in order to find out if non-covalently conjugated HSA affects the fluorescence of FR670. Addition of 1000 mg/L HSA raised the value of the fluorescence intensity 5.6-fold (fig. 2.21.). The position of the fluorescence maximum is shifted to 700 nm.

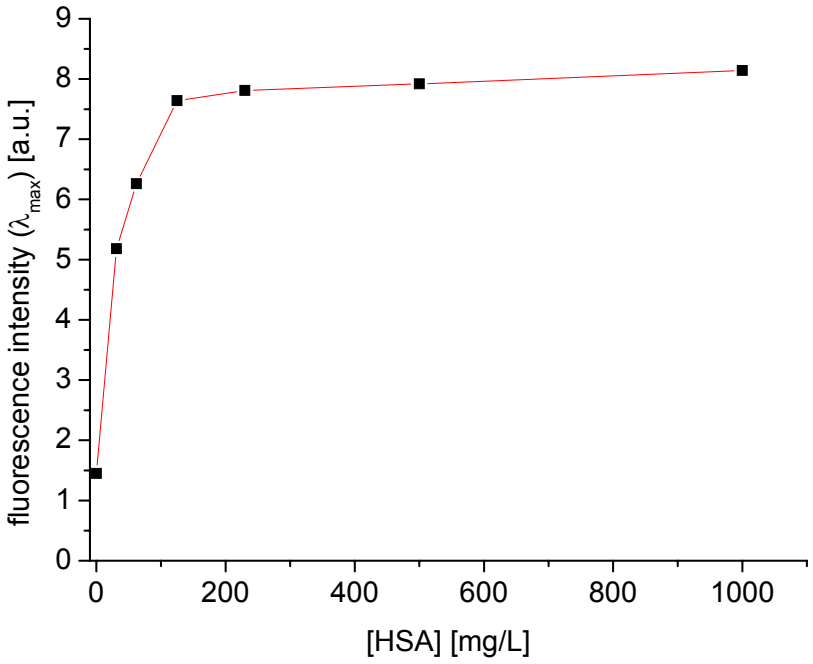

Figure 2.21. Plot of the fluorescence intensities of FR670 (free dye) at the emission maximum versus the concentration of added HSA. [FR670]= $3.8 \cdot 10^{-7}$ mol/L. λ_{exc}=640 nm.

The quantum yield of FR670/HSA is 0.08 at a DPR of 1.2 and decreases to 0.02 at a DPR of 2.7. The dye undergoes self-quenching at high DPRs. At a DPR of 5 fluorescence is not detectable any more.

2.2.5. OB630

OB630 is a saccharide-reactive label. Such labels contain a phosphoramidite (PAM) group that binds to the 5'-hydroxy group of the desoxyribose of oligonucleotides. The squaraine is well soluble in chloroform which is important in the automated synthesis of labeled oligonucleotides.

Synthesis

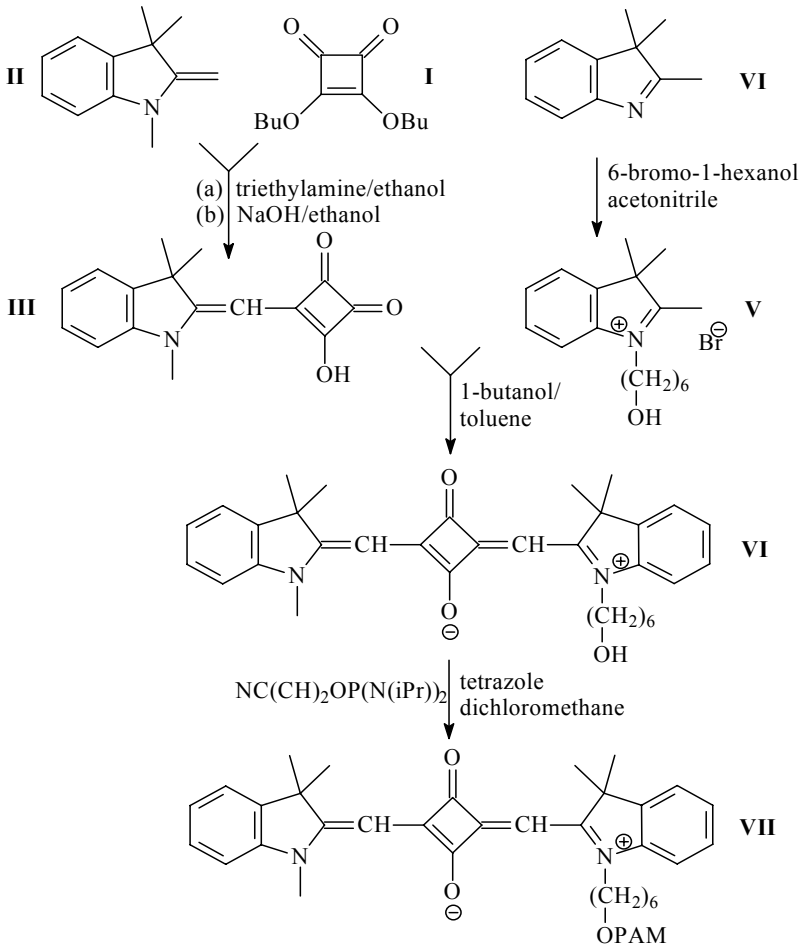

Figure 2.22. Synthesis of OB630 (VII).

OB630 can be synthesized via a four step reaction (fig. 2.22). First, 2-methylene-1,3,3-trimethylindoline (**II**) and 3,4-dibutoxy-3-cyclobutene-1,2-dione (**I**) react in ethanol in presence of catalytic amounts of triethylamine [in analogy to 8, 9, 10] to give the butyl ester of the semi-substituted squaric acid derivative. The butyl ester is cleaved with NaOH in ethanol. The semi-substituted squaric acid derivative (**III**) reacts with 1-(6-hydroxyhexyl)-2,3,3-trimethyl-3*H*-indolium bromide (**V**) which was synthesized by quaternation of 2,3,3-trimethyl-3*H*-indole (**IV**) with 6-bromo-1-hexanol to give OB630-OH (**VI**) which is purified by column chromatography. Activation of the dye to the reactive phosphoramidite is carried out with 2-cyanoethyl-N,N,N',N',-tetraisopropyl-phosphordiamidite in dichloromethane with catalytic amounts of tetrazole [12].

Spectral Properties of OB630 and its Oligonucleotide Conjugates

OB630 has an absorption maximum at 628 nm and an emission maximum at 637 nm in methanol. The following molar absorbances were determined: $\varepsilon_{628\ nm}$ (MeOH) = 200,000

L/(mol·cm), $\varepsilon_{280\ nm}$ (MeOH) = 10,000 L/(mol·cm), $\varepsilon_{260\ nm}$ (MeOH) = 8,000 L/(mol·cm). The quantum yield of the free dye in methanol is 0.07 and rises to 0.25 if OB630 is labeled to a 15-mer oligonucleotide. The absorption and emission maxima shift to 632 nm and 643 nm, respectively, in this case.

2.2.6. OG670

OB670 is another saccharide-reactive label. It has a chemical structure very similar to OB630 with one oxygen atom at the squaric acid moiety substituted by a dicyanomethylene group. The dicyanometylene group causes a bathochromic shift of the absorption maximum of 40 nm.

Synthesis

The synthesis of OG670 is carried out in complete analogy to the synthesis of OB630 using 2-(2,3-dibutoxy-4-oxo-2-cyclobutenyliden)malonodinitrile instead of 3,4-dibutoxy-3-cyclobutene-1,2-dione.

Spectral Properties of OB670 and its Oligonucleotide Conjugates

OB670 has an absorption maximum at 668 nm and an emission maximum at 687 nm in methanol. The following molar absorbances were determined: $\varepsilon_{668\ nm}$ (MeOH) = 180,000 L/(mol·cm), $\varepsilon_{280\ nm}$ (MeOH) = 13,000 L/(mol·cm), $\varepsilon_{260\ nm}$ (MeOH) = 12,000 L/(mol·cm). The quantum yield of the free dye in methanol is 0.09 and rises to 0.13 if OB630 is labeled to a 15-mer oligonucleotide. The absorption and emission maxima shift to 667 nm and 681 nm, respectively, in this case.

2.3. Non-covalent Protein Staining

In previous sections it has been shown several times that some of the new dyes reported here undergo a strong increase in fluorescence intensity if contacted with HSA. This effect may be used to detect and visualize the presence of proteins via fluorescence, e.g. in electrophoretic protein separation or in proteomics in general. The following table 2.1 gives the dyes and the maximal enhancement effect on addition of HSA. It can be seen that the dyes FR661 and FR662 are most suitable in that respect. It should be noted, however, that this finding cannot be generalized, because many more proteins need to be studied first.

In addition dissociation constants K_D^* are listed in table 2.1. K_D^* is the concentration of HSA needed to bind half of the free dye. The value n gives the number of dye molecules bound per HSA.

Table 2.1. Changes in Fluorescence Intensity of Free Dyes on Addition of Excess of Human Serum Albumin ([HSA] = 1000 mg/L), the Respective Dissociation Constants K_D^*, and the Number of Dye Molecules *n* Bound per HSA.

Dye (carboxy form)	Concentration of the Dye [mol/L]	Change in Fluorescence Intensity	K_D^* [mol/L]	n
FO546	$6.3 \cdot 10^{-7}$	2-fold enhancement	$5.3 \cdot 10^{-7}$	1.2
FO548	$1.4 \cdot 10^{-6}$	no change	--	--
FR642	$3.6 \cdot 10^{-7}$	3.1-fold enhancement	$6.1 \cdot 10^{-7}$	0.6
FR646	$1.7 \cdot 10^{-6}$	20% decrease	--	--
FR661	n.d.	8.4-fold enhancement	$6.1 \cdot 10^{-6}$	n.d.
FR662	$6.8 \cdot 10^{-7}$	8.1-fold enhancement	$6.8 \cdot 10^{-7}$	1.0
FR670	$3.8 \cdot 10^{-7}$	5.6-fold enhancement	$4.6 \cdot 10^{-7}$	0.8

K_D^* values were determined graphically as described in chapter 4.5.

The fluorescence intensities of the dyes FO546, FR642, FR661, FR662, and FR670 increase upon addition of HSA. The reason is that the dyes interact non-covalently with the protein. The chromophores might be attached onto the surface or in the hydrophobic domains of HSA. Fluorescence intensity increases, because on the one hand the fluorophore is shielded from the water molecules which are known to quench fluorescence, and on the other hand the dye is rigidized upon attachment to the protein and the degree of freedom of rotation and vibration is suppressed. This effect is quite strong in the case of the squaraine dyes where the fluorescence intensity rises up to 8-fold upon addition of 1000 mg/L HSA. The fluorescence of the cyanines FO546 and FR642 rises only 2- and 3-fold, respectively. In contrast, the cyanine dye FO548 is not affected at all, and FR646 shows even a small decrease of the fluorescence intensity upon addition of HSA.

2.4. Conclusions

The cyanines and the squaraines were chosen as a group of reactive labels because of their long-wavelengh absorbance and their relative small molecular size. All dyes contain only one

reactive group which avoids crosslinking. Various cyanine and squaraine labels were synthesized. The absorption maxima of the free dyes are in the range of 545 nm to 668 nm, the emission maxima are between 562 nm and 687 nm. The labels exhibit high molar absorbances between 86,000 L/(mol·cm) and 220,000 L/(mol·cm). Table 2.2 summarizes the structures and spectral properties of the newly synthesized labels.

The fact that all labels are unsymmetrical dyes implies that the purification of the dyes is very sophisticated. A number of by-products are formed which have to be removed by column chromatography. The following digital photography (fig. 2.23) shows a chromatography column separating the raw product of an unsymmetrical dye.

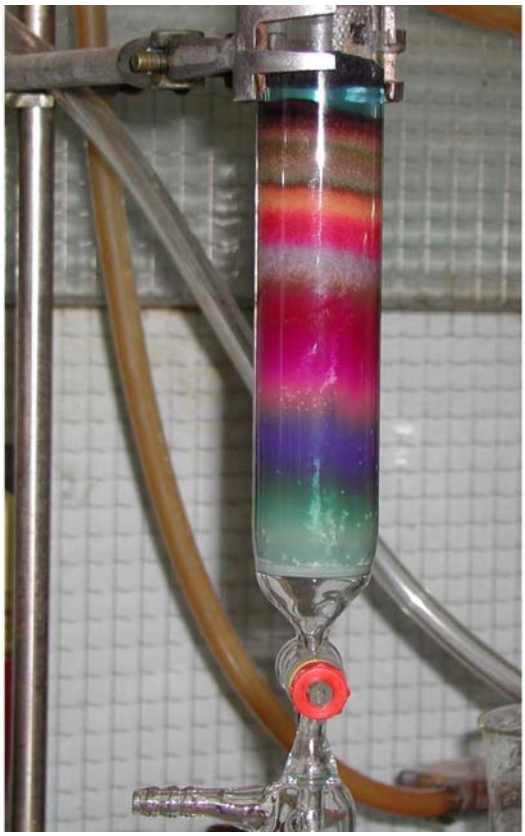

Figure 2.23. Photography of a chromatographic column separating the raw product in the synthesis of an unsymmetrical dye.

Table 2.2. Overview of the structures and spectral properties of the synthesized labels.

Name	Structure	λ_{abs} [nm]	λ_{em} [nm]	ε [L/mol·cm]	ϕ
FO544	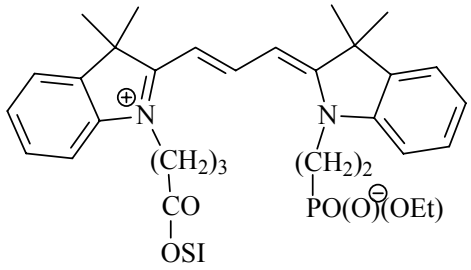	545	562	*n.d.*	*n.d.*
FO545	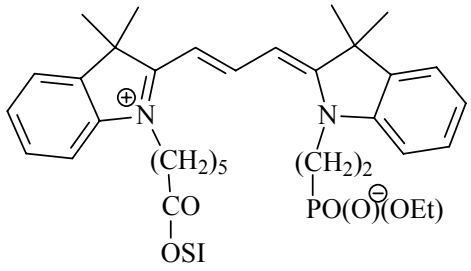	545	562	110,000	0.03
FO546	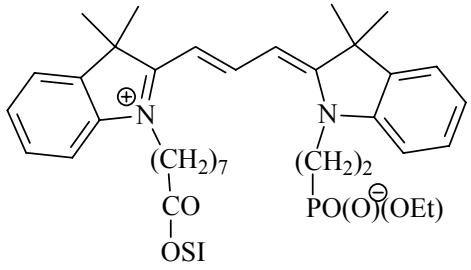	545	562	86,000	0.04
FO548	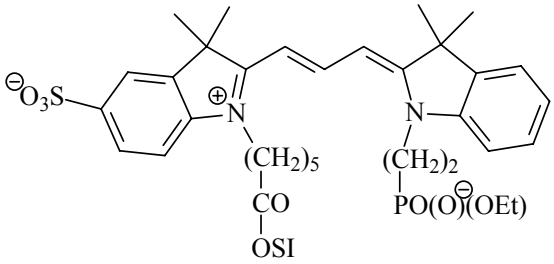	548	562	155,000	0.05
FR642	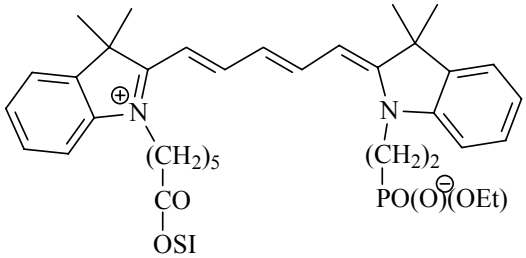	642	663	170,000	0.17
FR646	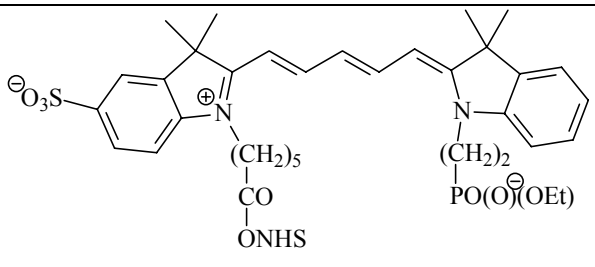	646	664	220,000	0.20

FR626	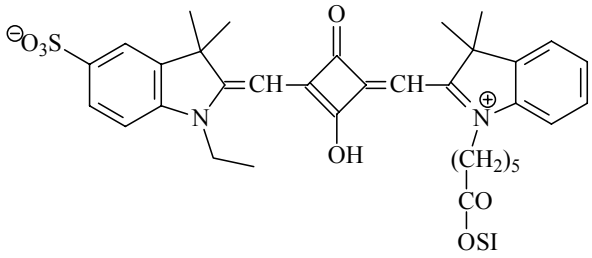	626	637	113,000	0.02
FR661	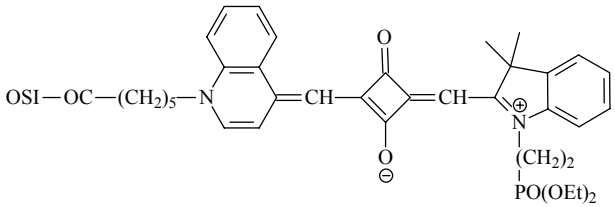	661	725	120,000	<0.005
FR662	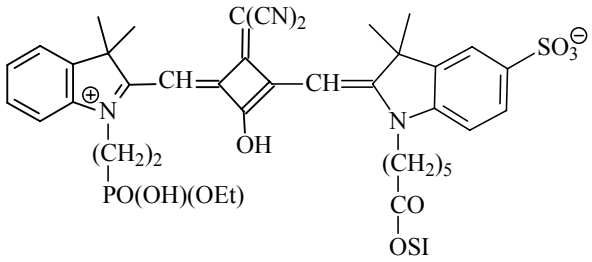	662	682	130,000	0.02
FR670	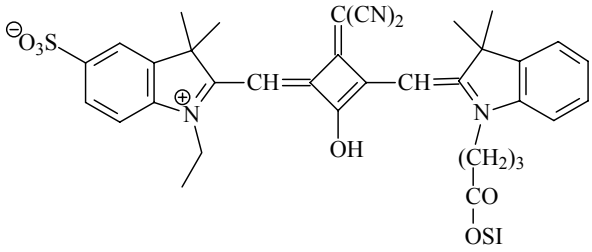	658	676	145,000	0.03
OB630*	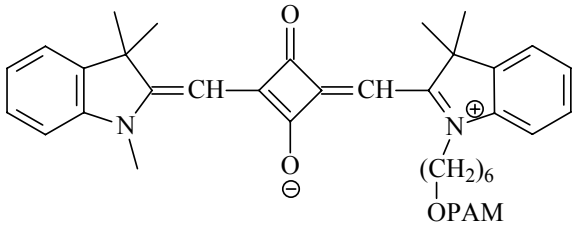	628	637	200,000	0.07
OG670*	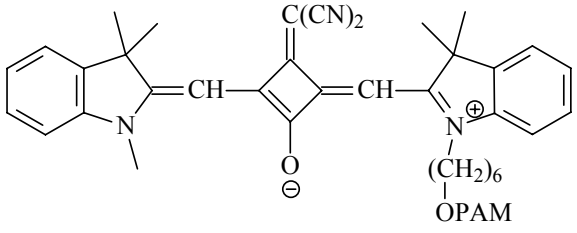	668	687	180,000	0.09

***** *in methanol, others in PBS*

Amine-Reactive Labels

The amine-reactive labels all carry groups which enhance their water solubility. Therefore they are all satisfactorily soluble in aqueous solution. Precipitation of the dye/protein conjugates was not observed even at high DPRs.

A comparison of FO544, FO545, and FO546 which have quite similar spectroscopic properties shows that the chemical stability of the OSI esters of these dyes is strongly dependent on the length of the spacer groups. If the spacer is short (C3 in FO544) the stability of the OSI ester is low, if the spacer is long (C7 in FO546) the stability of the OSI ester is high both in solution and in solid state. Although it is possible to use freshly activated FO544 and FO545 for labeling, the use of FO546 is preferred due to its stability in solid state over months.

The fluorescence intensities of the labels (except FR661) generally increase upon covalent binding to protein. The extent of the increase is dependent on the dye-to-protein ratio (DPR). The highest quantum yields are found at DPR values between 1 and 2, because at higher DPRs the dyes undergo self-quenching, and fluorescence quantum yields decrease. Labeling to amino-modified oligonucleotides enhances the fluorescence intensities of the dyes up to 7-fold (FO546).

Saccharide-Reactive Labels

The saccharide-reactive phosphoramidites OB630 and OG670 are well soluble in chloroform. Their solubility in water is good enough to suppress precipitation of the labeled oligonucleotides in aqueous solution. The fluorescence intensities of OB630 and OG670 rise 3.5- and 1.5-fold, respectively, upon labeling to 15-mer oligonucleotides.

Energy Transfer Pairs

All dyes described previously are promising labels for use in fluorescence resonance energy transfer (FRET) studiesbecause the emission spectra of the donor dyes efficiently overlap the absorption spectra of the acceptor dyes. Fluorescent acceptors are used instead of quenchers [13, 14] because in this case ratiometric data evaluation is possible. Ratiometric applications eliminate distortions of data caused e.g. by instrumental factors such as illumination stability or by changes of the probe concentration because of evaporation of solvent.

The emission spectra of FO544, FO545, FO546, and FO548 sufficiently overlap the absorption spectra of FR642 and FR646. Any combination in which FO544, FO545, FO546, or FO548 serve as the donor dyes and FR642 or FR646 are used as acceptor dyes could be

used for FRET measurements. OB630 and OG670 can serve as donor-acceptor pair for oligonucleotide measurements.

FR646 and FR662 cannot be used as a donor-acceptor-pair, because the emission maxima of the two dyes are too close to each other. The resolution of both emission peaks is not possible because only one broad emission band is detected. In this case FR661 could be used as acceptor because of its large Stokes' shift. But the fluorescence of FR661 is very weak, and therefore ratiometric data evaluation is not possible in this case. FR662 can serve as acceptor dye if for example a ruthenium complex (e.g. $[Ru(bpy)_2(mcbpy)]$) [15, 16] with an absorption maximum of about 450 nm and a large Stokes' shift is used as donor.

The use of the synthesized labels as donor–acceptor-pairs in FRET studies is shown in chapter 3. Immunoassays were performed as well as hybridization assays.

2.5. References

[1] M. Arbter (2000) Diode Laser Compatible Cyanine and Squarylium Dyes, *Diploma Thesis,* University of Regensburg (Germany).

[2] S. R. Mujumdar, R. B. Mujumdar, C. M. Grant, and A. S. Waggoner (1996) Cyanine-Labeling Reagents: Sulfobenzindocyanine Succinimidyl Esters. *Bioconjugate Chem* **7,** 356-362.

[3] B. Oswald, L. Patsenker, J. Duschl, H. Szmacinski, O. S. Wolfbeis, and E. Terpetschnig (1999) Synthesis, Spectral Properties, and Detection Limits of Reactive Squaraine Dyes, a New Class of Diode Laser Compatible Fluorescent Protein Labels. *Bioconjugate Chem.* **10**, 925-931.

[4] H. E. Fierz-David, L. Blangley (Eds.) (**1943)** *Grundlegende Operationen der Farbenchemie*, 5. Aufl., 123.

[5] R. B. Mujumdar, L. A. Ernst, S. R. Mujumdar, C. J. Lewis, A. S. Waggoner (1993) Cyanine dye labeling reagents: sulfoindocyanine succinimidyl esters. *Bioconjugate Chem.* **4,** 105-111.

[6] B. Oswald, M. Gruber, M. Böhmer, F. Lehmann, M. Probst, and O. S. Wolfbeis (2001) Novel Diode Laser-compatible Fluorophores and Their Application to Single Molecule Detection, Protein Labeling and Fluorescence Resonance Energy Immunoassay. *Photochem. Photobiol.* **74(2)**, 237-245.

[7] B. Wetzl (2002) New Rhodamines and Squarylium Dyes for Biological Applications, *Diploma Thesis,* University of Regensburg (Germany).

[8] E. Terpetschnig and J. R. Lakowicz (1993) Synthesis and Characterization of Unsymmetrical Squaraines: A New Class of Cyanine Dyes. *Dyes and Pigments* **21**, 227-234.

[9] E. Terpetschnig, H. Szmacinski, and J. R. Lakowicz (1993) Synthesis, Spectral Properties and Photostabilities of Unsymmetrical Squaraines; A New Class of Fluorophores with Long-Wavelength Excitation and Emission. *Anal. Chim. Acta* **282**, 633-641.

[10] B. Oswald, L. Patsenker, J. Duschl, H. Szmacinski, O. S. Wolfbeis, and E. Terpetschnig (1999) Synthesis, Spectral Properties, and Detection Limits of Reactive Squaraine Dyes, a New Class of Diode Laser Compatible Fluorescent Protein Labels. *Bioconjugate Chem.* **10**, 925-931.

[11] B. Oswald (2000) New Long-Wavelength Fluorescent Labels for Bioassays, *Dissertation*, University of Regensburg (Germany).

[12] G. M. Little, R. Raghavachari, N. Narayanan, and H. L. Osterman (2000) Fluorescent Cyanine Dyes, *U.S. Patent 6,0276,709.*

[13] S. Tyagi (2000) Wavelength-shifting molecular beacons. *Nature Biotech.* (**18**). 1191-1196.

[14] S. Tyagi and F. R. Kramer (1996) Molecular Beacons: Probes that Fluoresce upon Hybridization. *Nature Biotech.* **14,** 303-308.

[15] E. Terpetschnig, H. Szmacinski, H. Malak, J. R. Lakowicz (1995) Metal-ligand complexes as a new class of long lived fluorophores for protein hydrodynamics, *Biophys. J.*, **68**, 342-350.

[16] C. M. Augustin, B. Oswald, and O. S. Wolfbeis (2002) Time-Resolved Luminescence Energy Transfer Immunobinding Study Using a Ruthenium-Ligand Complex as a Donor Label, *Anal. Biochem.,* **305**, 166-172.

3. Applications

This chapter deals with the applicability of the new labels presented in chapter two. The labels were used as donor and acceptor dyes in FRET studies. Binding studies of antigen-antibody complexes and homogenous immunoassays were performed using HSA/anti-HSA as a model system. Cytometric measurements for the quantification of HSA show the applicability of the labels in flow cytometry. In addition, various hybridization studies are shown: binding studies, determinations of molecular distances, and competitive assays. The applicability of a fluorescent dUTP in fluorescence in situ hybridization (FISH) is shown as well.

3.1. Immunostudies

In this work immunostudies were performed on the system HSA/anti-HSA. Binding studies, homogenous competitive immunoassays, and cytometric measurements are shown in the following.

3.1.1. Binding Studies

Binding studies were performed using various donor-acceptor pairs. Figure 3.1 shows how energy transfer can occur in this system. HSA (Ag) is labeled with the donor dye (orange), and anti-HSA (Ab) is labeled with the acceptor dye (red). When the antigen-antibody reaction takes place the complex is formed and labeled HSA occupies the specific binding sites at the labeled anti-HSA. Donor and acceptor come into close proximity and fluorescence resonance energy transfer can occur [1, 2].

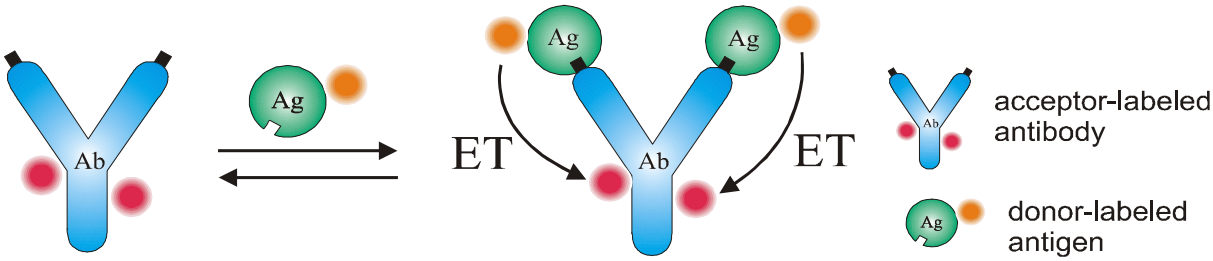

Figure 3.1. Scheme for energy transfer on the system HSA/anti-HSA

FO546/HSA-FR642/anti-HSA

A representative binding study based on energy transfer measurements is shown in figure 3.2. HSA was labeled with FO546 at a DPR of 2.1. Anti-HSA was labeled with FR642 at a DPR of 2.5. FO546/HSA of constant concentration ([HSA] = $1.0 \cdot 10^{-7}$ mol/L) was titrated with

various amounts of FR642/anti-HSA in molar ratios of 1:0, 1:0.25, 1:0.5, 1:1, 1:2, and 1:4. The fluorescence intensity of FO546/HSA decreases to 60% with increasing amounts of FR642/anti-HSA due to energy transfer. The fluorescence intensity of FR642/anti-HSA increases on the one hand due to the energy transfer, on the other hand due to the fact that the acceptor itself is directly photo-excited to a certain degree. Besides, fluorescence increases additionally with increasing amounts of acceptor. The fluorescence of FR642/anti-HSA without donor (0:4) is shown in figure 3.2.

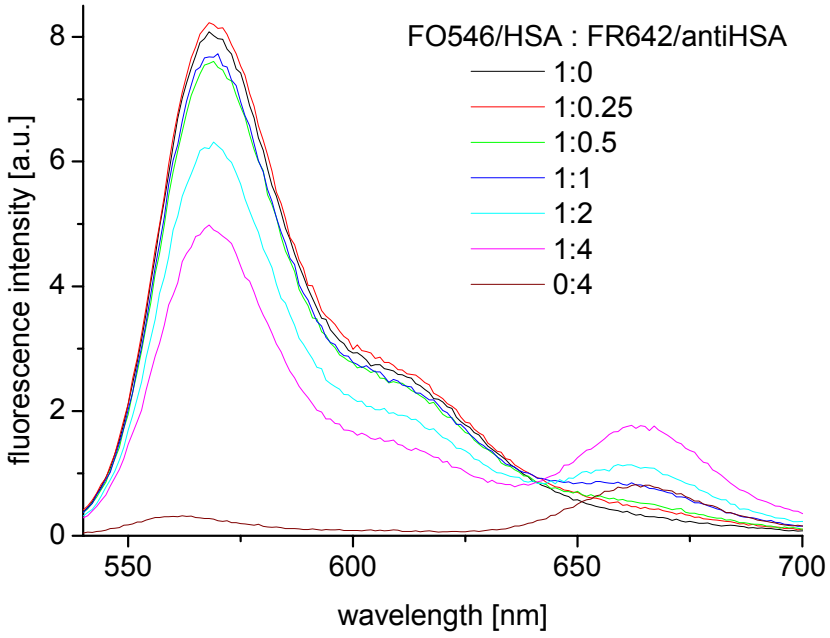

Figure 3.2. Energy transfer study in which FO546/HSA (DPR = 2.1) of constant concentration was titrated with FR642/anti-HSA (DPR = 2.5) (λ_{exc} = 520 nm). [HSA] = $1.0 \cdot 10^{-7}$ mol/L.

Figure 3.3 shows the fluorescence spectra of FO546/HSA (DPR = 2.1) of constant concentration ([HSA] = $1.0 \cdot 10^{-7}$ mol/L) titrated with increasing amounts of free FR642. Molar ratios are 1:0, 1:0.625, 1:1.25, 1:2.5, 1:5, and 1:10 and correspond to the concentrations of FR642 in the binding study shown in figure 3.2. This measurement was performed in order to find out wether free acceptor dye affects the fluorescence of the donor labeled HSA. The fluorescence intensity of FO546/HSA is reduced to 90% upon addition of a ten-fold excess of free FR642. The fluorescence intensity of FR642 increases with increasing amounts of FR642. Measurement of the fluorescence intensity of FR642 without FO546/HSA (0:10) shows that this increase is mainly caused by direct excitation of the acceptor and only a small part contributes to energy transfer.

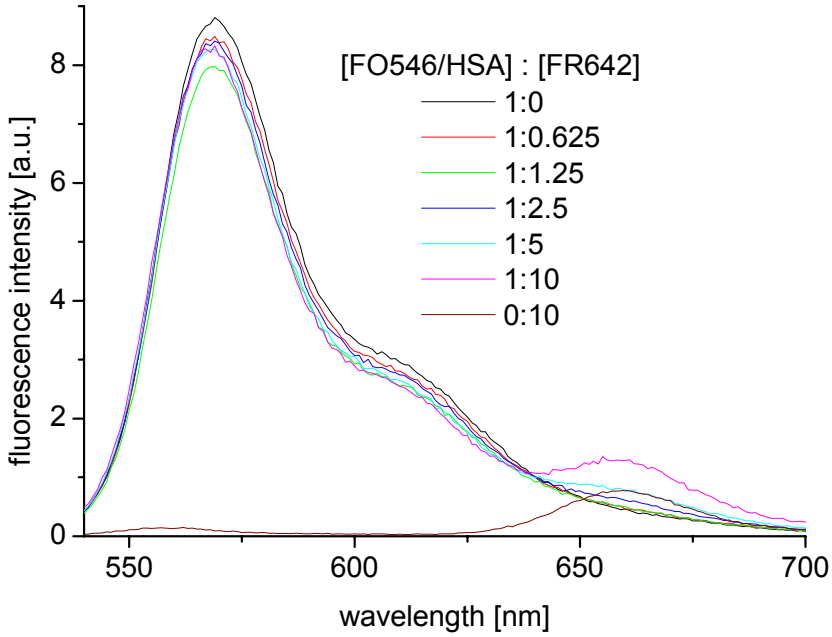

Figure 3.3. Fluorescence spectra of FO546/HSA (DPR = 2.1) of constant concentration titrated with free FR642 (λ_{exc} = 520 nm). [HSA] = $1.0 \cdot 10^{-7}$ mol/L.

The effect of non-labeled anti-HSA on the fluorescence of FO546/HSA (DPR = 2.1) was proved in addition. FO546/HSA of constant concentration ([HSA] = $1.0 \cdot 10^{-7}$ mol/L) was titrated with various amounts of anti-HSA in molar ratios of 1:0, 1:0.25, 1:0.5, 1:1, 1:2, and 1:4. No effect was observed of the anti-HSA concentration on fluorescence intensity.

Figure 3.4 shows ratiometric plots of the three measurements. The fluorescence intensities at 664 nm are divided by the fluorescence intensities at 569 nm. These values are plotted versus the ratio of the concentration of the titrators (FR642/anti-HSA, FR642, or anti-HSA) and the concentration of FO546/HSA. It is clearly visible that non-labeled anti-HSA (blue line) has no effect on the fluorescence of FO546/HSA. On addition of free FR642 a raise of the ratio of the fluorescence intensities appears (red line). A straight line would be achieved if there was no energy transfer and if only the fluorescence intensity of the acceptor alternated and the fluorescence of the donor was constant. The curve obtained in this case is not exactly straight which might tribute to the fact that a small part of the free acceptor molecules bind non-covalently to the donor labeled HSA molecules whereupon energy transfer can take place to a certain extent. It is expected that on addition of FR642/anti-HSA to FO546/HSA a sigmoidal binding curve should be obtained. In this case only a part of the binding curve is visible. The point of saturation, this means the point where addition of more

acceptor labeled anti-HSA causes no changes in the ratio of the fluorescence intensities is not visible.

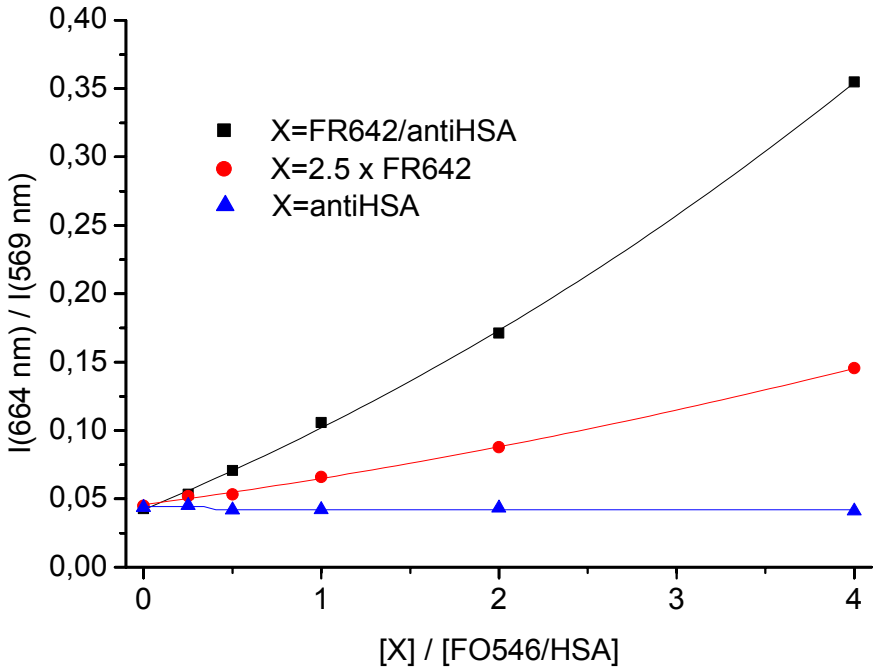

Figure 3.4. Ratiometric plot of the ratios of the fluorescence intensities at 664 nm and 569 nm versus the ratios of the concentrations of titrators (FR642/anti-HSA, FR642, or anti-HSA) and the concentration of FO546/HSA.

Figure 3.5 and figure 3.6 show another binding study on the system FO546/HSA-FR642/anti-HSA. Here the DPR of FO546/HSA has been reduced to 1.7 and the DPR of FR642/anti-HSA has been raised to 5.9. In this case the fluorescence of FR642/anti-HSA caused by direct excitation and not by energy transfer is small because at high DPR the quantum yield of the dye is weak (see figure 3.5; 0:4). The fluorescence intensity of the donor decreases to 40% upon addition of a four-fold excess of FR642/anti-HSA (fig. 3.5; 1:4) compared to the intensity without acceptor (fig. 3.5; 1:0). The fluorescence intensity of the acceptor (fig. 3.5; 1:4) increases more than eight-fold compared to the fluorescence of FR642/anti-HSA without donor (fig. 3.5; 0:4).

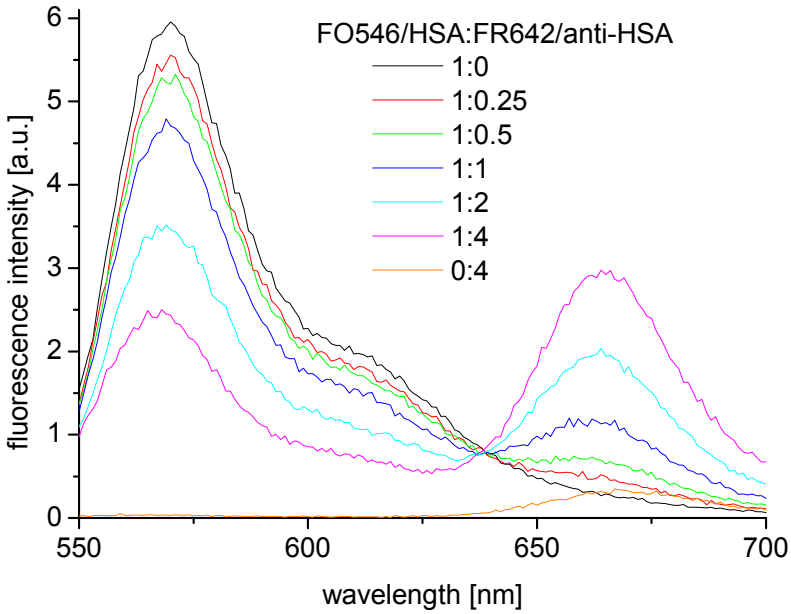

Figure 3.5. Energy transfer study in which FO546/HSA (DPR = 1.7) of constant concentration was titrated with FR642/anti-HSA (DPR = 5.9) (λ_{exc} = 520 nm). [HSA] = $1.0 \cdot 10^{-7}$ mol/L.

The plot of the ratios of the fluorescence intensities at 664 nm and 568 nm versus the ratios of the concentration of FR642/anti-HSA and of FO546/HSA gives a sigmoidal curve. Saturation is nearly reached at a four-fold excess of FR642/anti-HSA.

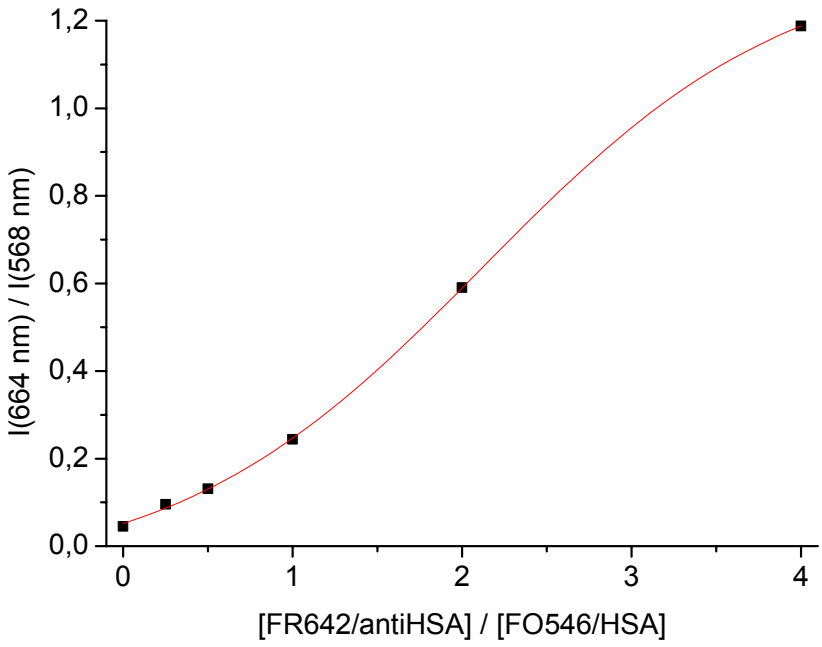

Figure 3.6. Plot of the ratios of the fluorescence intensities at 664 nm and 568 nm versus the ratios of the concentrations of FR642/anti-HSA and the concentration of FO546/HSA.

In the energy transfer system shown in figure 3.4 (black line) almost equal DPRs of the donor and acceptor conjugates, respectively, were used. In contrast, in the system shown in figure 3.6, the DPR of the acceptor conjugate is much higher than that of the donor conjugate. This system gives a sigmoidal binding curve which is preferred to the curve obtained in figure 3.4.

FO548/HSA-FR646/anti-HSA

Figure 3.7 shows an energy transfer study on the system FO548/HSA-FR646/anti-HSA. HSA was labeled with FO548 at a DPR of 3.6. Anti-HSA was labeled with FR646 at a DPR of 1.5. FO548/HSA of constant concentration ([HSA] = $2.0 \cdot 10^{-8}$ mol/L) was titrated with various amounts of FR646/anti-HSA in molar ratios of 1:0, 1:0.25, 1:0.5, 1:1, 1:2, and 1:4. The fluorescence intensity of the donor decreases to 50% upon addition of a four-fold excess of FR646/anti-HSA (fig. 3.7; 1:4) compared to the intensity without acceptor (fig. 3.7; 1:0). The fluorescence intensity of the acceptor (fig. 3.7; 1:4) increases nearly three-fold compared to the fluorescence of FR646/anti-HSA without donor (fig. 3.7; 0:4). The ratiometric plot (fig.3.7, right) shows the sigmoidal binding curve of the system.

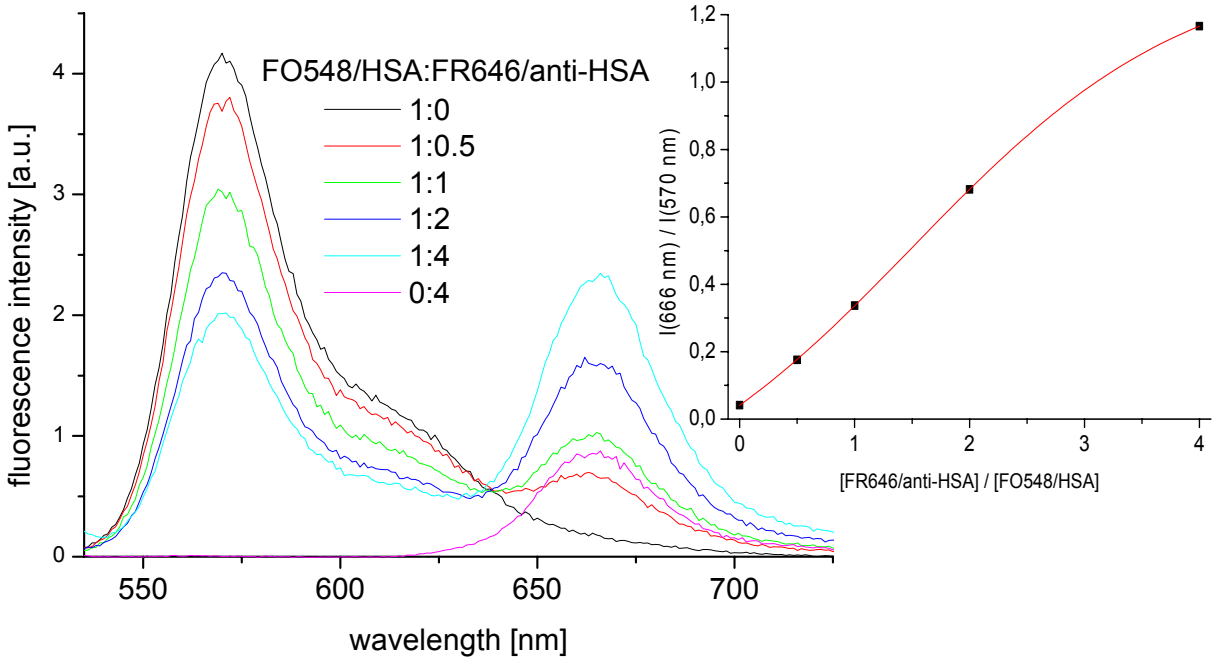

Figure 3.7. Energy transfer study in which FO545/HSA (DPR = 3.6) of constant concentration was titrated with FR646/anti-HSA (DPR = 1.5) (λ_{exc} = 520 nm). [HSA] = $2.0 \cdot 10^{-8}$ mol/L.

[Ru(bpy)$_2$(mcbpy)]/HSA-FR662/anti-HSA

In figure 3.8 an energy transfer study is shown in which a ruthenium complex serves as the donor dye. It should be mentioned that the donor is not fluorescent but phosphorescent. The ruthenium complex [Ru(bpy)$_2$(mcbpy)](PF$_6$)$_2$ [3, 4, 5] shown in figure 3.8 on the right side was activated to the OSI ester by standard methods and was labeled to HSA with a DPR of 10.3. The absorption maximum of the conjugate is at 460 nm and the emission maximum is at 635 nm, i.e. the Stokes' shift is as large as 175 nm. The acceptor FR662 was labeled to anti-HSA with a DPR of 7.8. [Ru(bpy)$_2$(mcbpy)]/HSA of constant concentration ([HSA] = $1.3 \cdot 10^{-7}$ mol/L) was titrated with various amounts of FR662/anti-HSA in molar ratios of 1:0, 1:0.125, 1:0.25, 1:0.5, 1:1, 1:2, and 1:4. The emission intensity of the donor decreases to 30% upon addition of a four-fold excess of FR662/anti-HSA (fig. 3.8; 1:4) compared to the intensity without acceptor (fig. 3.8; 1:0). The fluorescence intensity of the acceptor in absence of donor (fig. 3.8; 0:4) is negligible, because the acceptor is not photo-excited at 460 nm.

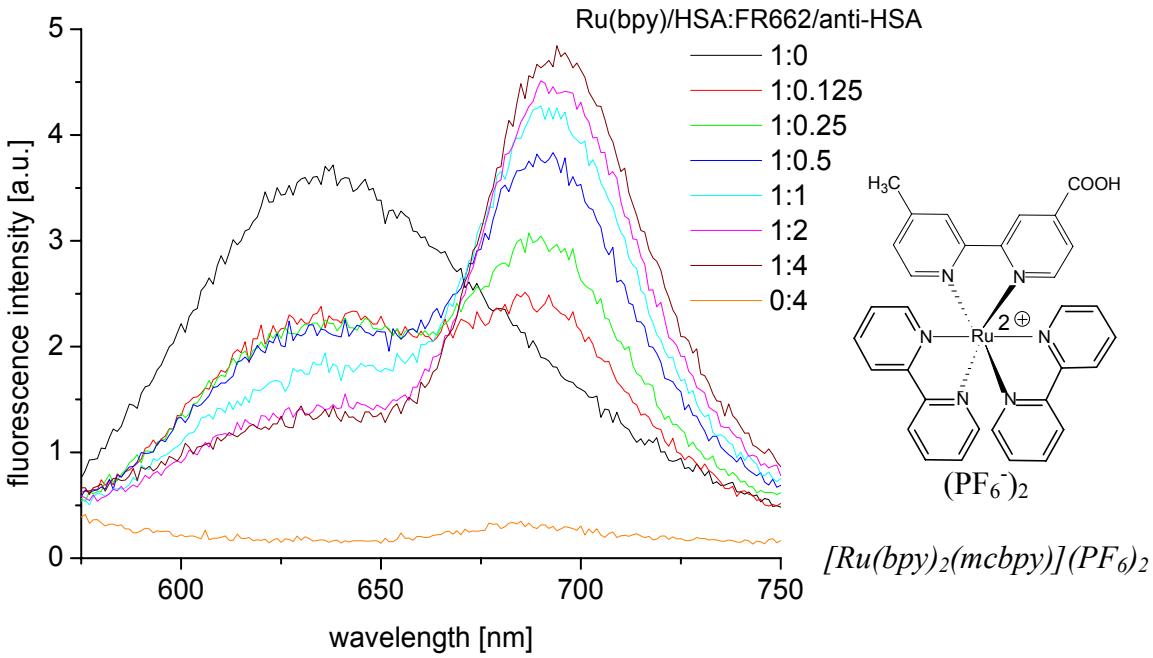

Figure 3.8. Energy transfer study in which $[Ru(bpy)_2(mcbpy)]$/HSA (D/P = 10.3) of constant concentration was titrated with FR662/anti-HSA (D/P = 7.8) (λ_{exc} = 460 nm). [HSA] = $1.3 \cdot 10^{-7}$ mol/L. The chemical structure of the ruthenium complex $[Ru(bpy)_2(mcbpy)](PF_6)_2$ is shown on the right side.

The plot of the ratios of the emission intensities at 693 nm and 635 nm versus the ratios of the concentration of FR662/anti-HSA and of $[Ru(bpy)_2(mcbpy)]$/HSA gives a sigmoidal curve (fig. 3.9). At a two-fold excess of FR662/anti-HSA saturation is nearly reached.

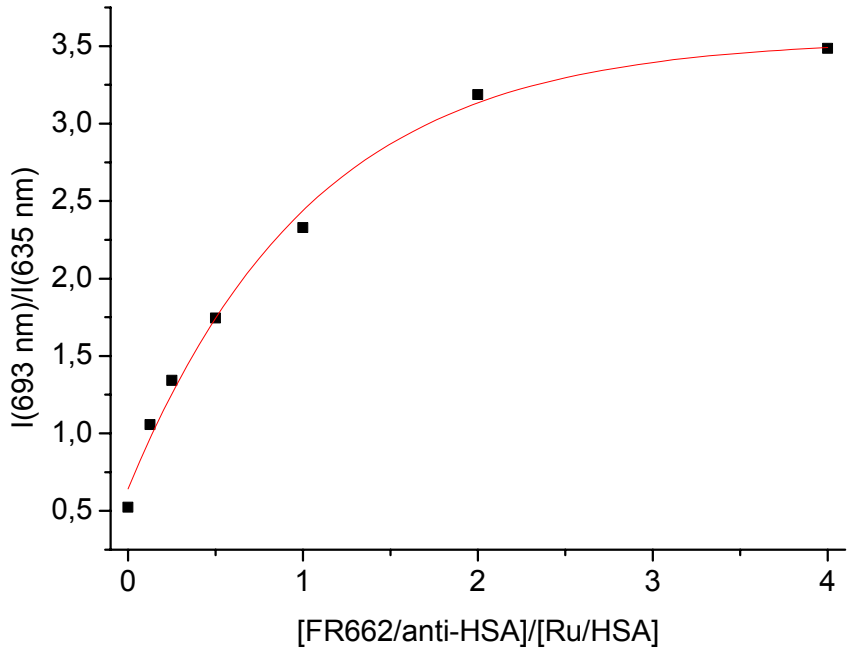

Figure 3.9. Ratiometric plot of the ratios of the fluorescence intensities at 693 nm and 635 nm versus the ratios of the concentrations of FR662/anti-HSA and the concentration of $[Ru(bpy)_2(mcbpy)]$/HSA.

3.1.2. Competitive Immunoassays

Competitive homogenous immunoassays on the system HSA/anti-HSA were performed using various donor/acceptor pairs. Figure 3.10 shows the scheme for the competitive immunoassay. Constant amounts of donor labeled HSA (Ag) were mixed with various quantities of non-labeled HSA (analyte). These solutions were diluted to a constant volume with PBS. An equal amount of acceptor labeled anti-HSA (Ab) was added and the solutions were incubated for 20 minutes at room temperature to allow the formation of the antigen-antibody complex.

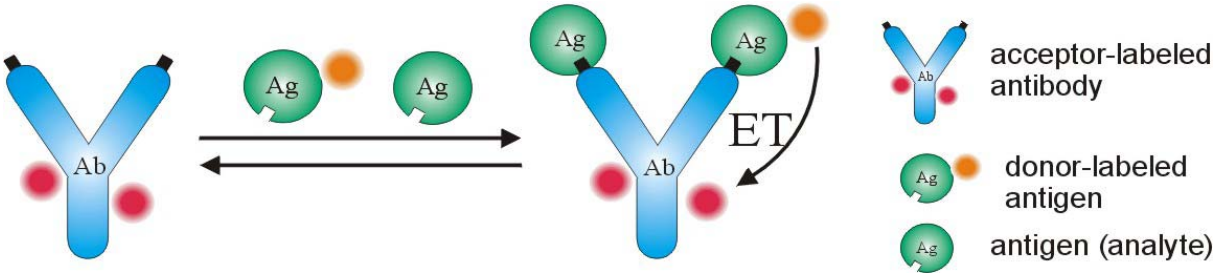

Figure 3.10. Scheme for the competitive immunoassay on the system HSA/anti-HSA.

Labeled and non-labeled HSA compete for the specific binding sites at the labeled antibody. If the fraction of non-labeled HSA is low, mainly labeled HSA binds to the labeled anti-HSA and energy transfer can occur. This leads to a decrease of the fluorescence intensity of the donor and an increase of the fluorescence intensity of the acceptor. If the fraction of non-labeled HSA is high, mainly non-labeled HSA binds to anti-HSA and energy transfer is reduced. This leads to an increase of the fluorescence intensity of the donor and to a decrease of the fluorescence intensity of the acceptor [1]. FRET immunoassays open the way to 2-wavelength immunoassays which are intrinsically self-referenced, because the signal is calculated from the fluorescence intensities at two wavelengths. Some examples for competitive homogenous immunoassays are shown in the following.

FO546/HSA-FR642/anti-HSA

Constant quantities of FO546/HSA with a DPR of 2.1 ([FO546/HSA] = $8.3 \cdot 10^{-8}$ mol/L) were mixed with various quantities of non-labeled HSA in molar ratios of 1:0, 1:0.25, 1:0.5, 1:1, 1:2, and 1:3. Constant amounts of FR642/anti-HSA with a DPR of 2.5 were added ([FR642/anti-HSA] = $8.3 \cdot 10^{-8}$ mol/L). Figure 3.11 (left) shows the plot of the fluorescence intensities versus the wavelength. The fluorescence intensity of the donor increases with increasing amounts of non-labeled HSA. The decrease of the acceptor fluorescence is not visible in this case.

The ratiometric plot is shown on the right side of figure 3.11. The ratio of the fluorescence intensities of the donor and the acceptor is plotted versus the ratio of the concentrations of non-labeled HSA and FO546/HSA. A sigmoidal binding curve is achieved. The use of this system enables determination of HSA in the concentration range of $4 \cdot 10^{-8}$ – $2.4 \cdot 10^{-7}$ mol/L. The concentration range was determined graphically.

The measurement was repeated using BSA instead of HSA in order to prove if protein which does not compete with FO546/HSA for the binding sites of FR642/anti-HSA affects the immunoassay system. In figure 3.11 (right side, red line) it can bee seen that addition of BSA has no effect on the FRET efficiency of the immunosystem.

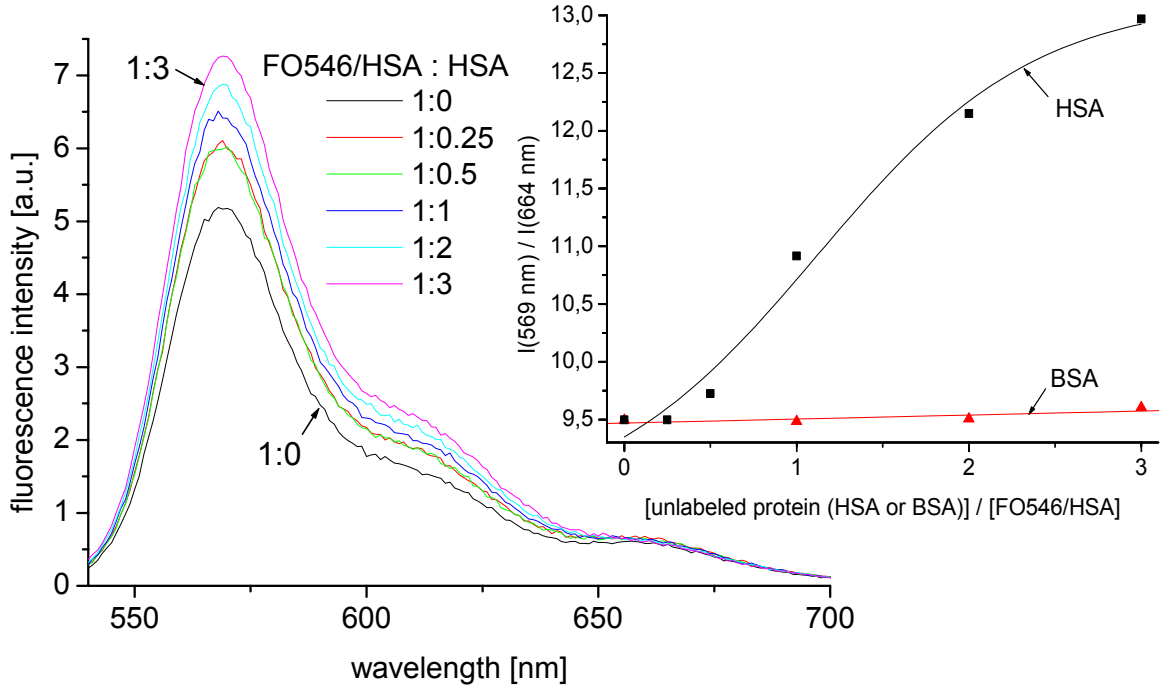

Figure 3.11. **Left side:** Competitive immunoassay in which FO546/HSA (DPR = 2.1) of constant concentration ([FO546/HSA] = $8.3 \cdot 10^{-8}$ mol/L) was mixed with various amounts of non-labeled HSA and constant quantities of FR642/anti-HSA (DPR = 2.5) ([FR642/anti-HSA] = $8.3 \cdot 10^{-8}$ mol/L). λ_{exc} = 520 nm.

Right side: Ratiometric plot of the immunoassay (black line) and the negative control (red line on bottom).

Figure 3.12 shows another immunoassay on the system FO546/HSA-FR642/anti-HSA. Here the DPR of FO546/HSA has been reduced to 1.7 and the DPR of FR642/anti-HSA has been raised to 5.9. Constant quantities of FO546/HSA ([FO546/HSA] = $8.3 \cdot 10^{-8}$ mol/L) were mixed with various quantities of non-labeled HSA in molar ratios of 1:0, 1:0.25, 1:0.5, 1:1, 1:2, and 1:4. Constant amounts of FR642/anti-HSA were added ([FR642/anti-HSA] = $8.3 \cdot 10^{-8}$ mol/L). Figure 3.12 (left side) shows the plot of the fluorescence intensities versus the wavelength. The increase of the fluorescence intensity of the donor upon addition of non-labeled HSA is much stronger in this case compared to the assay in figure 3.11. In fact, a slight decrease of the fluorescence intensity of the acceptor is visible.

The ratiometric plot is shown on the right side of figure 3.12. The ratio of the fluorescence intensities of the donor and the acceptor is plotted versus the ratio of the concentrations of non-labeled HSA and FO546/HSA. A sigmoidal binding curve is obtained.

The use of this system enables determination of HSA in the concentration range of $2 \cdot 10^{-8}$ – $1.6 \cdot 10^{-7}$ mol/L which was evaluated graphically.

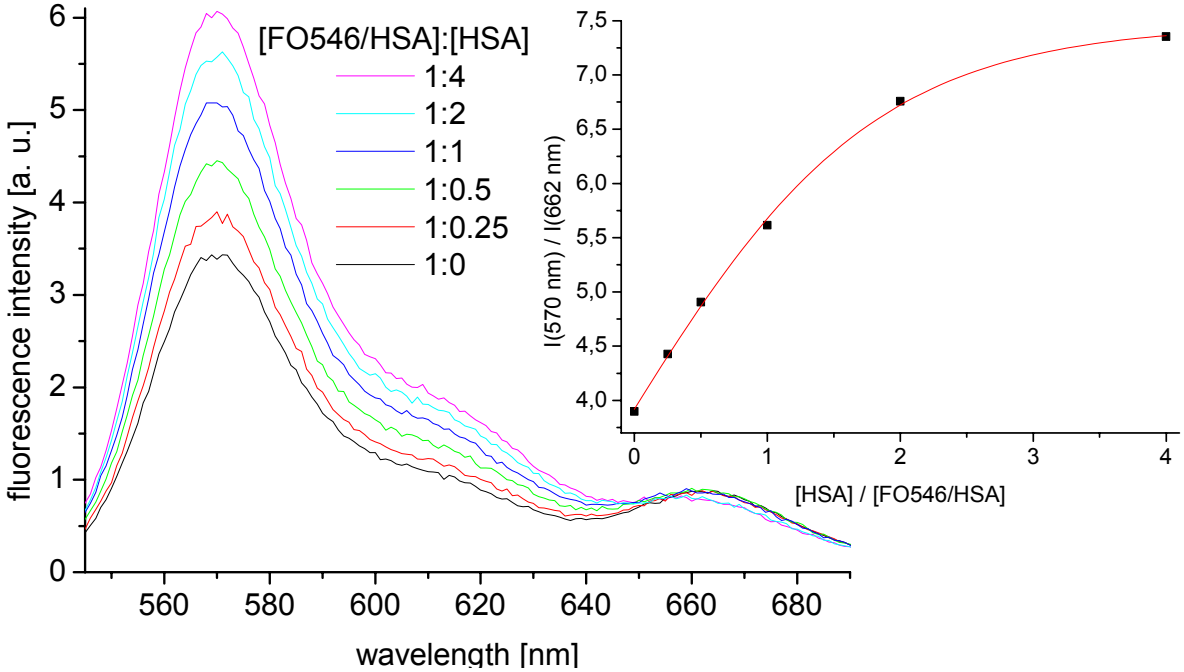

Figure 3.12. **Left side:** Competitive immunoassay in which FO546/HSA (DPR = 1.7) of constant concentration ([FO546/HSA] = $8.3 \cdot 10^{-8}$ mol/L) was mixed with various amounts of non-labeled HSA and constant quantities of FR642/anti-HSA (DPR = 5.9) ([FR642/anti-HSA] = $8.3 \cdot 10^{-8}$ mol/L). λ_{exc} = 520 nm.
Right side: Ratiometric plot.

FO548/HSA-FR646/anti-HSA

Two homogenous competitive immunoassays based on the system FO548/HSA-FR646/anti-HSA are shown in figure 3.13 and 3.14. Constant amounts of FO548/HSA with a DPR of 3.6 were mixed with various quantities of non-labeled HSA in molar ratios of 1:0, 1:0.125, 1:0.25, 1:0.5, 1:1, 1:2, and 1:4. Constant quantities of FR642/anti-HSA with a DPR of 1.5 were added. The assay shown in figure 3.13 contains equimolar amounts of labeled HSA and anti-HSA ([FO548/HSA] = [FR642/anti-HSA] = $1.7 \cdot 10^{-8}$ mol/L). The assay shown in figure 3.14 contains a two-fold excess of labeled anti-HSA ([FO548/HSA] = $1.4 \cdot 10^{-8}$ mol/L, [FR642/anti-HSA] = $2.8 \cdot 10^{-8}$ mol/L). The left sides in figures 3.13 and 3.14 show the plots of the fluorescence intensities versus the wavelength. In both assays the fluorescence intensity of the donor increases with increasing fractions of non-labeled HSA while the fluorescence intensity of the acceptor decreases.

The ratiometric plots are shown on the right sides in figures 3.13 and 3.14. The ratio of the fluorescence intensities of the donor and the acceptor is plotted versus the ratio of the concentrations of non-labeled HSA and FO548/HSA. Sigmoidal binding curves are obtained. The slope of the binding curve in figure 3.13. is high at concentration ratios in the range of 0.125 - 2. This enables determination of HSA in the concentration range of $2 \cdot 10^{-9}$ – $3.5 \cdot 10^{-8}$ mol/L. At higher concentrations of HSA the slope of the binding curve is low, because saturation is nearly reached. Accurate determinations of HSA concentrations in this concentration range are not possible.

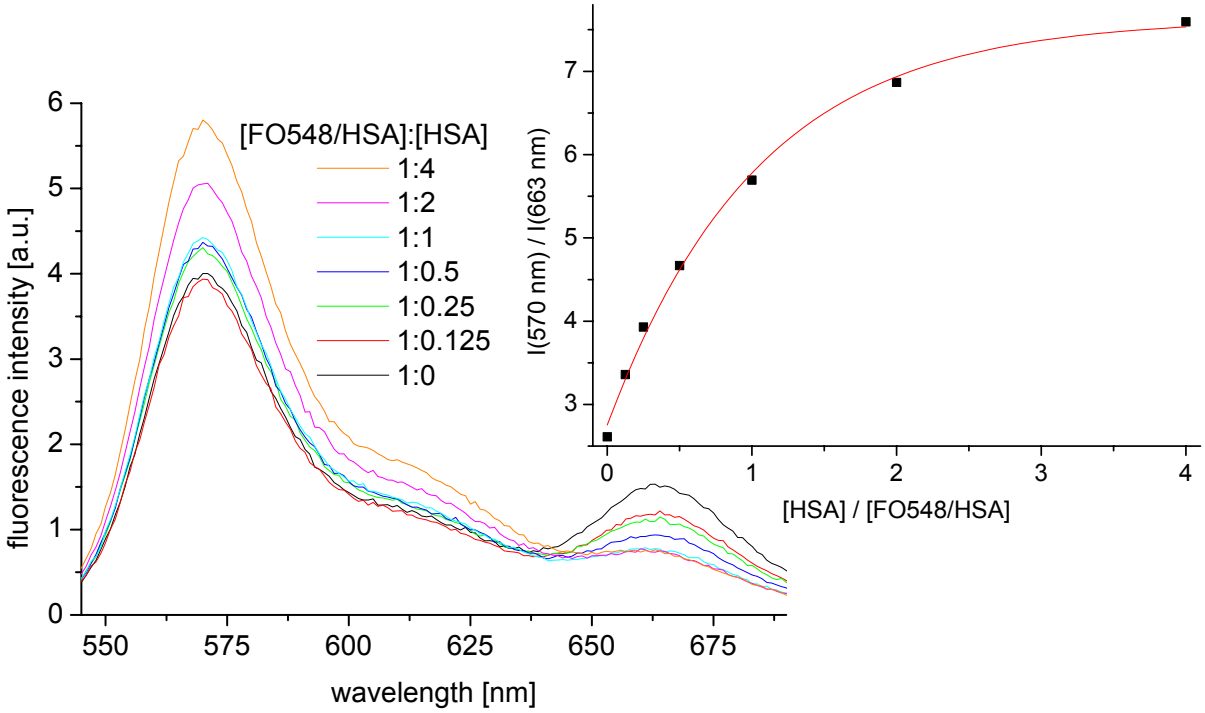

Figure 3.13. **Left side:** Competitive immunoassay in which FO548/HSA (DPR = 3.6) of constant concentration ([FO548/HSA] = $1.7 \cdot 10^{-8}$ mol/L) was mixed with various amounts of non-labeled HSA and constant quantities of FR646/anti-HSA (DPR = 1.5) ([FR642/anti-HSA] = $1.7 \cdot 10^{-8}$ mol/L). λ_{exc} = 520 nm.
Right side: Ratiometric plot of the immunoassay.

The slope of the binding curve in figure 3.14 at low HSA concentrations is lower than that in figure 3.13, indicating that at low HSA concentrations ($2 \cdot 10^{-9}$ – $3 \cdot 10^{-8}$ mol/L) the system shown in figure 3.13 is favored. At higher HSA concentrations ($3 \cdot 10^{-8}$ – $5.5 \cdot 10^{-8}$ mol/L) the system shown in figure 3.14 is favored, because at a four-fold excess of HSA still saturation is not reached.

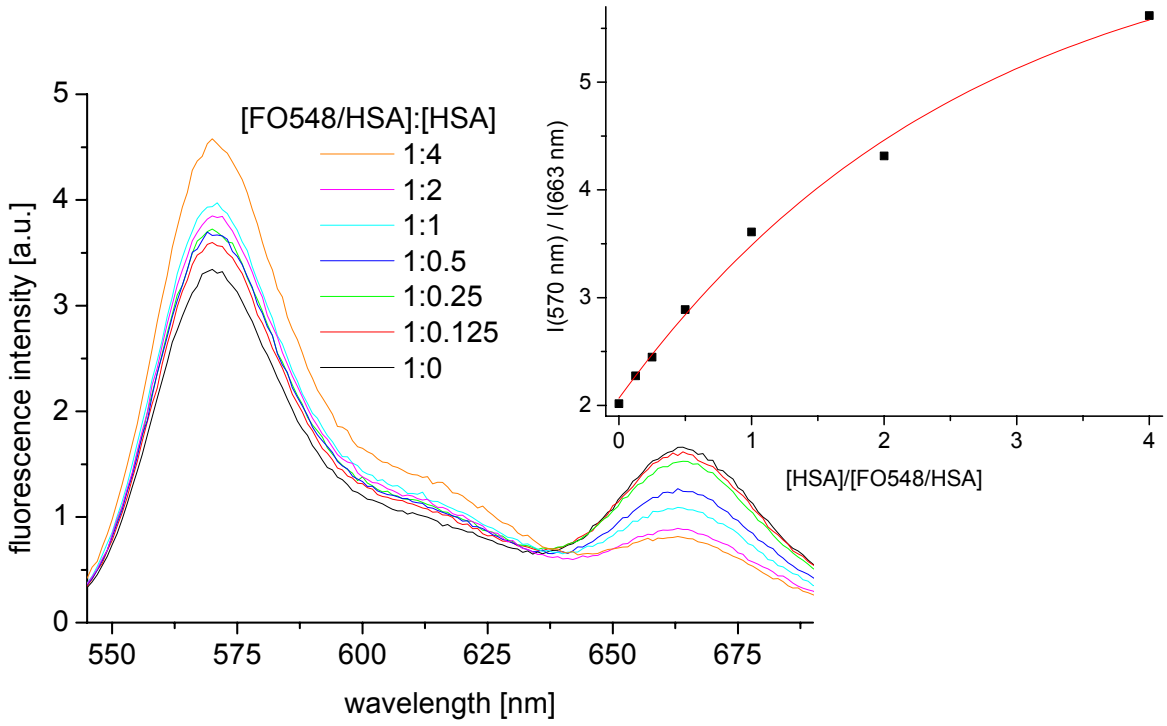

Figure 3.14. **Left side:** Competitive immunoassay in which FO548/HSA (DPR=3.6) of constant concentration ([FO548/HSA] = $1.4 \cdot 10^{-8}$ mol/L) was mixed with various amounts of non-labeled HSA and a two-fold excess of FR646/anti-HSA (DPR=1.5) ([FR642/anti-HSA] = $2.8 \cdot 10^{-8}$ mol/L). λ_{exc}=520 nm.
Right side: Ratiometric plot.

3.1.3. Cytometric Measurements

Flow cytometry allows the simultaneous quantitative measurement of up to 100 different diagnostic parameters in a single drop of a sample (Luminex™ technology). At the same time it may even save time compared to a single parameter measurement using conventional methods. Due to its high flexibility, the technology can be used to measure numerous diagnostic analytes if it undergoes a specific molecular interaction with a partner molecule, e.g. an antibody, an enzyme or a substrate, any ligand or receptor, or a complementary nucleic acid.

The antigen-antibody interaction takes place on the surface of the microspheres. The extent to which the antibody has interacted with the immobilized antigen is measured using a fluorescent label. Usually, polystyrene particles serve as a solid phase. Thousands of microspheres are analyzed per second individually. The kind of assay may be encoded as well by rendering the beads fluorescent using a second (encoding) color that typically has a red

fluorescence. Flow cytometric assays involve less washing steps, enable working with whole blood, and can be fully programmed. Hence, they represent a substantial advantage over previous assays protocols. [6]

The assay is demonstrated using the system HSA/anti-HSA. Figure 3.15 shows the antigen-antibody system attached to the surface of the microsphere.

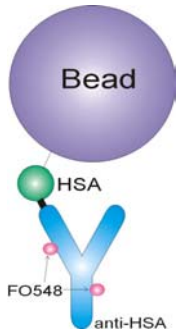

Figure 3.15. Scheme of a bead carrying the antigen-antibody system.

Polystyrene beads of 5.4 µm diameter were activated with sulfo-NHS and EDC. The reactive particles were incubated with HSA solutions of various concentrations (0-500 µg/mL). Anti-HSA was labeled with FO548 at a DPR of 2.1. The beads loaded with HSA were then incubated with solutions of labeled antibody. The concentrations of the anti-HSA solutions were in the range of 0-131 µg/mL. The beads were washed and submitted to the flow cytometer. HSA is detectable in the 10 - 120 µg/mL concentration range as can be seen from figure 3.16.

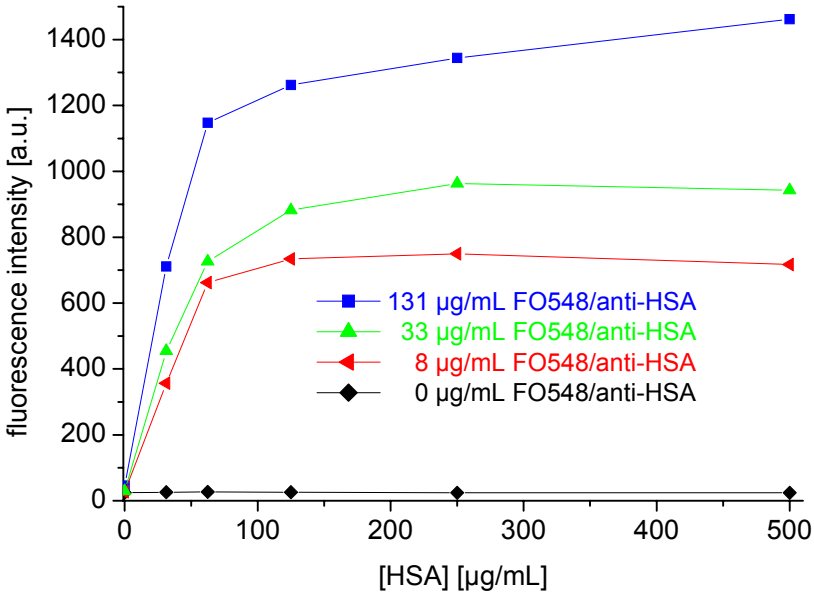

Figure 3.16. Flow cytometric assay of HSA using FO548 labeled anti-HSA.

3.2. Hybridization Studies

Various hybridization studies were performed. In the following, binding studies and homogenous competitive hybridization studies based on FRET are shown. In these cases 15-mer oligonucleotides were labeled with saccharide reactive PAMs, or amino-modified oligonucleotides were labeled with OSI esters. (The sequences of the oligonucleotides can be found in chapter 4.1.1).

3.2.1. Binding Studies

FO548/oligo1-FR646/oligo3

Various energy transfer systems were tested. A representative energy transfer measurements is shown in figure 3.17. FO548 was labeled to the 5'-end of an amino-modified 15-mer oligonucleotide (oligo1). FO646 was labeled to the 3'-end of a complementary amino-modified 15-mer oligonucleotide (oligo3). The donor FO548/oligo1 of constant concentration ([FO548/oligo1] = $2 \cdot 10^{-7}$ mol/L) was titrated with various amounts of acceptor FR646/oligo3. Molar ratios are 1:0, 1:0.25, 1:0.5, 1:0.75, 1:1, 1:2, and 1:4. The fluorescence intensity of FO548/oligo1 decreases to 9% with increasing amounts of FR646/oligo3 and the fluorescence intensity of FR646/oligo3 increases due to energy transfer.

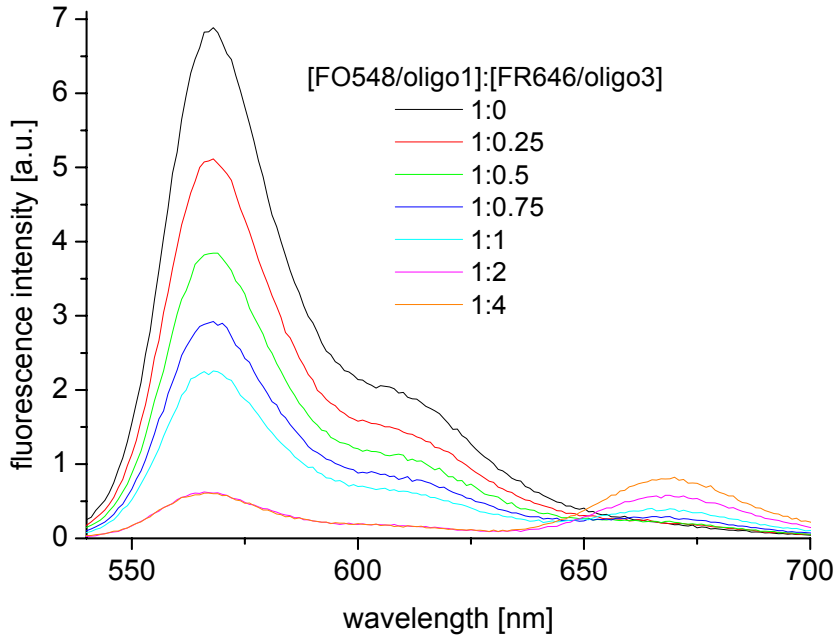

Figure 3.17. Energy transfer study in which FO548/oligo1 of constant concentration ([FO548/oligo1] = $2 \cdot 10^{-7}$ mol/L) was titrated with FR646/oligo3 (λ_{exc} = 520 nm).

Figure 3.18 shows the plot of the ratio of the fluorescence intensities at 668 nm and 568 nm versus the ratio of the concentration of FR646/oligo3 and the concentration of FO548/oligo1 (black line). In addition, ratiometric plots of a titration of FO548/oligo1 with free FR646 (red line) and with non-labeled complementary oligonucleotide (oligo3) (blue line) are shown. It is clearly visible that the influence of free acceptor and of non-labeled oligonucleotide on the energy transfer is negligible.

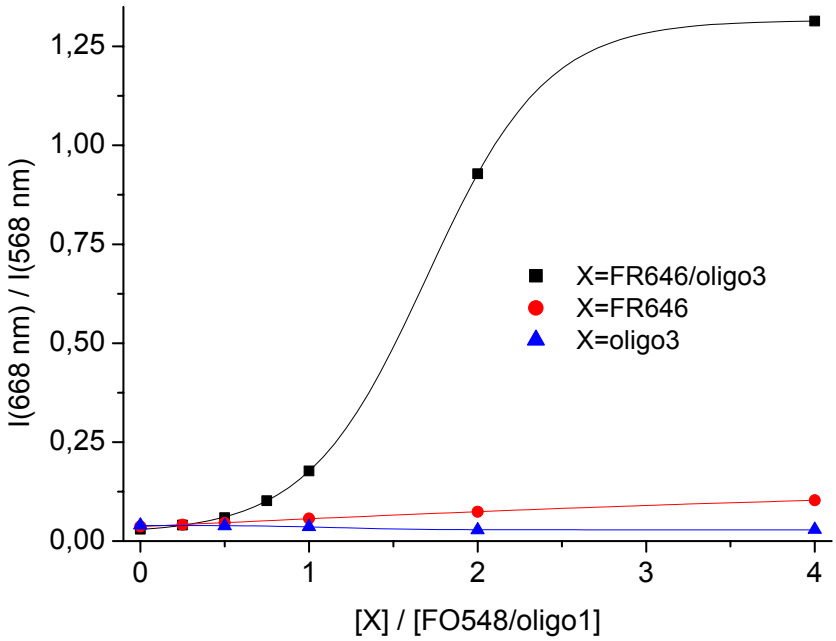

Figure 3.18. Plot of the ratio of the fluorescence intensities at 668 nm and 568 nm versus the ratio of the concentration of titrators (FR646/oligo3, FR646, or oligo3) and the concentration of FO548/oligo1.

The R_0 value and the average distance between the donor and the acceptor molecules were calculated according to the method described in capter 1.3. The R_0 value of the system FO548/oligo1-FR646/oligo3 is 5.9 nm. The average distance between the donor and the acceptor is 4.0 nm.

OB630/oligo5-OG670/oligo4

Two complementary oligonucleotides were labeled at the respective 5'-ends, the one with the phosphoramidite OB630 (oligo5), and on the other with the phosphoramidite OG670 (oligo4). Figure 3.19 shows the titration of the donor OB630/oligo5 at constant concentration ([OB630/oligo5] = $2 \cdot 10^{-7}$ mol/L) with various amounts of acceptor OG670/oligo4. Molar ratios are 1:0, 1:0.25, 1:0.5, 1:1, 1:2, and 1:4. The fluorescence intensity of OB630/oligo5

decreases to 40% with increasing amounts of OG670/oligo4. The fluorescence spectrum of OG670/oligo4 without donor (fig. 3.19; orange line) shows that the acceptor is directly excited at 600 nm. The fluorescence of the acceptor increases not only due to an increase in energy transfer but also due to higher concentration. The ratiometric plot of the measurement is shown on the right side of figure 3.19. At a four-fold excess of OG670/oligo4 saturation is nearly reached.

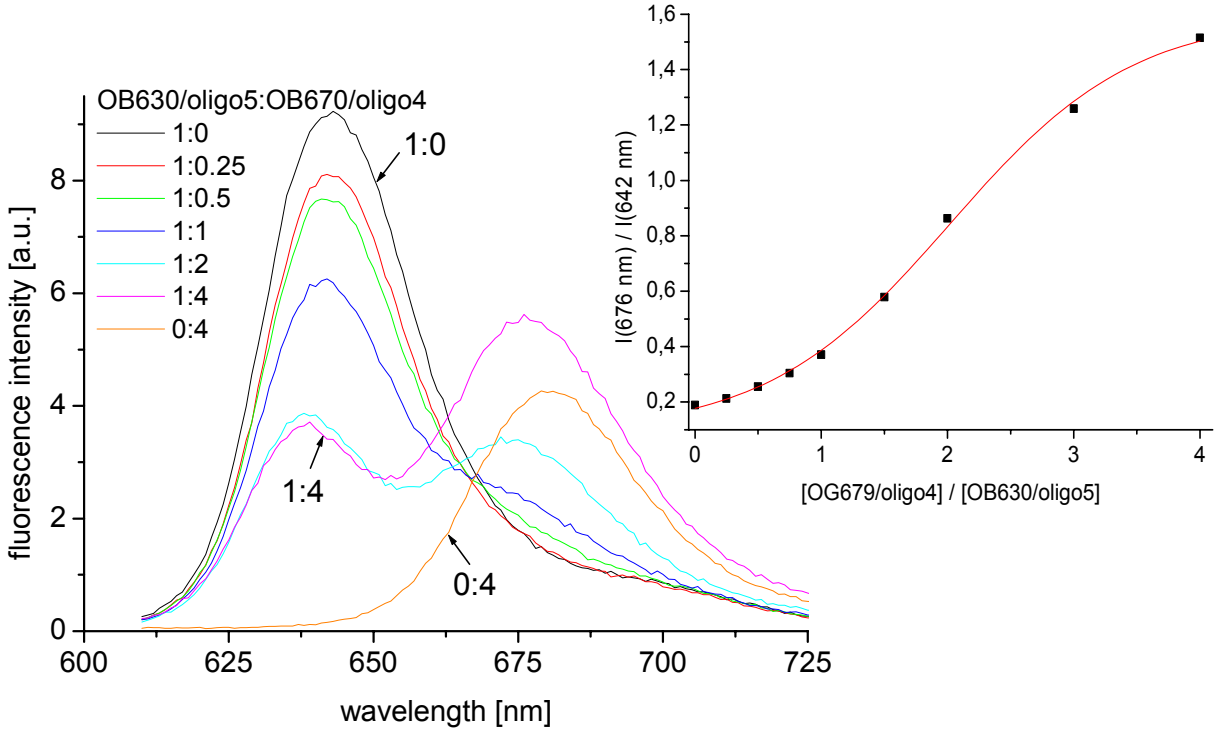

Figure 3.19. Energy transfer study in which OB630/oligo5 of constant concentration ([OB630/oligo5] = $2 \cdot 10^{-7}$ mol/L) was titrated with OG670/oligo4 (λ_{exc} = 600 nm).

The R_0 value of the system OB630/oligo5-OG670/oligo4 was calculated to be 6.3 nm. The average distance between the donor and the acceptor molecules is 6.0 nm.

FO546/oligo1-FR642/oligo2 and FO546/oligo1-FR642/oligo3

The donor FO546/oligo1 was titrated with acceptor FR642/oligo2 (fig. 3.20) and FR642/oligo3 (fig. 3.21), respectively. The fluorescence intensity of the donor decreases to 55% (fig. 3.20) and 13% (fig. 3.21), respectively, with increasing quantities of acceptor, while the fluorescence intensity of the acceptor increases due to energy transfer. In both cases the donor dye FO546 is labeled to the 5'-end of oligo1. In figure 3.20 the acceptor is attached to the 5'-end, in figure 3.21 to the 3'-end of the complementary oligonucleotide. The decreased

energy transfer efficiency (figure 3.20) in comparison to that shown in figure 3.21 shows that the donor-acceptor distance is much larger in case of 5'-5' labeling.

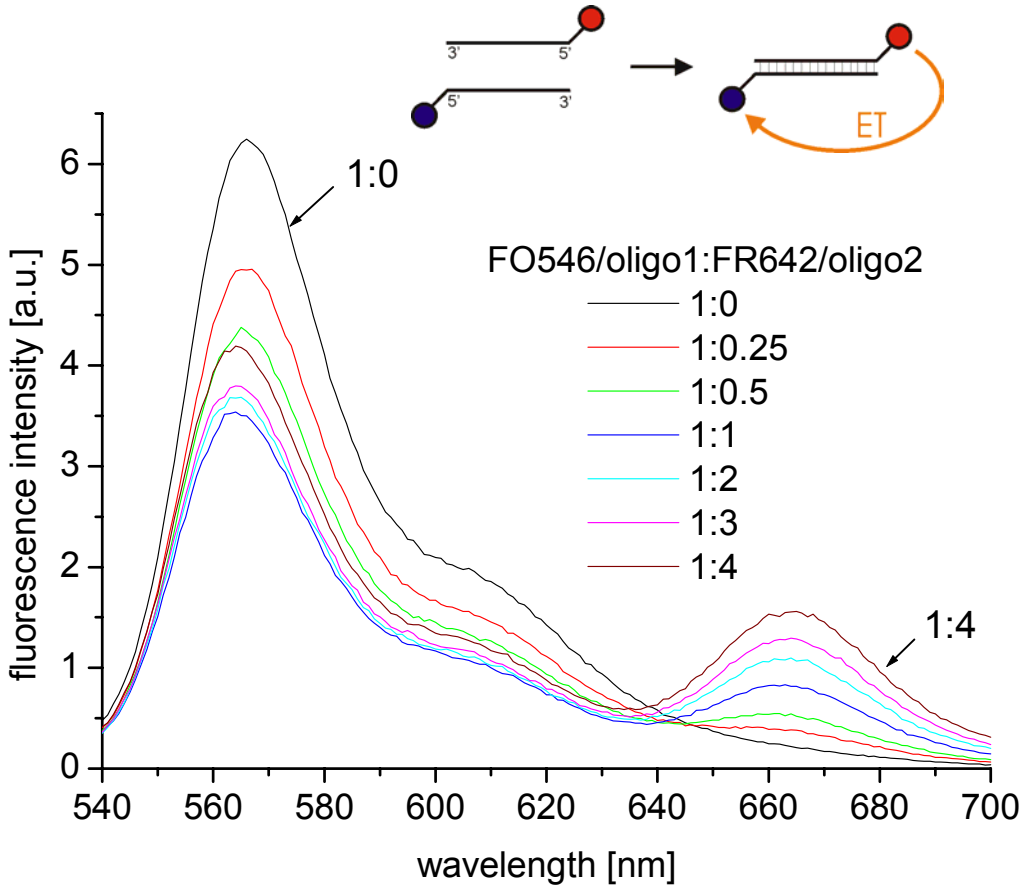

Figure 3.20. Energy transfer study in which FO546/oligo1 of constant concentration ([FO546/oligo1] = $1.0 \cdot 10^{-7}$ mol/L) was titrated with FR642/oligo2 (λ_{exc} = 530 nm).

The R_0 value of the system FO546/oligo1-FR642/oligo2 was calculated to be 5.8 nm. The average distance between the donor and the acceptor molecules is 5.5 nm. The calculations were carried out according to the method described in chapter 1.3.

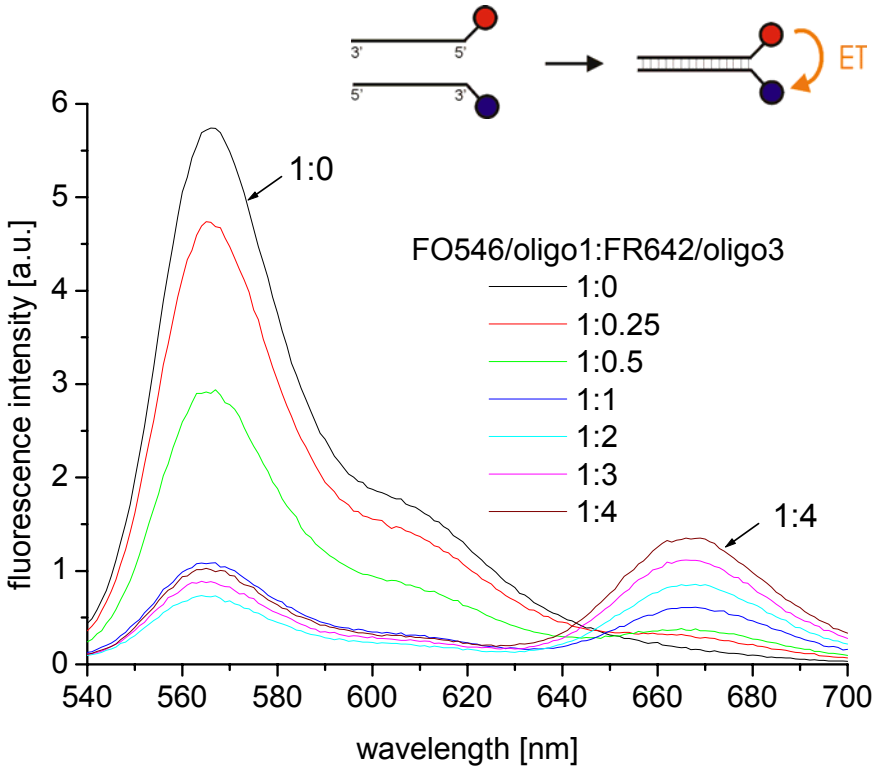

Figure 3.21. Energy transfer study in which FO546/oligo1 ([FO546/oligo1] = $1.0 \cdot 10^{-7}$ mol/L) was titrated with FR642/oligo3 (λ_{exc} = 530 nm).

The R_0 value of the system FO546/oligo1-FR642/oligo3 was calculated to be 5.9 nm. The average distance between the donor and the acceptor molecules is 4.3 nm.

Figure 3.22 shows the so-called binding curves, the plot of the ratio of the two peak intensities versus the concentration ratio of the labeled oligonucleotides. In both cases saturation of the curve is nearly reached at a two-fold excess of acceptor. The energy transfer rate is much higher if FR642/oligo3 is used as acceptor instead of FR642/oligo2, because in this case the distance between donor and acceptor is much shorter.

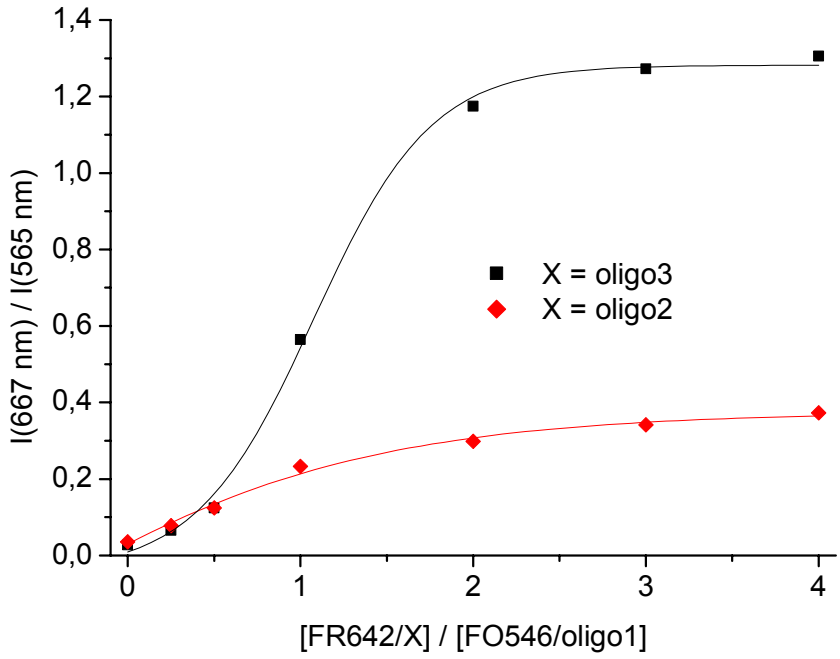

Figure 3.22. Plot of the ratio of the fluorescence intensities at 667 nm and 565 nm versus the ratio of the concentration of titrators (FR642/oligo2 and FR642/oligo3) and the concentration of FO546/oligo1.

The Förster radii (R_0) of the donor-acceptor pairs are summarized in table 3.1. They all are around 6 nm. In comparison to existing systems (2.2 nm in [7], 4.9 nm in [8]), the R_0 values of the used dye pairs are higher which enables energy transfer measurements over larger distances. This is of special significance in case of 5'-5' labeling. If the R_0 values were smaller, the energy transfer efficiency would be to low to be detected.

The average distances between the donor and acceptor molecule were computed using these R_0 values. If the position of the labels is 5' (donor) and 3' (acceptor) the average donor-acceptor distance was found to be around 4 nm. If both donor and acceptor are attached to the 5'-ends of the complementary oligonucleotides, the average donor-acceptor distance was found to be around 6 nm (table 3.1.). The calculated values are average distances because the flexible spacer groups between oligonucleotide and dye result in a variable distance of the fluorophores to each other.

Table 3.1. Calculated R_0 values and average distances between donor and acceptor molecules.

Donor	Acceptor	R_0 [nm]	Distance [nm]	Labeling Positions
FO548/oligo1	FR646/oligo3	5.9	4.0	5' – 3'
OB630/oligo5	OG670/oligo4	6.3	6.0	5' – 5'
FO-C7/oligo1	FR642/oligo2	5.8	5.5	5' – 5'
FO-C7/oligo1	FR642/oligo3	5.9	4.3	5' – 3'

R_0 values were calculated by Jörg Enderlein, Forschungszentrum Jülich, Institute of Biological Information Processing I, 52425 Jülich, Germany. Calculations were carried out according to the method described in chapter 1.3.

3.2.2. Competitive Hybridization Assays

FO548/oligo1-FR646/oligo3

Figure 3.23 shows a competitive hybridization assay in which FR646/oligo3 of constant concentration ([FR646/oligo3] = $1.7 \cdot 10^{-7}$ mol/L) and various amounts of non-labeled oligo3 were mixed, and a constant amount of FO548/oligo1 ([FO548/oligo1] = $1.7 \cdot 10^{-7}$ mol/L) was added. The fluorescence of the donor increases with increasing fractions of oligo3. The acceptor is displaced by non-labeled oligonucleotide and energy transfer efficiency is reduced. In this case the decrease of the acceptor intensity is not visible due to the low fluorescence intensity of the acceptor. The plot of the ratio of the two peak intensities versus the concentration ratio of the non-labeled oligonucleotides to the acceptor shows the binding curve very well (fig. 3.23; left side). Saturation is reached at am about 3-fold excess of oligo3. Determination of analyte concentration is possible in the dynamic range from $4 \cdot 10^{-8}$ mol/L to $2 \cdot 10^{-7}$ mol/L which was determined graphically. A negative control with oligo8 which neither hybridizes with FO548/oligo1 nor with FR646/oligo3 was performed for the purpose of comparison. The binding curve shows that in this case energy transfer is not affected at all (fig. 3.23; left side, red line).

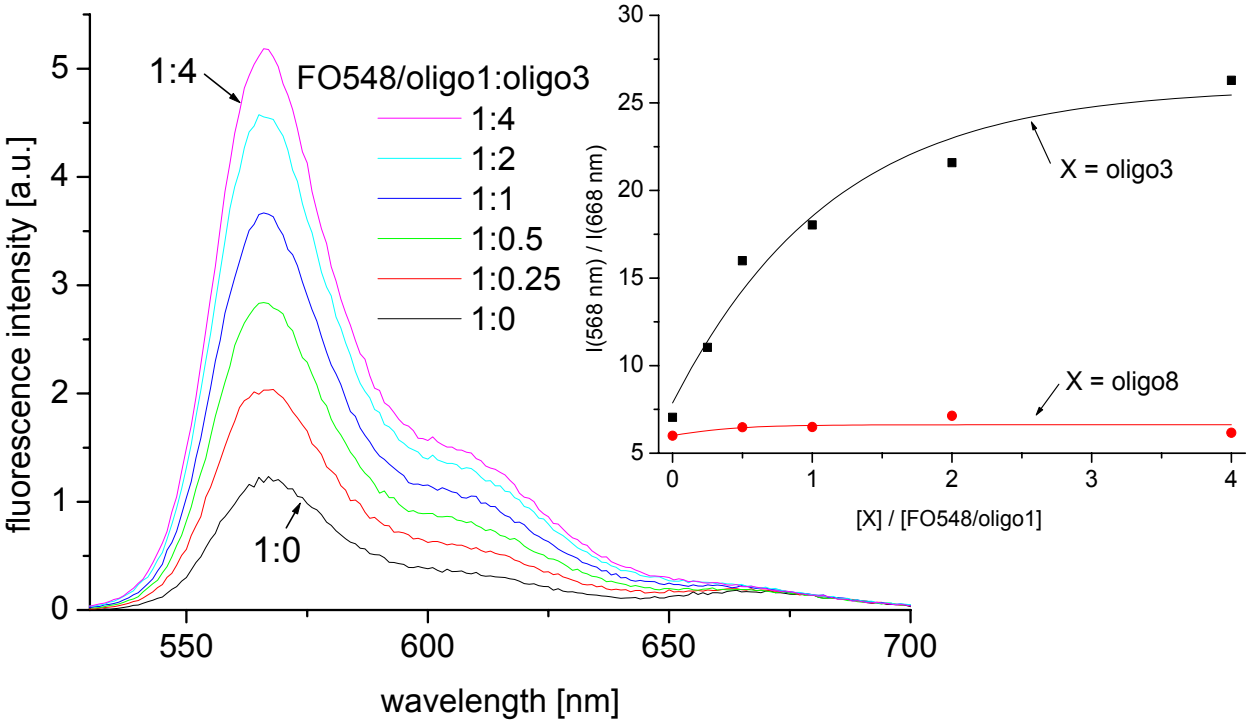

Figure 3.23. **Left side:** Competitive immunoassay in which FR646/oligo3 of constant concentration ([FR646/oligo3] = $1.7 \cdot 10^{-7}$ mol/L) was mixed with various amounts of non-labeled oligo3 and constant quantities of FO548/oligo1 ([FO548/oligo1] = $1.7 \cdot 10^{-7}$ mol/L). λ_{exc} = 500 nm.

Right side: Plot of the ratio of the two peak intensities versus the concentration ratio of the non-labeled oligonucleotides and FO548/oligo1.

OB630/oligo5-OG670/oligo4

The effect of single mismatches in an oligonucleotide on the hybridization rate was examined via a competitive hybridization assay on the system OB630/oligo5-OG670/oligo4. The donor of constant concentration ([OB630/oligo5] = $1.67 \cdot 10^{-7}$ mol/L) was mixed with the following non-labeled oligonucleotides: oligo3 (no mismatch), oligo6 (single mismatch), or oligo7 (double mismatch). Constant quantities of acceptor ([OG670/oligo4] = $1.67 \cdot 10^{-7}$ mol/L) were added. The binding curves are shown in figure 3.24. Oligo3 which is complementary to OG670/oligo4 shows the most efficient binding (fig. 3.24; black line). If one single mismatch is introduced into the center of the oligonucleotide (oligo6) binding is expected to be reduced. This effect is displayed in figure 2.24 (red line). Using oligo6 (single mismatch) the ratio I(642 nm)/I(674 nm) is reduced to 75% in comparison to oligo3. If a second mismatch next to the first one is introduced, this effect is enhanced (blue line). I(642 nm)/I(674 nm) drops to

25% compared to oligo3. Determination of the concentration of oligo3 is possible in the dynamic range from $8 \cdot 10^{-8}$ mol/L to $5 \cdot 10^{-7}$ mol/L which was determined graphically.

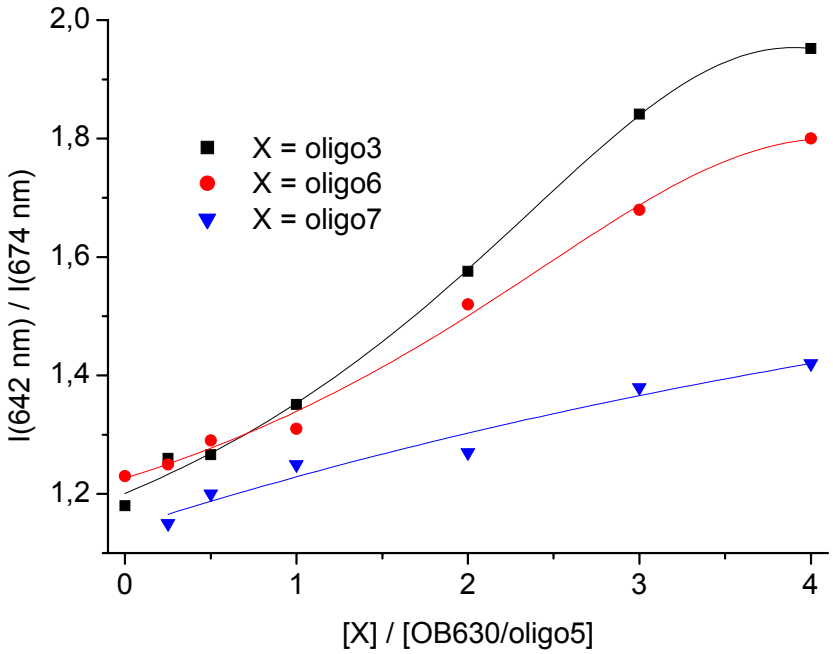

Figure 3.24. Competitive hybridization assays in which OB630/oligo5 (donor) of constant concentration ([OB630/oligo5] = $1.67 \cdot 10^{-7}$ mol/L) was mixed with oligo3 (no mismatch), oligo6 (single mismatch), or oligo7 (double mismatch), and constant quantities of OG670/oligo4 (acceptor) ([OG670/oligo4] = $1.67 \cdot 10^{-7}$ mol/L) were added. λ_{exc} = 600 nm.

3.2.3. Fluorescence in Situ Hybridization (FISH)

A common method of introducing fluorophores into probe DNA is to use fluorescent bases. The reactive amino group attached to dUTP can be coupled to a wide variety of reactive fluorophores, including OSI esters (see figure 3.25.).

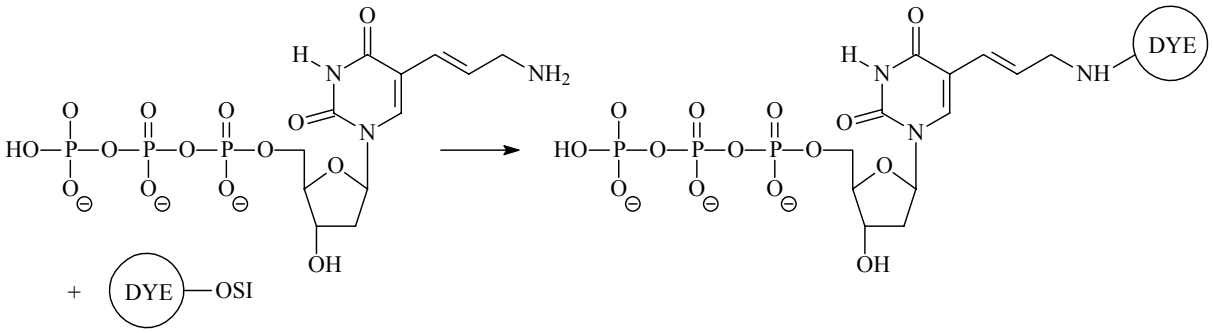

Figure 3.25. Scheme for the reaction of aminoallyl dUTP with the OSI ester of a fluorescent dye.

In this work, FR661 and PB634 were conjugated to aminoallyl dUTP. The labeled dUTP was employed in PCR producing specific sequences of DNA (known as the *probe*) which were labeled with fluorescent molecules throughout their lengths. A mixture of probes specific for many regions along the length of one specific chromosome, in our case the mouse Y-chromosome, was produced and applied in fluorescence in situ hybridization (FISH).

FISH is a highly versatile method based on the ability of DNA to hybridize to its complementary sequence [9]. First, the biological material has to be fixed to preserve morphology. Then, the double strands of DNA in both the probe DNA and the chromosome DNA have to denature so that they can hybridize to each other. This is done by heating the DNA (70 - 80 °C). After that, the probe is placed on a slide and a glass coverslip is placed on top. The slide is then placed in a 37 °C incubator for several hours for the probe to hybridize with the target chromosome. The probe DNA seeks out its target sequence on the specific chromosome and binds to it. The strands slowly reanneal. Then the slide is washed to remove any of the probe that did not bind to chromosomes. A differently colored fluorescent dye is added to the slide to stain all of the chromosomes so that they may then be viewed using a fluorescence microscope [10, 11].

Such an experiment was performed with a probe which contained aminoallyl dUTP. It is possible to clearly visualize under a fluorescence microscope that the probe labeled with PB634 has hybridized to the mouse Y-chromosome. Figure 3.26 shows the mouse metaphase

recorded with a b/w CCD camera. The chromosomes in figure 3.26 are miscolored, where the X-chromosomes are colored blue and the Y-chromosome is colored green.

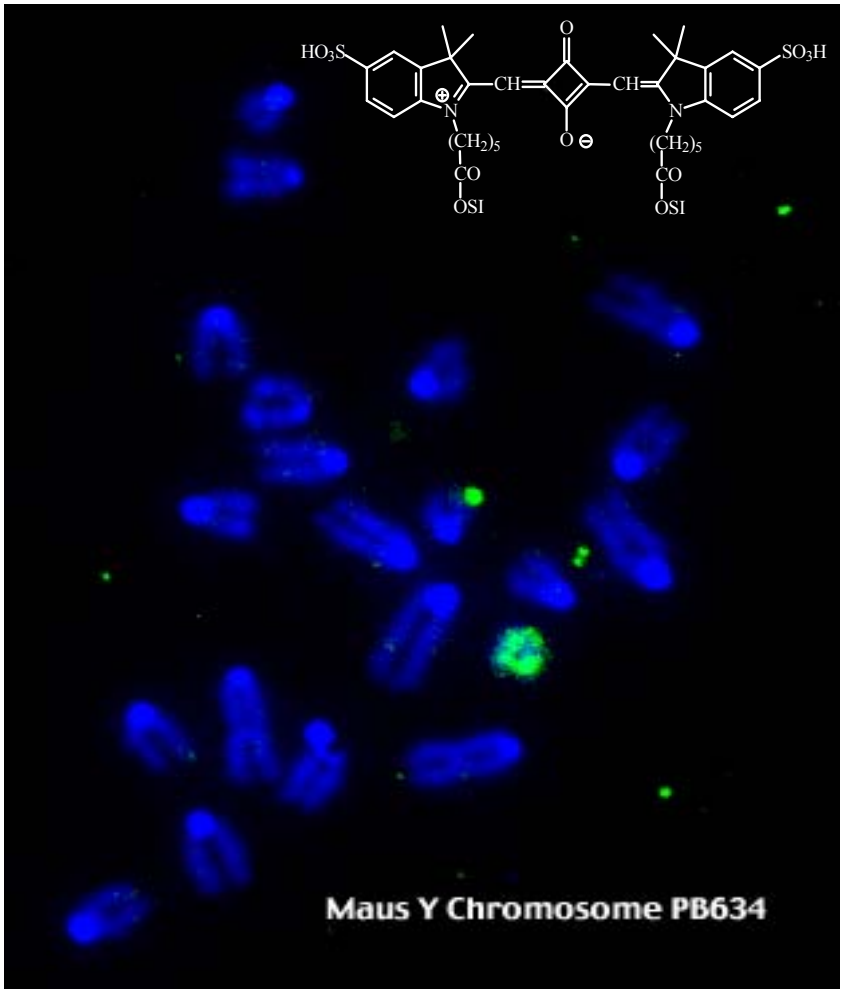

Figure 3.26. Mouse metaphase recorded with a b/w CCD camera. The chromosomes are painted in blue and the Y-chromosome is painted in green.

In contrast to the above result, a FISH using DNA probes labeled with FR661 yielded no results, because the fluorescence of the DNA probes was too weak to be detected by fluorescence microscope.

3.3. Conclusions

Immunosystems

In this work immunostudies were performed on the system HSA/anti-HSA. Binding studies were performed on the systems FO546/HSA-FR642/anti-HSA, FO548/HSA-FR646/anti-HSA, and [Ru(bpy)$_2$(mcbpy)]/HSA-FR662/anti-HSA. All of these systems worked properly and gave sigmoidal binding curves. The shape of the curve strongly depends on the DPRs of

the donor and acceptor conjugates, respectively. The influence of non-labeled anti-HSA on the fluorescence of donor labeled HSA is negligible. Free acceptor dye may have influence on the ratiometric plot, because on the one hand it can be excited by the light source and on the other hand it might bind non-covalently to HSA which enables non-desired energy transfer. The use of a ruthenium comlex with a large Stokes' shift as donor dye has the advantage that at the excitation wavelenght of 460 nm the acceptor is not excited by the light source.

Homogenous competitive immunoassays were shown using the systems FO546/HSA-FR642/anti-HSA, FO548/HSA-FR646/anti-HSA. These systems can be used for the determination of HSA concentrations in the range of $2 \cdot 10^{-9}$ - $2.5 \cdot 10^{-7}$ mol/L. A larger concentration range could be obtained by further variations of the DPRs or by variation of the concentrations or ratios of donor and acceptor. It was proved that BSA has no influence on the immunosystem.

A cytometric measurement has been performed to show the applicability of the dyes in flow cytometry. The introduced systems can be used for the determination of HSA concentrations in the range of 0 - 120 µg/mL ($1.5 \cdot 10^{-7}$ - $1.8 \cdot 10^{-8}$ mol/L).

Hybridization Systems

Hybridization binding studies were carried out on the systems FO548/oligo1-FR646/oligo3, oligo5/oligo4, FO546/oligo1-FR642/oligo2, and FO546/oligo1-FR642/oligo3. The Förster radii (R_0) of the donor-acceptor pairs are all are around 6 nm. The average donor-acceptor distance was found to be around 4 nm if the position of the labels was 5' (donor) and 3' (acceptor), and 6 nm if both donor and acceptor were attached to the 5'-ends of the complementary oligonucleotides.

Competitive hybridization assays were performed on the systems FO548/oligo1-FR646/oligo3 and OB630/oligo5-OG670/oligo4. The presented competitive assays enable determination of oligonucleotide concentrations in the range of $4 \cdot 10^{-8}$ to $6 \cdot 10^{-6}$ mol/L. In addition these measurements enable the distinction of oligonucleotides without, with a single, or with a double mismatch in their sequence.

Fluorescence in situ hybridization (FISH) was carried out using DNA probes labeled with PB634 and FR661, respectively. Good results were only achieved with PB634, because the fluorescence intensity of FR661 was too weak to be detected via fluorescence microscopy.

3.4. References

[1] B. Oswald, F. Lehmann, L. Simon, E. Terpetschnig, and O. S. Wolfbeis (2000) Red Laser Induced Fluorescence Energy Transfer in an Immunosystem, *Anal. Biochem.* **280**, 272-277.

[2] B. Oswald, M. Gruber, M. Böhmer, F. Lehmann, M. Probst, and O. S. Wolfbeis (2001) Novel Diode Laser-compatible Fluorophores and Their Application to Single Molecule Detection, Protein Labeling and Fluorescence Resonance Energy Immunoassay. *Photochem. Photobiol.* **74 (2)**, 237-245.

[3] E.Terpetschnig, H. Szmacinski, H Malak, J. R. Lakowicz, (1995) Metal-ligand complexes as a new class of long lived fluorophores for protein hydrodynamics, *Biophys. J.*, **68**, 342-350.

[4] A. Dürkop, F. Lehmann, O. S. Wolfbeis (2002) Polarization Immunoassays Using Reactive Ruthenium Metal Ligand Complexes as Labels, *Anal. Bioanal. Chemistry,* **372**, 688-694.

[5] C. M. Augustin, B. Oswald, and O. S. Wolfbeis (2002) Time-Resolved Luminescence Energy Transfer Immunobinding Study Using a Ruthenium-Ligand Complex as a Donor Label, *Anal. Biochem.,* **305**, 166-172.

[6] O. S. Wolfbeis, M. Böhmer, A. Dürkop, J. Enderlein, M. Gruber, I. Klimant, C. Krause, J. Kürner, G. Liebsch, Z. Lin, B. Oswald, and M. Wu (2002) Advanced Luminescent Labels, Probes, and Beads, and Their Application to Luminescence Bioassay, and Imaging *in* Springer Series in Fluorescence, (Kraayenhof, R., Ed.), Springer Verlag, Berlin-Heidelberg.

[7] Masuko, M. *et al.* (2000) Fluorescence Resonance Energy Transfer from Pyrene to Perylene Labels for Nucleic Acid Hybridization Assays under Homogeneous Solution Conditions. *Nucleic Acids Res.* **28,** e34, 2-8.

[8] R. A. Cardullo, S. Agrawal, C. Flores, P. C. Zamecnik, and D. E. Wolf (1988) Detection of Nucleic Acid Hybridization by Nonradiative Fluorescence Resonance Energy Transfer, *Procl. Natl. Acad. Sci.,* **85,** 8790-8794.

[9] http://www.thenhs.com/regionalgenetics/FISH/fishintro.htm

[10] http://www.waisman.wisc.edu/cytogenetics/procedures/FISH/FISHmethod.html

[11] http://biochem.boehringer-mannheim.com/Prod_Inf/Manuals/InSitu/p19-25.pdf

4. Experimental Part

4.1. Materials and Methods

4.1.1. Chemicals, Solvents, Proteins and Oligonucleotides

All chemicals and solvents used were purchased from Acros (Geel, Belgium), Aldrich (Steinheim, Germany), Fluka (Buchs, Switzerland), Merck (Darmstadt, Germany) or Sigma (Steinheim, Germany). All chemicals were of analytical grade and were used as received. Anhydrous dichloromethane and DMF were prepared following standard procedures [1]. Water was doubly destilled. HSA and anti-HSA were obtained from Sigma. DNA oligonucleotide syntheses, phosphoramidite labeling, and molecular beacon synthesis were carried out by Metabion (Martinsried, Germany). The following sequences were used: oligo1: amino-5'-CCG GCA GCA AAA TGT-3', oligo2: amino-5'-ACA TTT TGC TGC CGG-3', oligo3: 5'-ACA TTT TGC TGC CGG-3'-amino, oligo4: 5'-CCG GCA GCA AAA TGT-3', oligo5: 5'-ACA TTT TGC TGC CGG-3', oligo6: 5'-ACA TTT TCC TGC CGG-3', oligo7: 5'-ACA TTT ACC TGC CGG-3, oligo8: 5'-GGC CGT CGT TTT ACA.

Phosphate buffer (PBS) of pH 7.2, 100 mM: 25.79 g of $Na_2HPO_4 \cdot 12\ H_2O$ and 4.37 g of $NaH_2PO_4 \cdot 2\ H_2O$ are dissolved in 1 L of doubly destilled water. Bicarbonate buffer (BCBS) of pH 9, 50 mM: 2.1 g of $NaHCO_3$ are dissolved in 500 mL of doubly destilled water. Triethylammonium acetate (TEAA) of pH 7.1, 0.1 M: 13.8 mL of triethylamine and 5.76 mL of acetic acid are mixed and diluted to 1 L with water. The buffers are adjusted to the corresponding pH value with 1 N HCl and 1 N NaOH, respectively. pH measurements were performed with a WTW pH 196 pH meter with temperature compensation.

4.1.2. Chromatography

For analytical thin-layer chromatography RP-18 (TLC) F_{254s} aluminum sheets and silica gel 60 F_{254} aluminum sheets (thickness 0.2 mm each) from Merck (Darmstadt, Germany) were used. Column chromatography was carried out using silica gel 60 (40-63 μm) as the stationary phase for non-polar substances and silica gel 60 RP-18 (40-63 μm) or LiChroprep RP-18 (40-63 μm) as the stationary phase for polar substances (all from Merck). HPLC was performed on a Knauer HPLC 64 apparatus. A Hibar pre-packed column RT (250 x 4 mm) packed with LiChrosorb RP 18 (10 μm) was used as the stationary phase.

Labeled protein was separated from unlabeled dye by gel permeation chromatography using Sephadex G-25 from Sigma as the stationary phase (2 x 12 cm column) and a 22 mM PBS of pH 7.2 as the eluent.

4.1.3. Melting Points

Melting points (m.p.) were measured with a melting point apparatus "Dr. Tottoli" from Büchi. They were determined in open capillary tubes and are not corrected.

4.1.4. Spectra

^{1}H-NMR spectra were recorded with a 250 MHz PFT-NMR spectrometer (AC 250 from Bruker) or a 400 MHz PFT-NMR spectrometer (ARX 400 from Bruker). The internal or external standard was tetramethylsilan (TMS) or the solvent. ^{31}P-NMR spectra were recorded with a 400 MHz PFT-NMR spectrometer (ARX 400 from Bruker) with H_3PO_4 as external standard. The chemical shifts are given in ppm. The following abbreviations were used to describe the signals: s = singlet, d = doublet, dd = doublet of doublets, dt = doublet of triplets, t = triplet, q = quartet, quin = quintet, m = multiplet, b = broad. Mass spectra were recorded with a Finnigan MAT 95 (fast-atom bombardment, FAB) and with a Finnigan SSQ 2000 (electro-spray ionization, ESI).

Absorption spectra were taken with a Cary 50 Bio UV-Visible Spectrophotometer from Varian. Emission spectra were recorded with a luminescence spectrometer Aminco Bowman (Series 2) from SLM with a standard 150 W xenon lamp as the excitation source.

4.2. Synthesis and Purification of the Dyes

4.2.1. FO544

4.2.1.1. 1-(3-Ethoxycarbonyl-propyl)-2,3,3-trimethyl-3*H*-indolium Bromide

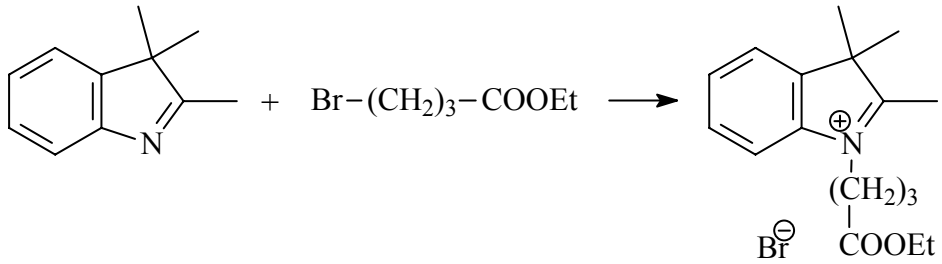

$C_{11}H_{13}N$	$C_6H_{11}BrO_2$	$C_{17}H_{24}BrNO_2$
159.23	195.06	354.29

5.00 mL (31.1 mmol) of 2,3,3-trimethyl-3*H*-indole and 4.45 mL (31.1 mmol) of ethyl-4-bromobutyrate are heated under stirring in a pressure tube to 110 °C under argon for 16 h. After cooling to room temperature the solid is dissolved in water and diethylether is added. The aqueous phase is extracted with diethylether. The aqueous phase is collected and water is removed on a rotary evaporator. The amorphous red residue is dried in a desiccator over P_2O_5. The residue is washed twice with 20 mL of acetone and a white powder remains.

Yield: 4.90 g, (13.8 mmol, 44%), white powder, $C_{17}H_{24}BrNO_2$ (354.29 g/mol).
^{1}H-NMR (DMSO, TMS external): δ 8.00 (m, 1H), 7.83 (m, 1H), 7.63 (m, 2H), 4.46 (t, 2H), 4.02 (q, b 2H), 2.83 (s, 3H), 2.08 (m, 2H), 1.53 (s, 6H), 1.14 (t, 3H).

4.2.1.2. 1-[2-(Diethoxyphosphoryl)-ethyl]-2,3,3-trimethyl-3*H*-indolium Bromide

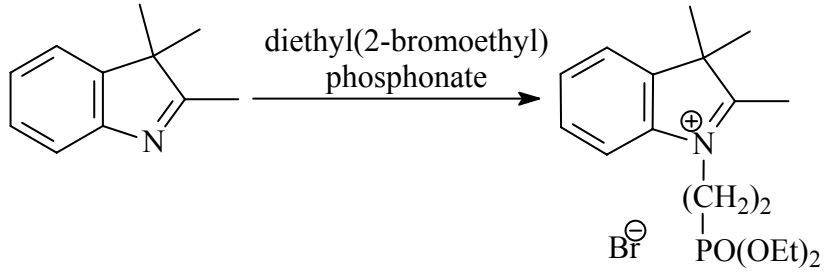

$C_{11}H_{13}N$ 159.23

$C_{17}H_{27}BrNO_3P$ 404.28

1.00 mL (991 mg, 6,22 mmol) of 2,3,3-trimethyl-3*H*-indole and 1.00 mL (1.35 g, 5.50 mmol) of diethyl(2-bromoethyl)phosphonate are dissolved in a mixture of 5 mL of water and 3 mL of ethanol. The solution is refluxed for 30 h. After cooling to room temperature the solvent is removed under reduced pressure. The residue is dissolved in water and extracted with diethylether. The aqueous phase is collected and water is removed on a rotary evaporator. The amorphous product is dried in a desiccator over P_2O_5 and then triturated with ethylacetate until the faintly purple product crystallizes.

Yield: 660 mg (1.63 mmol, 30%), faintly purple powder, $C_{17}H_{27}BrNO_3P$ (404.29 g/mol).
m.p.: 108 °C, R_f (silica gel RP-18, methanol): 0.67.
^{1}H-NMR (D_2O, TMS external): δ 7.69-7.40 (m, 4H), 4.66 (m, 2H), 3.94 (m, 4H), 2.63 (s, 3H), 2.55 (m, 2H), 1.43 (s, 6H), 1.06 (t, 6H). (Singlet for 2-methyl does not appear in D_2O.)
FAB-MS: m/e (M^+, cation) for $C_{17}H_{27}NO_3P$, calculated 324.4, found 324.3.

4.2.1.3. FO544-Acid

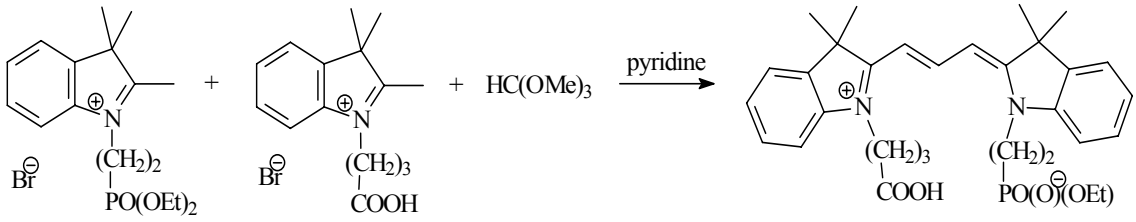

$C_{17}H_{27}BrNO_3P$ 404.28 | $C_{15}H_{20}BrNO_2$ 326.23 | $C_4H_{10}O_3$ 120.15 | $C_{31}H_{39}N_2O_5P$ 550.63

1.20 g (2.96 mmol) of 1-[2-(diethoxyphosphoryl)ethyl]-2,3,3-trimethyl-3*H*-indolium bromide and 1.05 g (2.96 mmol) of 1-(3-ethoxycarbonyl-propyl)-2,3,3-trimethyl-3*H*-indolium bromide are heated in 12 mL of pyridine to 95 °C until the educts dissolve. 400 µL (3.64 mmol) of 1,1,1-trimethoxymethane are added and the solution is kept at 95 °C for 15 h. After cooling to room temperature the purple solution is slowly dropped into 150 mL of diethylether whereas the purple product precipitates. The suspension is allowed to stand for 30 minutes. Diethylether is decanted. The precipitate is dissolved in 10 mL of methanol. 10 mL of water and 276 mg of K_2CO_3 are added and the solution is refluxed for 5 h. The solvent is removed on a rotary evaporator. The raw product is purified by column chromatography using silica gel 60 RP-18 (40-63 µm) as the stationary phase and a methanol/water mixture (50:50 v/v) as the eluent.

Yield: 118 mg (0.21 mmol, 7%), purple powder, $C_{31}H_{39}N_2O_5P$ (550.63 g/mol).

R_f (silica gel RP-18, methanol:water 75:25 v/v): 0.58.

^{1}H-NMR (d_4-methanol): δ 7.88 (t, 1H), 6.87 (m, 2H), 6.80-6.75 (m, 4H),6.63, (m, 2H), 5.84 (dd, 2H), 3.65 (m, 2H), 3.54 (t, 2H), 3.30 (quin, 2H), 1.72 (t, 2H), 1.49-1.33 (m, 4H), 1.10 (s, 6H), 1.09 (s, 6H), 1.60 (t, 3H).

4.2.1.4. FO544-OSI Ester

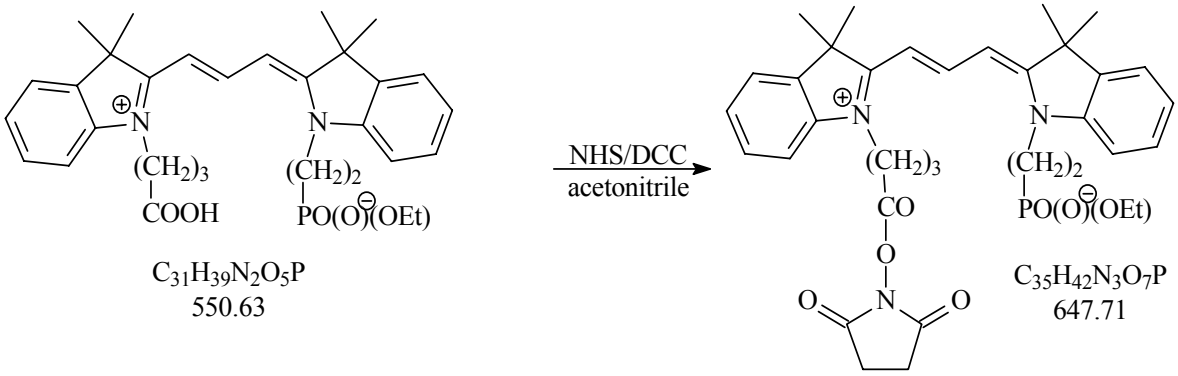

$C_{31}H_{39}N_2O_5P$ 550.63 → $C_{35}H_{42}N_3O_7P$ 647.71

28.5 mg (51.7 µmol) of FO544-acid, 11.9 mg (103 µmol) of NHS and 21.4 mg (103 µmol) of DCC are dissolved in 1 mL of dry acetonitrile. The solution is stirred at room temperature for 20 h. The solvent is removed on a rotary evaporator and the raw product is washed with diethylether. The OSI ester is used without further purification.

Yield: 23.0 mg (41.8 µmol, 81%), purple powder, $C_{35}H_{42}N_3O_7P$ (647.71 g/mol).

R_f (silica gel RP-18, methanol:water 75:25 v/v): 0.42.

4.2.2. FO545

4.2.2.1. 1-(5-Carboxypentyl)-2,3,3-trimethyl-3*H*-indolium Bromide

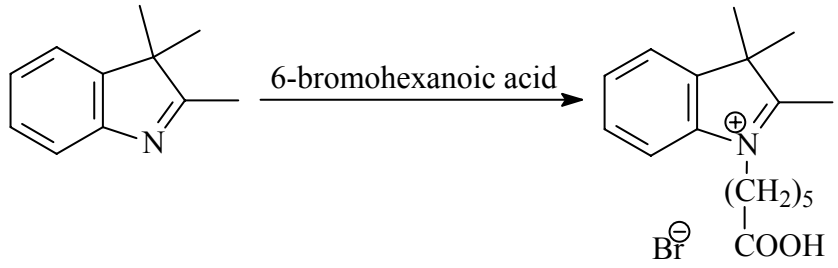

$C_{11}H_{13}N$
159.23

$C_{17}H_{24}BrNO_2$
354.29

1.00 mL (991 mg, 6.22 mmol) of freshly distilled 2,3,3-trimethyl-3*H*-indole and 1.23 g (6.22 mmol) of 6-bromohexanoic acid are heated to 110 °C under argon for 18 h. After cooling to room temperature the solid is dissolved in water and extracted with ether. The aqueous phase is collected and water is removed on a rotary evaporator. The product is dried in a desiccator over P_2O_5.

Yield: 1.61 g (4.54 mmol, 73%), faintly purple powder, $C_{17}H_{24}BrNO_2$ (354.29 g/mol).

R_f (silica gel RP-18, methanol): 0.61.

^{1}H-NMR (DMSO, TMS external): δ 7.96 (m, 1H), 7.84 (m, 1H), 7.62 (m, 2H), 4.44 (t, 2H), 2.83 (s, 3H), 2.22 (t, 2H), 1.83 (m, 2H), 1.55 (m, 2H), 1.52 (s, 6H), 1.41 (m, 2H).

4.2.2.2. FO545-Acid

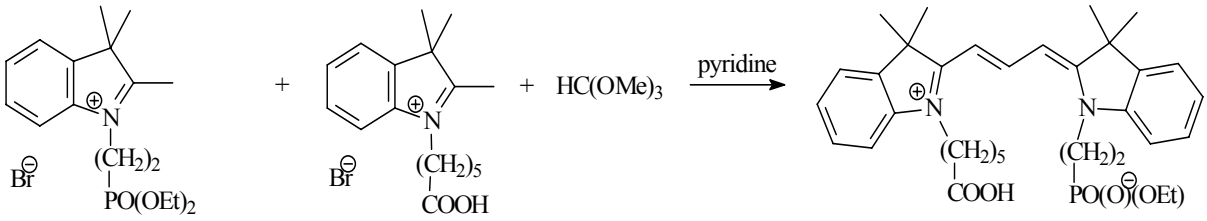

$C_{17}H_{27}BrNO_3P$ 404.28 | $C_{17}H_{24}BrNO_2$ 354.29 | $C_4H_{10}O_3$ 120.15 | $C_{33}H_{43}N_2O_5P$ 578.69

1.20 g (2.96 mmol) of 1-[2-(diethoxyphosphoryl)ethyl]-2,3,3-trimethyl-3*H*-indolium bromide and 1.05 g (2.96 mmol) of 1-(5-carboxypentyl)-2,3,3-trimethyl-3*H*-indolium bromide are heated in 12 mL of pyridine to 95 °C until the educts dissolve. 400 µL (3.64 mmol) of 1,1,1-trimethoxymethane are added and the solution is kept at 90 °C for 18 h. After cooling to room temperature diethylether is added until the purple product precipitates. The raw product is purified by two steps of column chromatography. In the first step silica gel 60 RP-18 (40-63 µm) was used as the stationary phase and a methanol/water mixture (50:50 v/v) containing 0.1% NH_3 as the eluent. Second LiChroprep RP-18 (40-63 µm) was used as the stationary phase and a methanol/water mixture (80:20 v/v) as the eluent.

Yield: 115.0 mg (0.20 mmol, 7%), purple powder, $C_{33}H_{43}N_2O_5P$ (578.69 g/mol).
R_f (silica gel RP-18, methanol:water 7:3 v/v): 0.26.
^{1}H-NMR (d_4-methanol, TMS): δ 8.54 (t, 1H), 7.52 (m, 2H), 7.47-7.28 (m, 6H), 6.50 (d, 1H), 6.46 (d, 1H), 4.30 (m, 2H), 4.16 (t, 2H), 3.97 (quin, 2H), 2.31 (t, 2H), 1.98 (m, 2H), 1.86 (t, 2H), 1.77 (s, 6H), 1.76 (s, 6H), 1.70 (m, 2H), 1.52 (m, 2H), 1.27 (t, 3H). ^{31}P{^{1}H}-NMR (d_4-methanol, H_3PO_4 external): δ 21.80.

4.2.2.3. FO545-OSI Ester

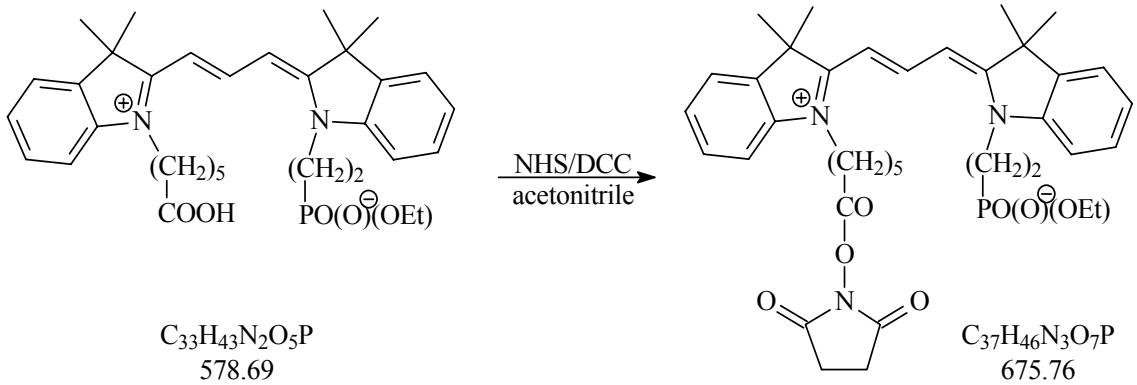

$C_{33}H_{43}N_2O_5P$ 578.69 | $C_{37}H_{46}N_3O_7P$ 675.76

30.0 mg (51.8 µmol) of FO545-acid, 11.9 mg (104 µmol) of NHS and 21.4 mg (104 µmol) of DCC are dissolved in 1 mL of dry acetonitrile. The solution is stirred at room temperature for 20 h. The solvent is removed on a rotary evaporator and the raw product is purified by column chromatography using LiChroprep RP-18 (40-63 µm) as the stationary phase and a water/acetone mixture (40:60 v/v) as the eluent.

Yield: 24.0 mg (35.5 µmol, 69%), purple powder, $C_{37}H_{46}N_3O_7P$ (675.76 g/mol).

R_f (silica gel RP-18, methanol:water 70:30 v/v): 0.16.

^{1}H-NMR (d_4-methanol, TMS): δ 8.54 (t, 1H), 7.53 (m, 2H), 7.46-7.28 (m, 6H), 6.48 (m, 2H), 4.30 (m, 2H), 4.16 (t, 2H), 3.97 (quin, 2H), 2.66 (s, 4H), 2.02 (m, 2H), 1.87 (t, 2H), 1.79 (m, 2H), 1.77 (s, 6H), 1.76 (s, 6H), 1.67 (m, 2H), 1.59 (m, 2H), 1.26 (t, 3H).

4.2.3. FO546

4.2.3.1. 1-(7-Carboxyheptyl)-2,3,3-trimethyl-3*H*-indolium Bromide

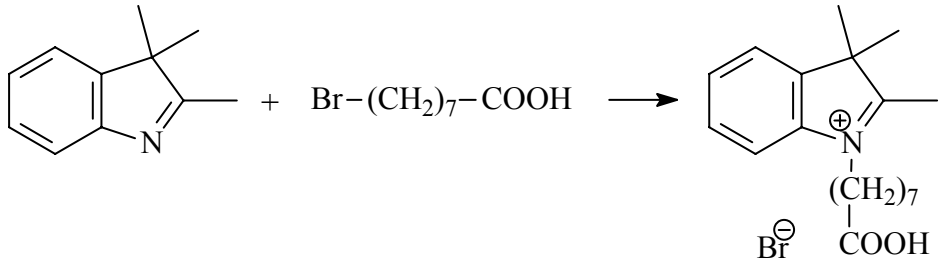

$C_{11}H_{13}N$	$C_8H_{15}BrO_2$	$C_{19}H_{28}BrNO_2$
159.23	223.11	382.34

1.00 mL (6.23 mmol) of 2,3,3-trimethyl-3*H*-indole and 1.39 g (6.23 mmol) of 8-bromooctanoic acid are heated under stirring in a pressure tube to 110 °C under argon for 16 h. After cooling to room temperature the solid is dissolved in 40 mL of water and 20 mL diethylether are added. The aqueous phase is extracted five times with 20 mL of diethylether. The aqueous phase is collected and the water is removed on a rotary evaporator. The amorphous red residue is dried in a desiccator over P_2O_5.

Yield: 2.12 g (5.54 mmol, 89%), amorphous brown solid, $C_{19}H_{28}BrNO_2$ (382.34 g/mol).

^{1}H-NMR (DMSO, TMS external): δ 7.95 (m, 1H), 7.82 (m, 1H), 7.62 (m, 2H), 4.44 (t, 2H), 2.83 (s, 3H), 2.18 (t, 2H), 1.81 (m, 2H), 1.52 (s, 6H), 1.48-1.26 (m, 8H).

4.2.3.2. FO546-Acid

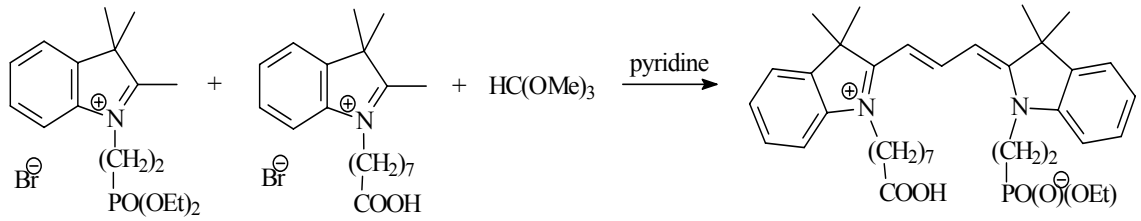

$C_{17}H_{27}BrNO_3P$ 404.28 | $C_{19}H_{28}BrNO_2$ 382.34 | $C_4H_{10}O_3$ 120.15 | $C_{35}H_{47}N_2O_5P$ 606.74

972 mg (2.40 mmol) of 1-[2-(diethoxyphosphoryl)ethyl]-2,3,3-trimethyl-3*H*-indolium bromide and 915 mg (2.40 mmol) of 1-(7-carboxyheptyl)-2,3,3-trimethyl-3*H*-indolium bromide are heated in 10 mL of pyridine to 90 °C until the educts dissolve. 324 µL (2.94 mmol) of 1,1,1-trimethoxymethane are added and the solution is kept at 90 °C for 18 h. After cooling to room temperature the purple solution is slowly dropped into 150 mL of diethylether whereas the purple product precipitates. The suspension is allowed to stand for 30 minutes. Diethylether is decanted. The precipitate is dissolved in 10 mL of methanol. 10 mL of water and 276 mg of K_2CO_3 are added and the solution is refluxed for 20 h. The solvent is removed on a rotary evaporator. The raw product is purified by column chromatography using silica gel 60 RP-18 (40-63 µm) as the stationary phase and a methanol/water mixture (50:50 v/v) as the eluent.

Yield: 93.0 mg (0.15 mmol, 6%), purple powder, $C_{35}H_{47}N_2O_5P$ (606.74 g/mol).

R_f (silica gel RP-18, methanol:water 7:3 v/v): 0.36.

^{1}H-NMR (d_4-methanol, TMS): δ 8.54 (t, 1H), 7.53 (m, 2H), 7.46-7.28 (m, 6H), 6.49 (t, 2H), 4.31 (m, 2H), 4.16 (t, 2H), 3.97 (quin, 2H), 2.24 (t, 2H), 2.02 (m, 2H), 1.84 (m, 2H), 1.76 (s, 12H), 1.59 (m, 2H), 1.44-1.32 (m, 6H), 1.26 (t, 3H).

4.2.3.3. FO546-OSI Ester

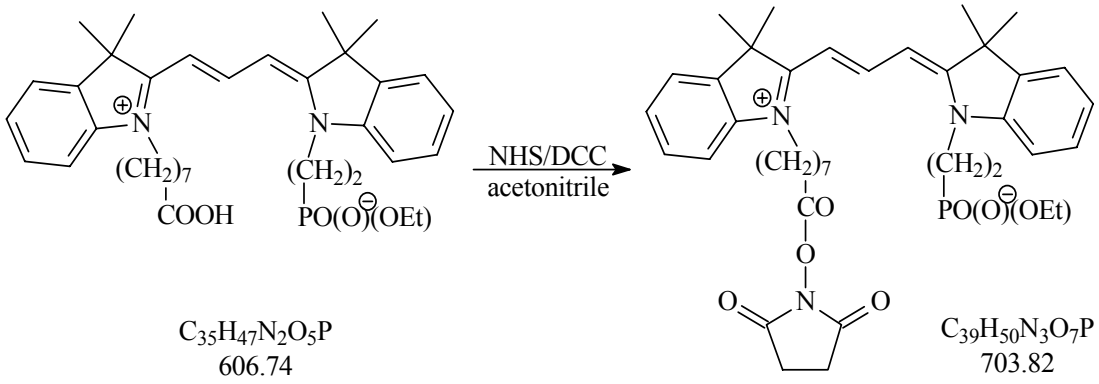

$C_{35}H_{47}N_2O_5P$ 606.74 | $C_{39}H_{50}N_3O_7P$ 703.82

150.0 mg (247.2 µmol) of FO546-acid, 42.6 mg (372 µmol) of NHS and 76.5 mg (372 µmol) of DCC are dissolved in 1 mL of dry acetonitrile. The solution is stirred at room temperature for 20 h. The solvent is removed on a rotary evaporator and the raw product is purified by column chromatography using LiChroprep RP-18 (40-63 µm) as the stationary phase and a water/acetone mixture (50:50 v/v) as the eluent.

Yield: 69.0 mg (96.6 µmol, 39%), purple powder, $C_{39}H_{50}N_3O_7P$ (703.82 g/mol).

R_f (silica gel RP-18, methanol:water 7:3 v/v): 0.08.

^{1}H-NMR (d_4-methanol, TMS): δ 8.54 (t, 1H), 7.53 (m, 2H), 7.47-7.28 (m, 6H), 6.49 (dd, 2H), 4.30 (m, 2H), 4.17 (t, 2H), 3.97 (quin, 2H), 2.77 (s, 4H), 2.61 (t, 2H), 2.01 (m, 2H), 1.86 (m, 2H), 1.76 (s, 6H), 1.75 (s, 6H), 1.72 (m, 2H), 1.49-1.40 (m, 6H), 1.27 (t, 3H).

4.2.4. FO548

4.2.4.1. 4-Hydrazino-benzenesulfonic acid

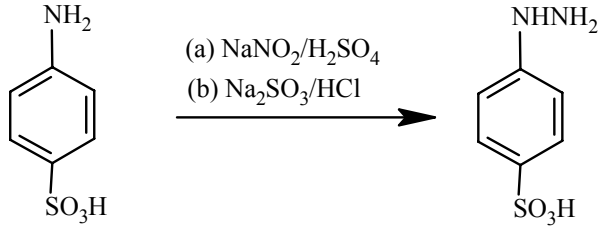

$C_6H_7NO_3S$
173.19

$C_6H_8N_2O_3S$
188.20

To a suspension of 104 g (0.60 mol) of 4-aminobenzenesulfonic acid in 400 mL of hot water 33 g of sodium carbonate are added. The solution is cooled to 5° C and 70 g of concentrated sulfuric acid is added slowly under rapid stirring. Then a solution of 42 g of sodium nitrite in 100 mL of water is added under cooling. The light yellow diazonium precipitate is filtered and washed with water. The wet diazonium compound is added to a stirred, cold solution (5° C) of 170 g of sodium sulfite in 500 mL of water. The solution which turns orange, is stirred under cooling for one hour, and then heated to reflux. Finally 400 mL of concentrated hydrochloric acid are added. First, the solution turns yellow, later the product precipitates as a white solid. For complete decoloration, 1-2 g of powdered zinc are added. The reaction mixture is cooled over night. The precipitate is filtered, washed with water and dried in an oven at 100 °C [2, 3].

Yield: 96 g (85%), white powder, $C_6H_8N_2O_3S$ (188.20 g/mol).

m.p.: > 250 °C (Lit.: 285 °C), R_f (RP-18, water:methanol 2:1 v/v): 0,95.

^{1}H-NMR (d_6-DMSO, TMS external): δ 10.00-9.70 (b, 2H), 8.30-8.20 (b, 1H), 7.50 (d, 2H), 6.80 (d, 2H).

4.2.4.2. Potassium 2,3,3-Trimethyl-3*H*-indole-5-sulfonate

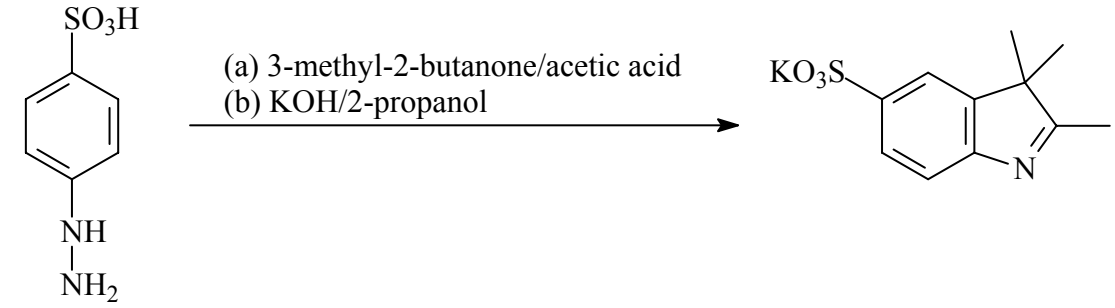

$C_6H_8N_2O_3S$
180.20

$C_{11}H_{12}KNO_3S$
277.38

2.28 g (12.1 mmol) of 4-hydrazinobenzenesulfonic acid and 2.3 mL (21.9 mmol) of 3-methyl-2-butanone are suspended in 15 mL of acetic acid and stirred at room temperature for one hour. Then the mixture is refluxed for 3 h. After cooling to room temperature, the solution is triturated with ether until the 2,3,3-trimethyl-3*H*-5-indolesulfonic acid crystallizes. The pink precipitate is filtered, washed with ether and then dissolved in methanol. To this solution a saturated solution of potassium hydroxide in 2-propanol is added until the precipitation of the yellow product is completed. The precipitate is filtered, washed with diethylether, and dried in a desiccator over P_2O_5 [3, 4].

Yield: 1.88 g (6.77 mmol, 56%) light-orange powder, $C_{11}H_{12}KNO_3S$ (277.37 g/mol).
m.p.: 246-250 °C (decomp.), R_f (RP-18, methanol:water 1:1 v/v): 0.82.
^{1}H-NMR (d_6-DMSO, TMS external): δ 7.70 (s, 1H), 7.60 (d, 1H), 7.35 (d, 1H), 2.30 (s, 3H), 1.30 (s, 6H).

4.2.4.3. 1-(5-Carboxypentyl)-2,3,3-trimethyl-3*H*-5-indoliumsulfonate

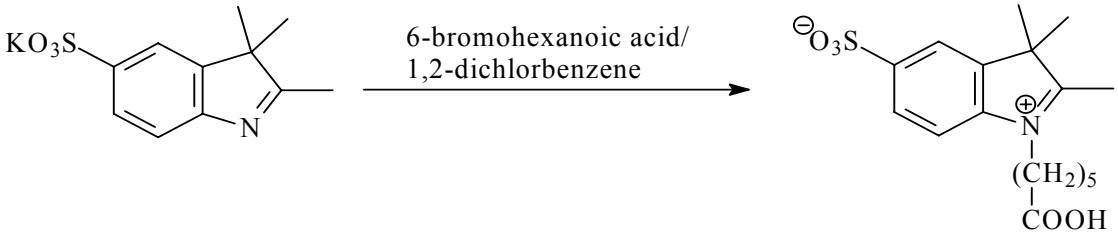

$C_{11}H_{12}KNO_3S$
277.38

$C_{17}H_{23}NO_5S$
353.43

3.18 g (11.0 mmol) of potassium 2,3,3-trimethyl-3*H*-5-indolesulfonate and 2.58 g (13.0 mmol) of 6-bromohexanoic acid are refluxed in 30 mL of 1,2-dichlorbenzene for 12 h. After cooling to room temperature the solvent is decanted. The pink precipitate is suspended in a 2-propanol/diethylether mixture (1:1 v/v), filtered, washed with diethylether and chloroform and dried in a desiccator over P_2O_5 [3, 4].

Yield: 3.82 g (10.8 mmol, 94%), pink powder, $C_{17}H_{23}NO_5S$ (353.43 g/mol).
m.p.: 135 °C (decomp.), R_f (RP-18, methanol:water 1:1 v/v): 0.79.
^{1}H-NMR (D_2O, TMS external): δ 8.00 (s, 1H), 7.89 (d, 1H), 7.77 (d, 1H), 4.38 (t, 2H), 2.25 (t, 2H), 1.86 (m, 2H), 1.48 (s, 6H), 1.59-1.29 (m, 4H) (Singlet for 2-methyl does not appear in D_2O).
FAB-MS: m/e ($M+H^+$, cation) for $C_{17}H_{24}NO_5S$, calculated 354.1, found 354.0.

4.2.4.4. FO548-Acid

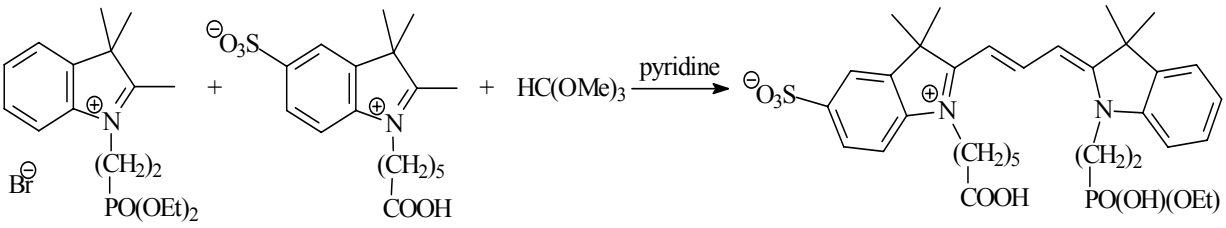

$C_{17}H_{27}BrNO_3P$ 404.28 + $C_{17}H_{23}NO_5S$ 353.43 + $C_4H_{10}O_3$ 120.15 → $C_{33}H_{43}N_2O_8PS$ 658.75

300 mg (0.74 mmol) of 1-[2-(diethoxyphosphoryl)ethyl]-2,3,3-trimethyl-3*H*-indolium bromide and 261 mg (0.74 mmol) of 1-(5-carboxypentyl)-2,3,3-trimethyl-3*H*-5-indoliumsulfonate are dissolved in 3 mL of pyridine. 100 µL (0.91 mmol) of 1,1,1-trimethoxymethane are added and the solution is heated to 90 °C for 4h. After cooling to room temperature 50 mL of ether are added, and the purple precipitate is filtered. The raw product is purified by column chromatography using silica gel 60 RP-18 (40-63 µm) as the stationary phase and a methanol/water mixture (50:50 v/v) as the eluent.

Yield: 44.0 mg (66.8 µmol, 9%), purple powder, $C_{33}H_{43}N_2O_8PS$ (658.75 g/mol).
R_f (silica gel RP-18, methanol:water 7:3 v/v): 0.81.
^{1}H-NMR (d_4-methanol, TMS): δ 8.56 (t, 1H), 7.91 (m, 2H), 7.55 (m, 2H), 7.45 (m, 2H), 7.38 (d, 1H), 6.58 (d, 1H), 6.47 (d, 1H), 4.34 (m, 2H), 4.16 (t, 2H), 3.99 (quin, 2H), 2.27 (t, 2H),

2.04 (m, 2H), 1.86 (t, 2H), 1.79 (s, 6H), 1.78 (s, 6H), 1.68 (m, 2H), 1.52 (m, 2H), 1.27 (t, 3H).

$^{31}P\{^{1}H\}$-NMR (d_4-methanol, H_3PO_4 external): δ 20.40.

ESI-MS: m/e ($M\text{-}H^+$, anion) for $C_{33}H_{42}N_2O_8PS$, calculated 657.2, found 657.0.

4.2.4.5. FO548-OSI Ester

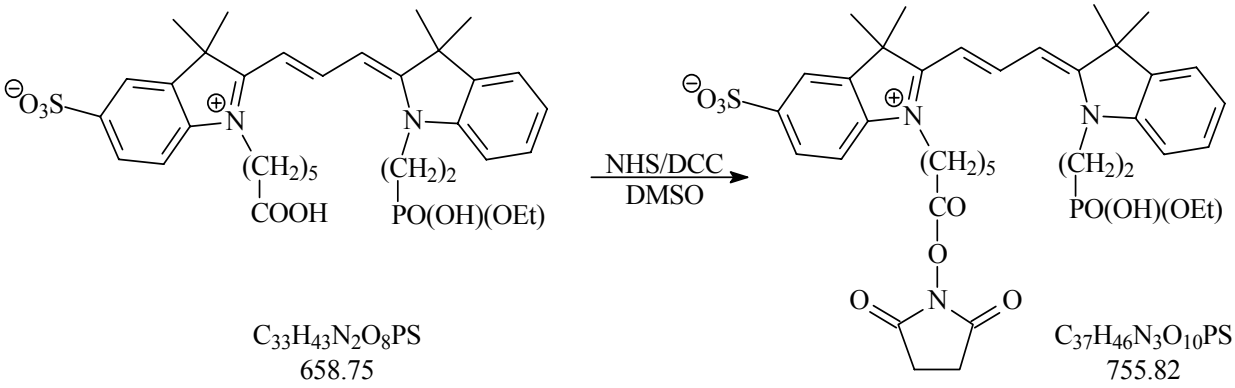

$C_{33}H_{43}N_2O_8PS$
658.75

$C_{37}H_{46}N_3O_{10}PS$
755.82

30 mg (45.6 µmol) of FO548-acid, 7.8 mg (68.1 µmol) of NHS, and 14.1 mg (68.1 µmol) of DCC are dissolved in 1 mL of dry DMSO. The solution is stirred at room temperature for 20 h. 5 mL of diethylether are added, and the purple precipitate is purified by column chromatography using LiChroprep RP-18 (40-63 µm) as the stationary phase and a water/acetonitrile mixture (75:25 v/v) as the eluent.

Yield: 16.0 mg (21.1 µmol, 46%), purple powder, $C_{37}H_{46}N_3O_{10}PS$ (755.82 g/mol).

R_f (silica gel RP-18, water:acetonitrile 3:1 v/v): 0.28.

^{1}H-NMR (d_4-methanol, TMS): δ 8.56 (t, 1H), 7.89 (m, 2H), 7.56 (d, 1H), 7.45 (m, 2H), 7.37 (m, 2H), 6.58 (d, 1H), 6.47 (d, 1H), 4.34 (m, 2H), 4.16 (t, 2H), 3.97 (quin, 2H), 2.67 (s, 4H), 2.22 (t, 2H), 2.04 (m, 2H), 1.85 (t, 2H), 1.79 (s, 6H), 1.78 (s, 6H), 1.70 (quin, 2H), 1.50 (quin, 2H), 1.27 (t, 3H).

ESI-MS: m/e ($M\text{-}H^+$, anion) for $C_{37}H_{45}N_3O_{10}PS$, calculated 754.3, found 754.0.

4.2.5. FR642

4.2.5.1. FR642-Acid

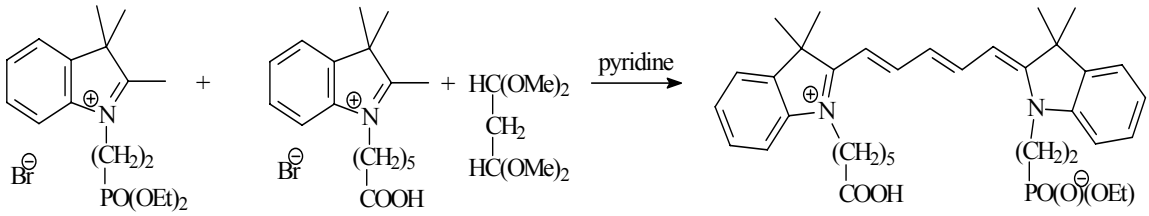

$C_{17}H_{27}BrNO_3P$ 404.28 | $C_{17}H_{23}BrNO_5S$ 354.29 | $C_7H_{16}O_4$ 164.20 | $C_{35}H_{45}N_2O_5P$ 604,73

671 mg (1.66 mmol) of 1-[2-(diethoxyphosphoryl)ethyl]-2,3,3-trimethyl-3*H*-indolium bromide and 588 mg (1,66 mmol) of 1-(5-carboxypentyl)-2,3,3-trimethyl-3*H*-indolium bromide are heated in 7 mL of pyridine to 95 °C until the educts dissolve. 330 µL (1.98 mmol) of 1,1,3,3-tetramethoxypropane are added and the solution is kept at 95 °C for 18 h. After cooling to room temperature diethylether is added until the blue product precipitates. The raw product is purified by two steps of column chromatography. In the first step silica gel 60 RP-18 (40-63 µm) is used as the stationary phase and a methanol/water mixture (50:50 v/v) containing 0.1% NH_3 as the eluent. Second LiChroprep RP-18 (40-63 µm) is used as the stationary phase and a methanol/water mixture (70:30 v/v) as the eluent .

Yield: 51.0 mg (84.3µmol, 5%), blue powder, $C_{35}H_{45}N_2O_5P$ (604.73 g/mol).

R_f (silica gel RP-18, methanol:water 80:20 v/v): 0.33.

^{1}H-NMR (d_4-methanol, TMS): δ 8.23 (dt, 2H), 7.48 (t, 2H), 7.40 (t, 2H), 7.39-7.22 (m, 4H), 6.65 (t, 1H), 6.32 (dd, 2H), 4.25 (m, 2H), 4.12 (t, 2H), 3.97 (quin, 2H), 2.30 (t, 2H), 1.98 (m, 2H), 1.83 (t, 2H), 1.72 (s, 6H), 1.71 (s, 6H), 1.69 (m, 2H), 1.49 (m, 2H), 1.28 (t, 3H).

^{31}P{^{1}H}-NMR (d_4-methanol, H_3PO_4 external): δ 20.62.

4.2.5.2. FR642-OSI Ester

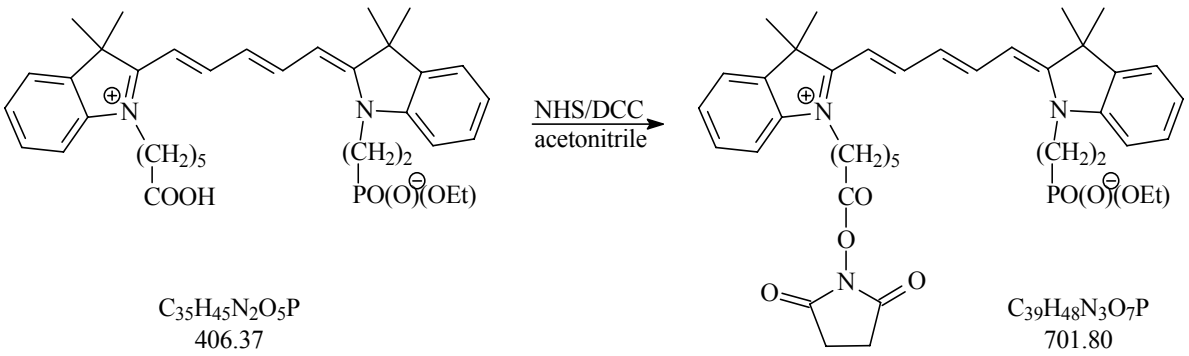

$C_{35}H_{45}N_2O_5P$ 406.37 | $C_{39}H_{48}N_3O_7P$ 701.80

30.0 mg (42.8 µmol) of FR642-acid, 9.8 mg (85.6 µmol) of NHS and 17.7 mg (85.6 µmol) of DCC are dissolved in 1 mL of dry acetonitrile. The solution is stirred at room temperature for 20 h. The solvent is removed on a rotary evaporator and the raw product is purified by column chromatography using LiChroprep RP-18 (40-63 µm) as the stationary phase and a water/acetone mixture (40:60 v/v) as the eluent.

Yield: 23.0 mg (32.7 µmol, 76%), blue powder, $C_{39}H_{48}N_3O_7P$ (701.80 g/mol).

R_f (silica gel RP-18, methanol:water 70:30 v/v): 0.08.

^{1}H-NMR (d_4-methanol, TMS): δ 8.23 (dt, 2H), 7.47 (t, 2H), 7.40 (m, 2H), 7.39-7.23 (m, 4H), 6.65 (t, 1H), 6.34 (dd, 2H), 4.25 (m, 2H), 4.12 (t, 2H), 3.97 (quin, 2H), 2.84 (s, 4H), 1.98 (m, 2H), 1.82 (m, 4H), 1.72 (s, 6H), 1.71 (s, 6H), 1.59 (m, 4H), 1.27 (t, 3H).

4.2.6. FR646

4.2.6.1. FR646-Acid

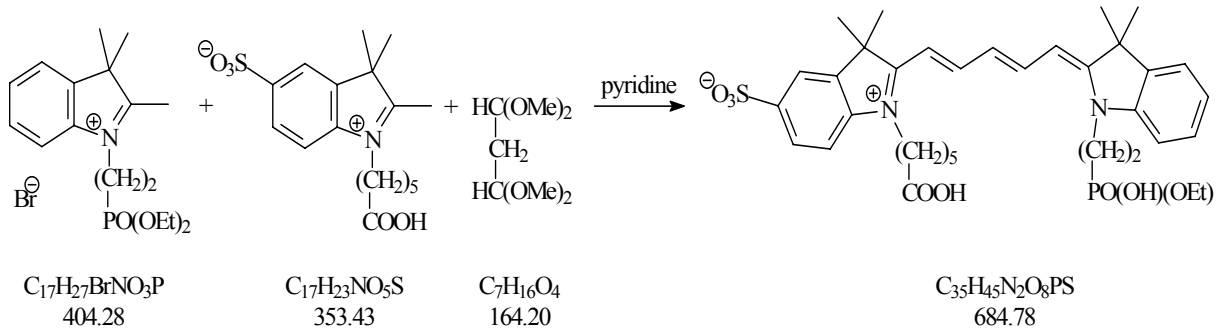

$C_{17}H_{27}BrNO_3P$ 404.28 | $C_{17}H_{23}NO_5S$ 353.43 | $C_7H_{16}O_4$ 164.20 | $C_{35}H_{45}N_2O_8PS$ 684.78

300 mg (0.74 mmol) of 1-[2-(diethoxyphosphoryl)ethyl]-2,3,3-trimethyl-3*H*-indolium bromide and 261 mg (0.74 mmol) of 1-(5-carboxypentyl)-2,3,3-trimethyl-3*H*-5-indoliumsulfonate are dissolved in 3 mL of pyridine. 150 µL (0.90 mmol) of 1,1,3,3-tetramethoxyproane are added and the solution is heated to 90 °C for 4h. After cooling to room temperature, 50 mL of diethylether are added, and the blue precipitate is filtered. The raw product is purified by column chromatography using silica gel 60 RP-18 (40-63 µm) as the stationary phase and a methanol/water mixture (50:50 v/v) as the eluent.

Yield: 46.0 mg (67.2 µmol, 9%), blue powder, $C_{35}H_{45}N_2O_8PS$ (684.78 g/mol).

R_f (silica gel RP-18, methanol:water 6:4 v/v): 0.69.

^{1}H-NMR (d_4-methanol, TMS): δ 8.30 (t, 1H), 8.25 (t, 2H), 7.86 (m, 2H), 7.51 (d, 1H), 7.42 (m, 2H), 7.30 (t, 2H), 6.68 (t, 1H), 6.43 (d, 1H), 6.28 (d, 1H), 4.30 (m, 2H), 4.09 (t, 2H), 3.97 (quin, 2H), 2.25 (t, 2H), 2.01 (m, 2H), 1.81 (t, 2H), 1.74 (s, 6H), 1.73 (s, 6H), 1.69 (t, 2H), 1.48 (m, 2H), 1.28 (t, 3H). ^{31}P{^{1}H}-NMR (d_4-methanol, H_3PO_4 external): δ 20.42.

ESI-MS: m/e ($M-H^+$, anion) for $C_{33}H_{42}N_2O_8PS$, calculated 683.3, found 683.0.

4.2.6.2. FR646-OSI Ester

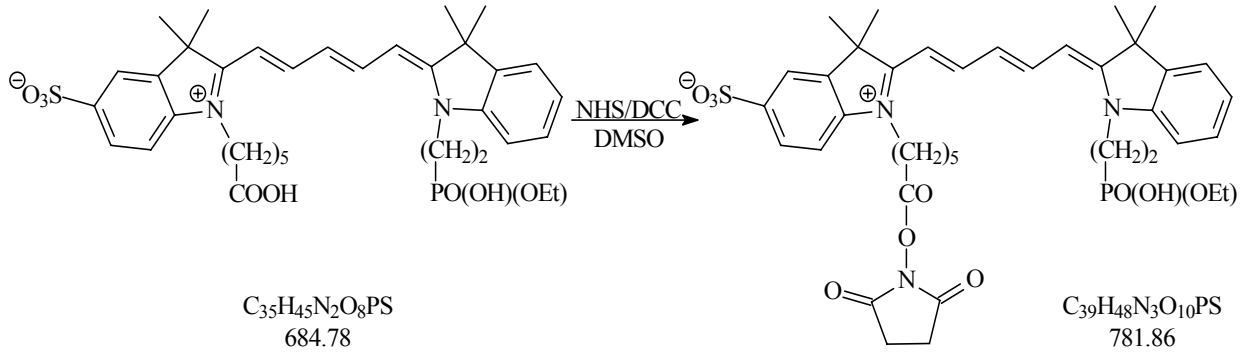

31.2 mg (45.6 µmol) of FR646-acid, 7.8 mg (68.1 µmol) of NHS, and 14.1 mg (68.1 µmol) of DCC are dissolved in 1 mL of dry DMSO. The solution is stirred at room temperature for 20 h. 5 mL of ether are added, and the blue precipitate is purified by column chromatography using LiChroprep RP-18 (40-63 µm) as the stationary phase and a water/acetonitrile mixture (3:1 v/v) as the eluent.

Yield: 12.9 mg (17.1 µmol, 37%), blue powder, $C_{39}H_{48}N_3O_{10}PS$ (781.86 g/mol).

R_f (silica gel RP-18, water:acetonitrile 3:1 v/v): 0.18.

^{1}H-NMR (d_4-methanol, TMS): δ 8.30 (t, 1H), 8.25(t, 2H), 7.86 (m, 2H), 7.52 (d, 1H), 7.42 (m, 2H), 7.30 (t, 2H), 6.68 (t, 1H), 6.42 (m, 1H), 6.28 (d, 1H), 4.30 (m, 2H), 4.09 (t, 2H), 3.97 (quin, 2H), 2.67(s, 4H), 1.98 (m, 2H), 1.83 (m, 2H), 1.74 (s, 6H), 1.73 (s, 6H), 1.72-1.47 (m, 6H), 1.28 (t, 3H).

4.2.7. FR626 [5]

4.2.7.1. 1-Ethyl-2,3,3-trimethyl-3*H*-5-indoliumsulfonate

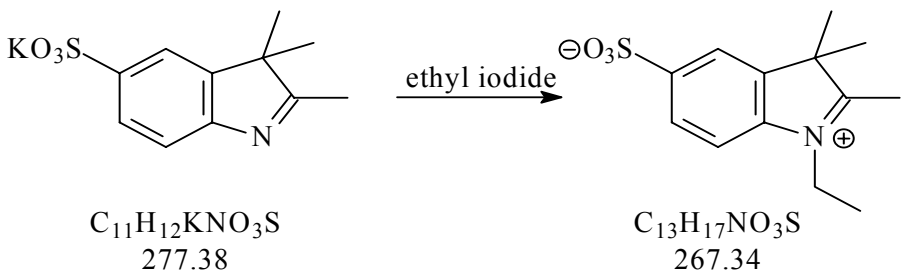

1.1 g (4.0 mmol) of potassium 2,3,3-trimethyl-3*H*-5-indolesulfonate are suspended in 10 mL of ethyl iodide. The reaction mixture is heated to 110 °C for 24 h in a sealed tube. After cooling to room temperature excess ethyl iodide is decanted and the residue is suspended in

10 mL of acetone and stirred at room temperature for 20 min. The solution is filtered, the residue is washed with acetone and diethylether and dried in a desiccator over P_2O_5 [4].

Yield: 320 mg (1.2 mmol, 30%), dark violet powder, $C_{13}H_{17}NO_3S$ (267.34 g/mol).
^{1}H-NMR: (d_6-DMSO, TMS external): δ 8.01 (s, 1H), 7.90 (d, 1H), 7.83 (d, 1H), 2.23 (q, 2H), 2.81 (s, 3H), 1.53 (s, 6H), 1.41 (t, 3H).

4.2.7.2. 3-Butoxy-4-(1-ethyl-3,3-dimethyl-1,3-dihydro-5-sulfonyl-indol-2-ylidenemethyl)-cyclobut-3-ene-1,2-dione

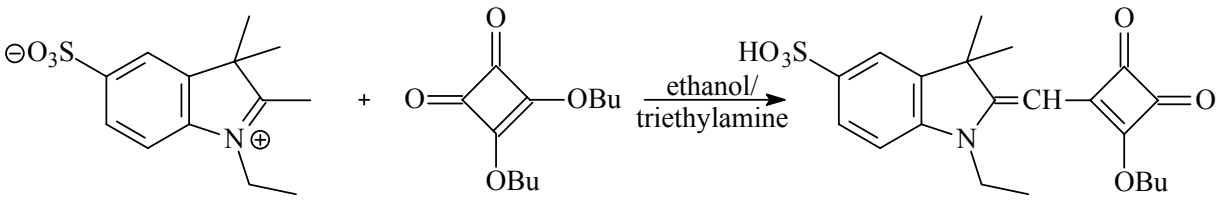

$C_{13}H_{17}NO_3S$ 267.34 | $C_{12}H_{18}O_4$ 226.27 | $C_{21}H_{25}NO_6S$ 419.49

500 mg (1.87 mmol) of 1-ethyl-2,3,3-trimethyl-3*H*-5-indoliumsulfonate and 500 µL (2.3 mmol) of 3,4-dibutoxy-3-cyclobutene-1,2-dione are dissolved in 20 mL of ethanol and 1 mL of triethylamine. The reaction mixture is refluxed at for 3 h. After cooling to room temperature, the solvent is removed under reduced pressure and the raw product is dissolved in a low amount of water and extracted three times with chloroform. Water is removed and the resulting brown-yellow product is pure enough for further reactions.

Yield: 380 mg (0.9 mmol, 48%), brown-yellow powder, $C_{21}H_{25}NO_6S$ (419.49 g/mol).

4.2.7.3. FR626-Acid

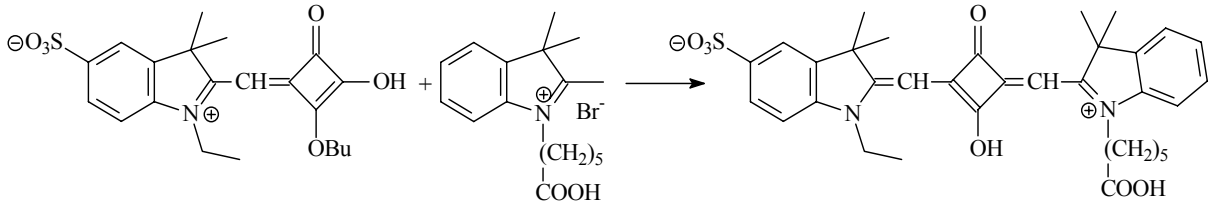

$C_{21}H_{25}NO_6S$ 419.49 | $C_{17}H_{24}BrNO_2$ 354.29 | $C_{34}H_{38}N_2O_7S$ 618.74

380 mg (0.9 mmol) of 3-butoxy-4-(1-ethyl-3,3-dimethyl-1,3-dihydro-5-sulfonyl-indol-2-ylidenemethyl)-cyclobut-3-ene-1,2-dione and 350 mg (1 mmol) of 1-(5-carboxypentyl)-2,3,3-trimethyl-3*H*-indolium bromide are dissolved in 20 mL of a 1-butanol/toluene mixture (1:1, v/v) and are refluxed for 14 h. The solvent is removed and the dye is purified by column chromatography using silica gel 60 RP-18 (40-63 µm) as the stationary phase and a methanol/water mixture (40:60, v/v) as the eluent.

Yield: 75 mg (0.12 mmol, 12%), blue powder, $C_{34}H_{38}N_2O_7S$ (618.74 g/mol).

R_f (methanol/water 5:5): 0.47.

^{1}H-NMR: (d_4-methanol, TMS external): δ 7.84 (m, 2H), 7.64-7.03 (m, 5H), 6.03 (s, 1H), 5.96 (s, 1H), 4.17 (m, 4H), 2.27-2.17 (m, 5H), 1.76 (s, 12H), 1.65 (m, 2H), 1.40 (m, 2H), 1.30 (m, 2H).

ESI-MS: m/e ($M-H^+$, anion) for $C_{34}H_{38}N_2O_7S$, calculated 617.4, found 617.3.

4.2.7.4. FR626-OSI Ester

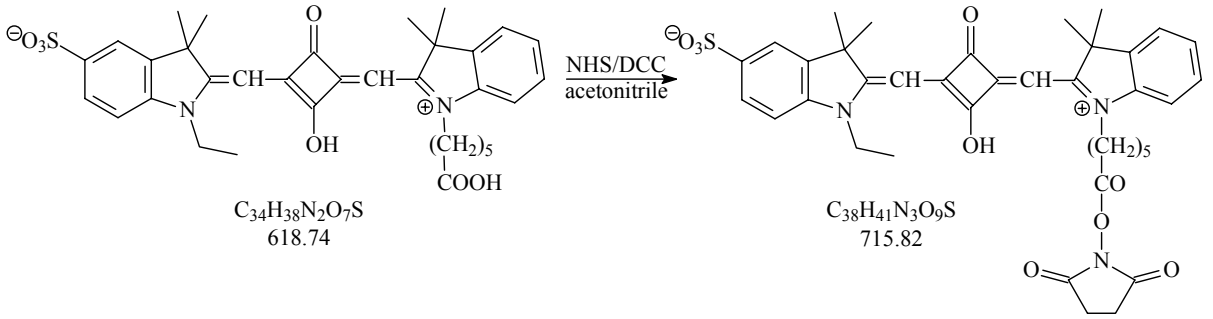

$C_{34}H_{38}N_2O_7S$ 618.74 | $C_{38}H_{41}N_3O_9S$ 715.82

60 mg (97 µmol) of FR626-acid, 17 mg (145 µmol) of NHS and 30 mg (145 µmol) of DCC are dissolved in 1 mL of dry acetonitrile. The solution is stirred at room temperature for 20 h. The solvent is removed on a rotary evaporator and the raw product is washed with diethylether. The OSI ester is used without further purification.

Yield: 51 mg (68 µmol, 70%), blue powder, $C_{38}H_{41}N_3O_9S$ (715.82 g/mol).

4.2.8. FR661

4.2.7.1. 6-(4-Methyl-1-quinolinium)hexanoic Acid Bromide

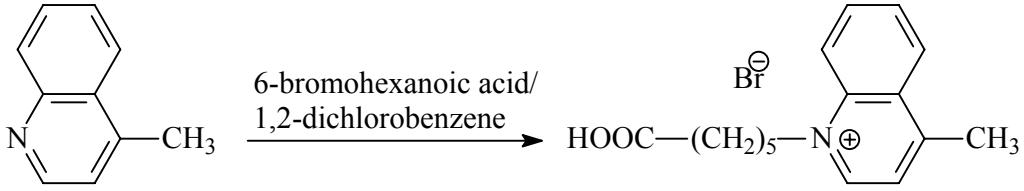

$C_{10}H_9N$
143.19

$C_{16}H_{20}BrNO_2$
338.24

5 g (35 mmol, 4.62 mL) of 4-methylquinoline and 6.81 g (35 mmol) of 6-bromohexanoic acid are dissolved in 50 mL of 1,2-dichlorobenzene. The reaction mixture is refluxed for 20 h. After cooling to room temperature, the solvent is decanted and the brown amorphous residue is triturated with few 2-propanol until it crystallizes. The white crystals are sucked off, washed with ether and dried in a desiccator over P_2O_5 [6].

Yield: 5.62 g (16.6 mmol, 47%), white powder, $C_{16}H_{20}BrNO_2$ (338.24 g/mol).
m.p.: 135-137 °C. R_f (silica gel RP-18, methanol): 0.58.
^{1}H-NMR (d_6-DMSO, TMS external): δ 9.40 (d, 1H), 8.60-8.50 (m, 2H), 8.25 (t, 1H), 8.05 (d, 2H), 4.95 (t, 2H), 2.45 (s, 3H), 2.20 (t, 2H), 1.95 (m, 2H), 1.55 (m, 2H), 1.40 (m, 2H).

4.2.8.2. 6-[4-(2-Butoxy-3,4-dioxo-cyclobut-1-enylmethylene)-4H-quinolin-1-yl]-hexanoic Acid

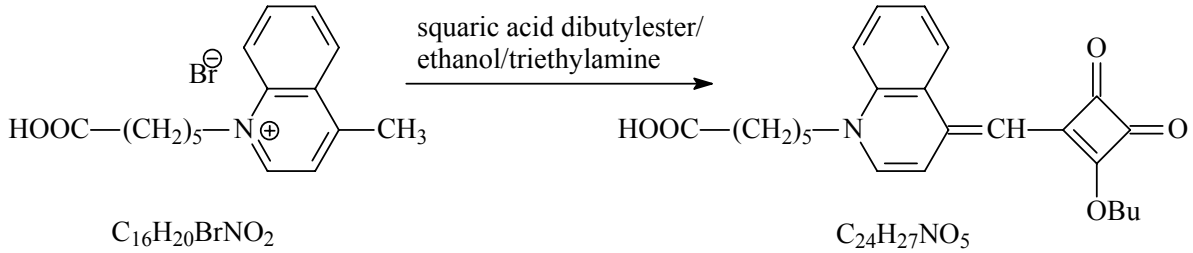

$C_{16}H_{20}BrNO_2$
338.24

$C_{24}H_{27}NO_5$
409.48

118 mg (0.35 mmol) of 6-(4-methyl-1-quinolinium)hexanoic acid bromide and 87.5 µL (0.40 mmol) of squaric acid dibutylester are dissolved in 5 mL of ethanol. 250 µL of triethylamine are added and the mixture is refluxed for 20 min. The solvent is removed on a rotary evaporator. The raw product is purified by column chromatography using silica gel 60 as the stationary phase and a chloroform/methanol mixture (90:10 v/v) as the eluent.

Yield: 41.0 mg (0.10 mmol, 29%), amorphous red product, $C_{24}H_{27}NO_5$ (409.48 g/mol).
R_f (silica gel, chloroform:methanol 90:10 v/v): 0.49.

^{1}H-NMR ($CDCl_3$, TMS): δ 8.13 (d, 1H), 7.92 (d, 1H), 7.60-7.53 (m, 1H), 7.35-7.29 (m, 2H), 7.14 (d, 1H), 6.04 (s, 1H), 4.81 (t, 2H), 4.03 (t, 2H), 2.37 (t, 2H), 1.81 (m, 4H), 1.69 (m, 2H), 1.49 (m, 4H), 0.99(t, 3H).

4.2.8.3. FR661-Butylester

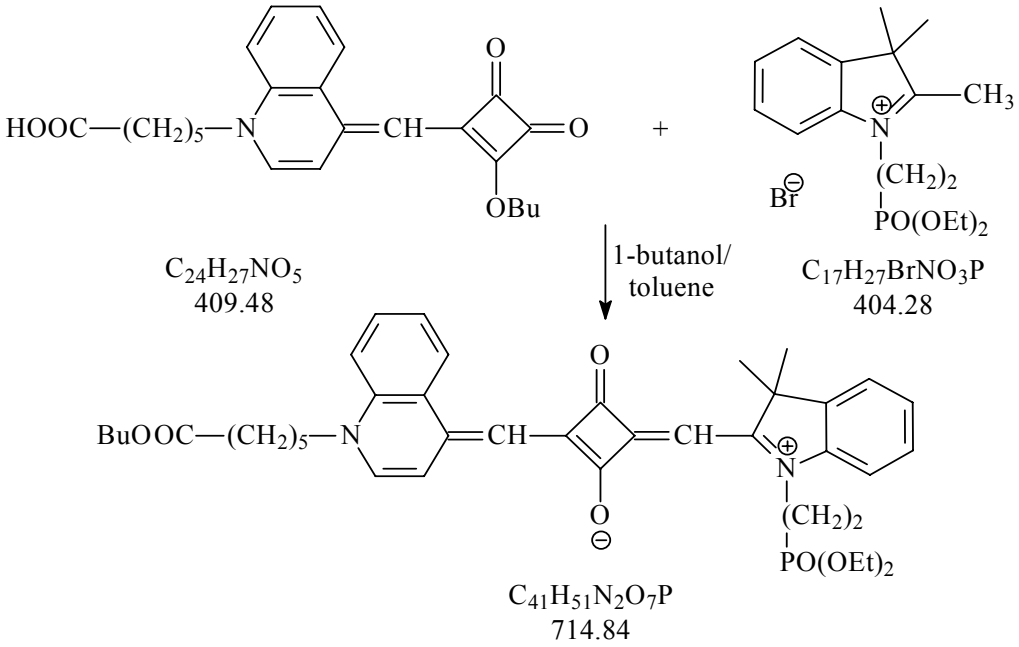

300 mg (0.68 mmol) of 1-(5-carboxypentyl)-4-(1-(2-butoxy-3,4-dioxo-1-cyclobutenyl) methylidene)-1,4-dihydroquinoline and 300 mg (0.74 mmol) of 1-[2-(diethoxyphosphoryl) ethyl]-2,3,3-trimethyl-3*H*-indolium bromide are dissolved in 60 mL of a 1-butanol/toluene mixture (1:1 v/v) and heated under reflux for 48 h. After cooling to room temperature the solvent is removed under reduced pressure. The raw product is purified by column chromatography using silica gel 60 as the stationary phase and a chloroform/methanol mixture (90:10 v/v) as the eluent.

Yield: 33.2 mg (45.5 µmol, 7%), amorphous green product, $C_{41}H_{51}N_2O_7P$ (714.84 g/mol).
R_f (silica gel, chloroform:methanol 90:10 v/v): 0.62.
^{1}H-NMR (d_4-methanol, TMS): δ 9.01 (d, 1H), 8.47 (d, 1H), 8.25 (d, 1H), 7.93 (m, 2H), 7.69 (t, 1H), 7.29 (m, 2H), 7.03 (m, 2H), 6.68 (s, 1H), 5.64 (s, 1H), 4.57 (t, 2H), 4.22-4.01 (m, 8H), 2.34 (t, 2H), 2.14-1.93 (m, 2H), 1.71-1.10 (m, 16H), 0.91 (t, 9H).
ESI-MS: m/e ($M+H^+$, cation) for $C_{41}H_{52}N_2O_7P$, calculated 715.4, found 715.4.

4.2.8.3. FR661-Acid

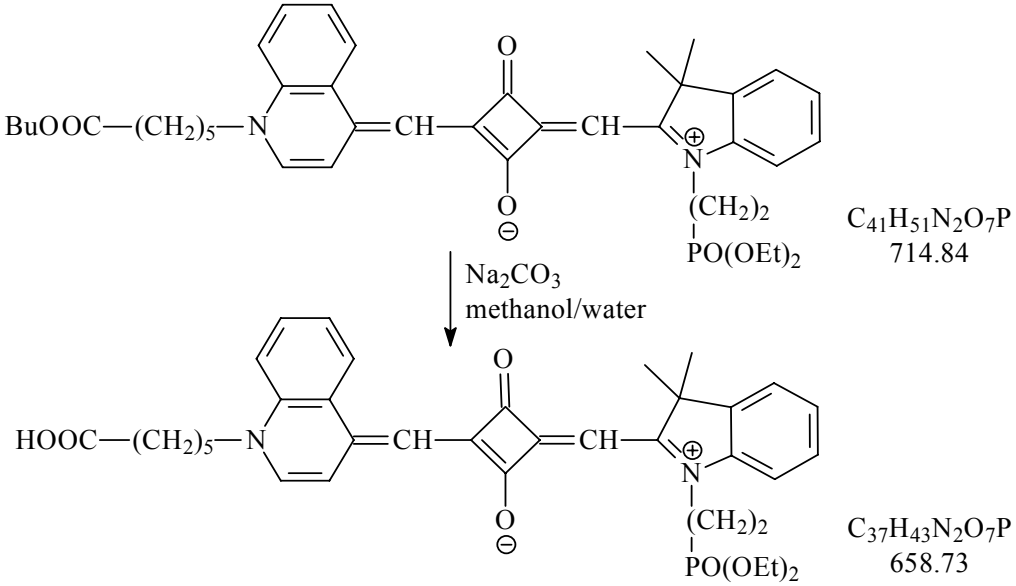

12 mg (16.4 µmol) of FR661-butylester are dissolved in 2 mL of a methanol/water mixture (1:1 v/v). A saturated solution of Na_2CO_3 in a methanol/water mixture (1:1 v/v) is added and the solution is stirred for 20 h at room temperature. The solvent is removed on a rotary evaporator. The raw product is purified by column chromatography using silica gel as the stationary phase and a chloroform/methanol mixture (60:40 v/v) as the eluent.

Yield: 8.0 mg (12.1 µmol, 74%), green powder, $C_{37}H_{43}N_2O_7P$ (658.73 g/mol).

R_f (silica gel, chloroform:methanol 90:10 v/v): 0.39.

ESI-MS: m/e ($M\text{-}H^+$, anion) for $C_{37}H_{42}N_2O_7P$, calculated 657.3, found 657.1.

4.2.8.4. FR661-OSI Ester

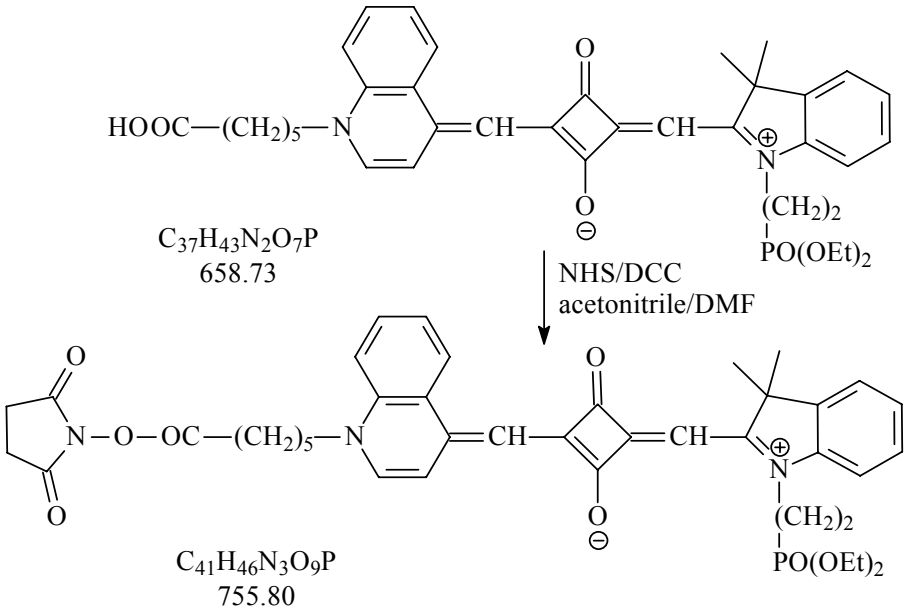

3.5 mg (5.3 µmol) of FR661-acid, 1.2 mg (10.6 µmol) of NHS, and 2.2 mg (10.6 µmol) of DCC are dissolved in 1 mL of an acetonitrile/DMF mixture (1:1 v/v). The solution is stirred at room temperature for 18 h. The solvent is removed on a rotary evaporator and the raw product is washed several times with diethylether.

Yield: 2.8 mg (3.7 µmol, 70%), green powder, $C_{41}H_{46}N_3O_9P$ (755.80 g/mol).

R_f (silica gel, chloroform:methanol 90:10 v/v): 0.51.

4.2.9. FR662

4.2.9.1. 2-(2,3-Dibutoxy-4-oxo-2-cyclobutenyliden)malonodinitrile

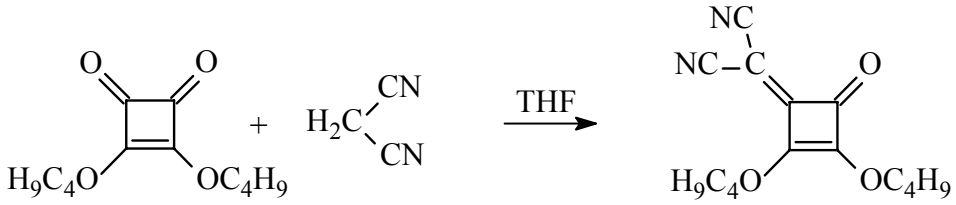

$C_{12}H_{18}O_4$	$C_3H_2N_2$	$C_{15}H_{18}N_2O_3$
226.27	66.06	274.32

2.16 mL (10 mmol) of squaric acid dibutylester are dissolved in 40 mL of anhydrous THF. 660 mg (10 mmol) of malonodinitrile are added under stirring. Then, a solution of 1.65 mL (12 mmol) of triethylamine in 3 mL of THF is added slowly via a dropping funnel. The solution is stirred at room temperature for 15 h. Then, 50 mL of dichloromethane and 100 mL of water are added. The product is extracted into the organic phase and separated. The aqueous phase is extracted twice with 20 mL of dichloromethane each. The organic phases are unified and dried over Na_2SO_4. The solvent is removed under vacuum and a yellow oil remains which is washed several times with diethylether [7, 8].

Yield: 1.7 g (63%), yellow oil, $C_{15}H_{18}N_2O_3$ (274.31 g/mol).

R_f (RP-18, methanol:water 2:1 v/v): 0.90.

CHN: calcd. C 65.68%, H 6.61%, N 10.21% found C 65.35%, H 6.51%, N 10.11%.

UV: λ (methanol) = 333 nm, 204 nm, IR: 2205 cm^{-1} (C≡N).

EI-MS: m/e (M^+, cation) for $C_{15}H_{18}N_2O_3$, calcd. 274.3, found 274.3.

4.2.9.2. {2-[2-(2-Butoxy-4-dicyanomethylene-3-oxo-cyclobut-1-enylmethylene)-3,3-dimethyl-2,3-dihydro-indol-1-yl]-ethyl}-phosphonic acid monoetyl ester

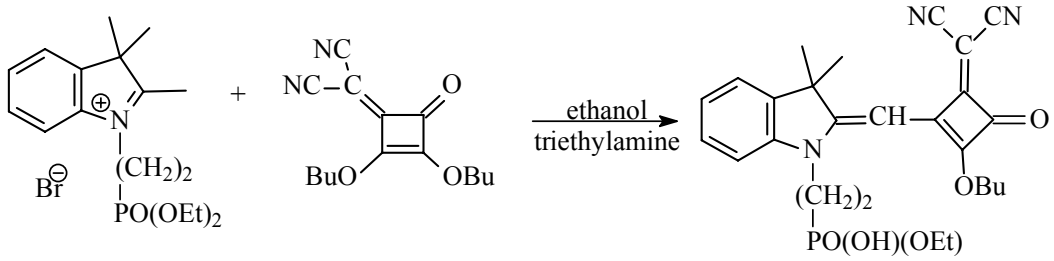

$C_{17}H_{27}BrNO_3P$ 404.28 | $C_{15}H_{18}N_2O_3$ 274.32 | $C_{26}H_{30}N_3O_5P$ 495.52

3.00 g (7.42 mmol) of 1-[2-(diethoxyphosphoryl)ethyl]-2,3,3-trimethyl-3*H*-indolium bromide and 2.00 mg (7.29 mmol) of 2-(2,3-dibutoxy-4-oxo-2-cyclobutenyliden)malonodinitrile are dissolved in 30 mL of ethanol. 1 mL of triethylamine is added and the solution is refluxed for 12 h. After cooling to room temperature the solvent is removed on a rotary evaporator. The brown residue is dissolved in 100 mL of water and extracted seven times with 30 mL of ether. The aqueous phase is collected and water is removed on a rotary evaporator. The raw intermediate is purified by column chromatography using silica gel 60 RP-18 (40-63 µm) as the stationary phase and a methanol/water mixture (50:50 v/v) as the eluent. The first orange fraction is collected and the solvent is removed on a rotary evaporator.

Yield: 1.95 g (53%), orange oil, $C_{26}H_{30}N_3O_5P$ (495.52 g/mol).

4.2.9.3. FR662-Butylester

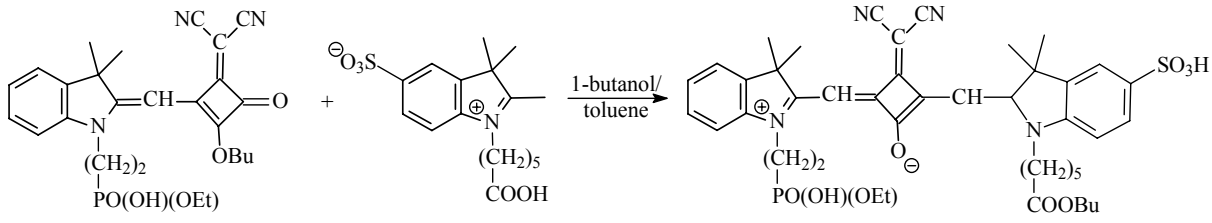

$C_{26}H_{30}N_3O_5P$ 495.52 | $C_{17}H_{23}NO_5S$ 353.43 | $C_{43}H_{52}N_4O_9PS$ 831.94

1.00 g (2.83 mmol) of 1-(5-carboxypentyl)-2,3,3-trimethyl-3*H*-5-indoliumsulfonate and 1.48 g (2.83 mmol) of {2-[2-(2-Butoxy-4-dicyanomethylene-3-oxo-cyclobut-1-enylmethylene)-3,3-dimethyl-2,3-dihydro-indol-1-yl]-ethyl}-phosphonic acid monoethyl ester are refluxed in 80 ml of a 1-butanol/toluene mixture (1:1 v/v) for 18 h. After cooling to room temperature the solvents are removed in vacuum. The raw product is purified by column chromatography

using silica gel 60 RP-18 (40-63 µm) as the stationary phase and a methanol/water mixture (50:50 v/v) as the eluent.

Yield: 290 mg (0.35 mmol, 12%), green crystals, $C_{43}H_{52}N_4O_9PS$ (831.94 g/mol).
R_f (silica gel RP-18, methanol:water 1:1 v/v): 0.13.
^{1}H-NMR (d_4-methanol, TMS): δ 7.87 (m, 2H), 7.54 (d, 1H), 7.49 (d, 1H), 7.41 (dt, 1H), 7.27 (m, 2H), 6.47 (s, 1H), 6.42 (s, 1H), 4.35 (m, 2H), 4.06 (m, 4H), 3.87 (quin, 2H), 2.33 (t, 2H), 2.08 (dt, 2H), 1.81 (m, 2H), 1.77 (s, 6H), 1.76 (s, 6H), 1.69 (t, 2H), 1.59 (m, 2H), 1.49 (m, 2H), 1.36 (m, 2H), 1.11 (t, 3H), 0.93 (t, 3H).
ESI-MS: m/e ($M-H^+$, anion) for $C_{43}H_{51}N_4O_9PS$, calculated 830.3, found 829.3.

4.2.9.4. FR662-Acid

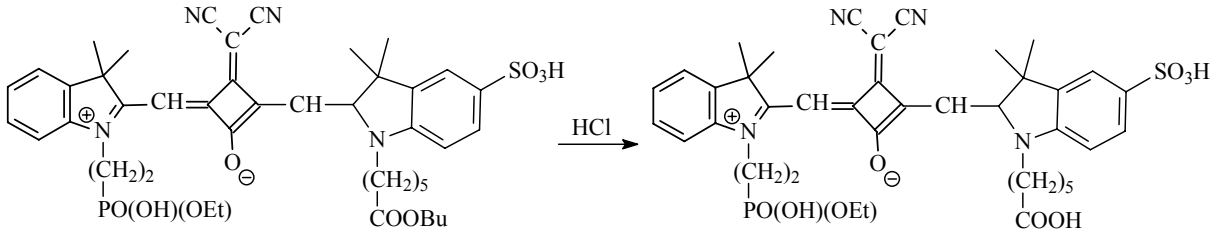

$C_{43}H_{52}N_4O_9PS$
831.94

$C_{39}H_{44}N_4O_9PS$
775.83

290 mg (0.35 mmol) of FR662-butylester are dissolved in 9 mL of water. 1 mL of 1N HCl is added and the mixture is refluxed for 2 h. The solvent is decanted and the raw product is purified by column chromatography using silica gel 60 RP-18 (40-63 µm) as the stationary phase and a methanol/water mixture (50:50 v/v) as the eluent.

Yield: 155 mg (0.20 mmol, 57%), green crystals, $C_{39}H_{44}N_4O_9PS$ (775.83 g/mol).
R_f (silica gel RP-18, methanol:water 1:1 v/v): 0.51.
^{1}H-NMR (d_4-methanol, TMS): δ 7.89 (m, 2H), 7.49 (d, 1H), 7.43-7.32 (m, 3H), 7.27 (t, 1H), 6.48 (s, 1H), 6.46 (s, 1H), 4.40 (m, 2H), 4.09 (m, 2H), 3.97 (quin, 2H), 2.30 (m, 4H), 1.83 (t, 2H), 1.78 (s, 6H), 1.76 (s, 6H), 1.68 (m, 2H), 1.51 (m, 2H), 1.16 (t, 3H).

4.2.9.5. FR662-OSI Ester

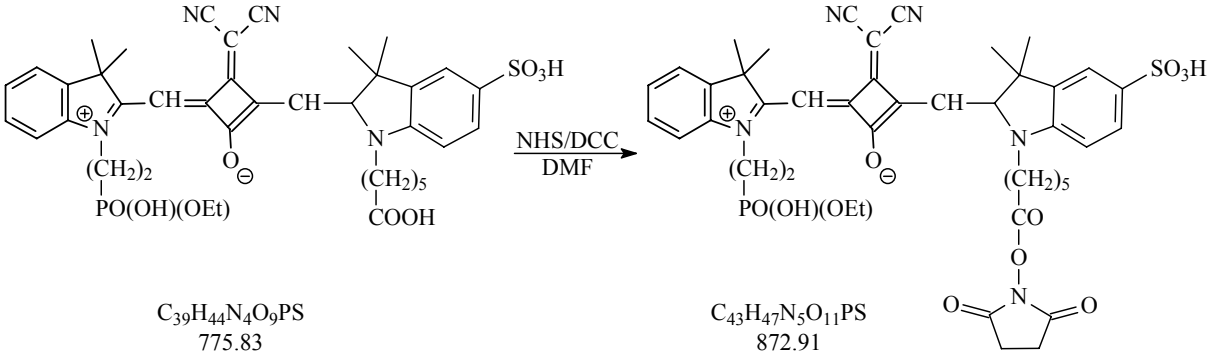

$C_{39}H_{44}N_4O_9PS$
775.83

$C_{43}H_{47}N_5O_{11}PS$
872.91

50.0 mg (64.4 µmol) of FR662-acid, 19.9 mg (96.6 µmol) of DCC and 11.1 mg (96.6 µmol) of NHS are dissolved in 1 mL of dry DMF. The solution is stirred for 20 h at room temperature. The reaction mixture is filtered and the solvent is removed in vacuum. The product is purified by column chromatography using silica gel 60 RP-18 (40-63 µm) as the stationary phase and a methanol/water mixture (80:20 v/v) as the eluent.

Yield: 26 mg (46%), green crystals, $C_{43}H_{47}N_5O_{11}PS$ (872.91 g/mol).
^{1}H-NMR (d_4-methanol, TMS): δ 7.87 (m, 2H), 7.50 (m, 2H), 7.39 (m, 1H), 7.27 (m, 1H), 6.46 (s, 1H), 6.42 (s, 1H), 4.38 (m, 2H), 4.06 (m, 2H), 3.87 (quin, 2H), 2.67 (s, 4H), 2.30 (t, 2H), 2.09 (dt, 2H), 1.82 (m, 2H), 1.77 (s, 6H), 1.76 (s, 6H), 1.68 (m, 2H), 1.51 (m, 2H), 1.11 (t, 3H).

4.2.10. FR670

4.2.10.1. FR670-Acid

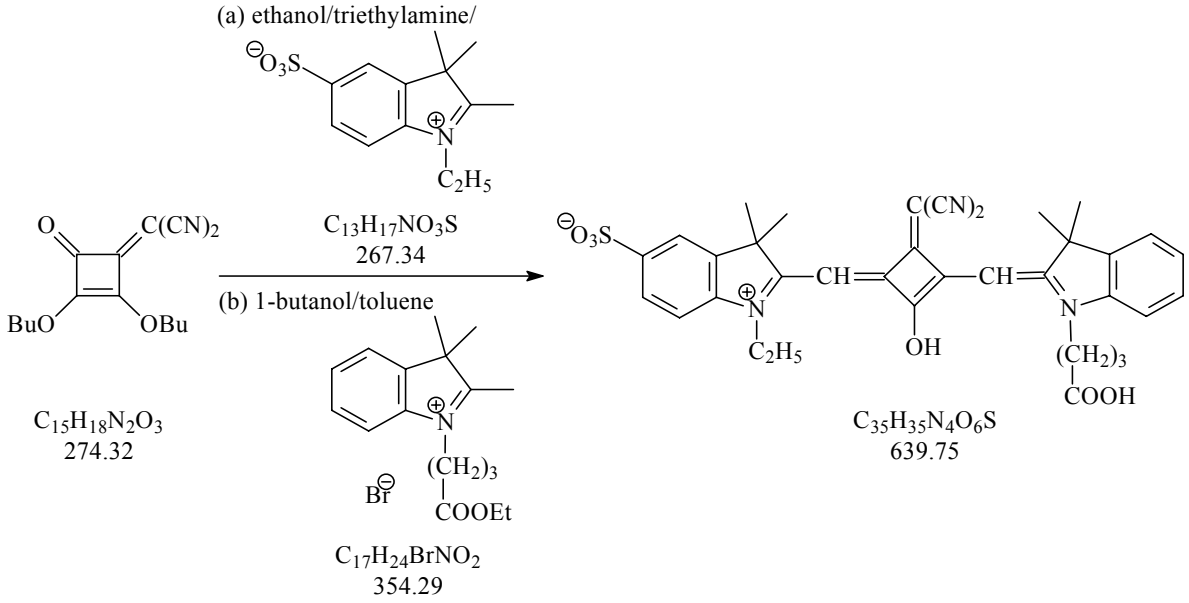

$C_{13}H_{17}NO_3S$
267.34

$C_{15}H_{18}N_2O_3$
274.32

$C_{17}H_{24}BrNO_2$
354.29

$C_{35}H_{35}N_4O_6S$
639.75

1.38 g (4.98 mmol) of 2-(2,3-dibutoxy-4-oxo-2-cyclobutenyliden)malonodinitrile and 1.33 g (4.98 mmol) of 1-ethyl-2,3,3-trimethyl-*3H*-5-indoliumsulfonate are dissolved in 60 mL of ethanol. 6 mL of triethylamine are added and the solution is refluxed for 6 h. After cooling to room temperature the solvent is removed on a rotary evaporator and an orange oil remains. The oil is dissolved in 75 mL of a 1-butanol/toluene mixture (2:1, v/v) and 1.76 g (4.98 mmol) of 1-(3-ethoxycarbonyl-propyl)-2,3,3-trimethyl-3*H*-indolium bromide are added. The solution is heated to 110 °C for 20 h. After cooling to room temperature the solvent is removed on a rotary evaporator. The dark green residue is dissolved in 40 mL of ethanol. 10 mL of ethanol, saturated with NaOH, are added and the green solution is heated to 50 °C, whereupon the color turns brown. After cooling to room temperature, HCl (35%) is added dropwise until neutral pH is reached. The solvent of the green solution is removed. The residue is suspended in an ethanol/acetone mixture (1:1, v/v). Unsoluble NaCl is sucked off. The solvent of the solution containing the raw product is removed, and the product is purified by column chromatography using silica gel 60 RP-18 (40-63 µm) as the stationary phase and a methanol/water mixture (40:60 v/v) as the eluent.

Yield: 171 mg (268 µmol, 5%), golden-green powder, $C_{35}H_{34}N_4O_6S$ (638.74 g/mol).
R_f (silica gel RP-18, methanol:water 8:2 v/v): 0.69.
^{1}H-NMR (d_4-methanol): δ 7.85 (m, 2H), 7.50 (m, 2H), 7.40 (dt, 1H), 7.28 (m, 1H), 6.46 (s, 1H), 6.40 (s, 1H), 4.18 (t, 2H), 4.10 (q, 2H), 2.34 (t, 2H), 2.07 (m, 2H), 1.37 (t, 3H).

4.2.10.2. FR670-OSI Ester

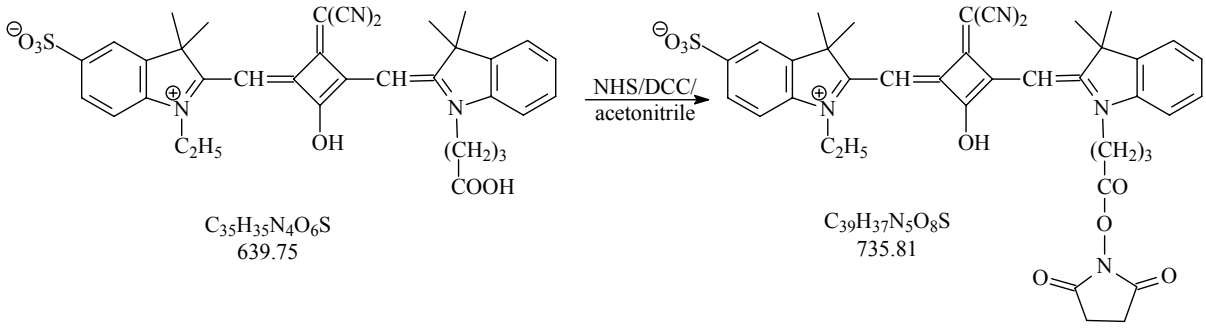

$C_{35}H_{35}N_4O_6S$
639.75

$C_{39}H_{37}N_5O_8S$
735.81

4.0 mg (6.25 µmol) of FR670-acid, 1.4 mg (12.5 µmol) of NHS, and 2.6 mg (12.3 µmol) of DCC are dissolved in 1 mL of acetonitrile. The solution is stirred at room temperature for 20 h. After filtration the solvent is removed on a rotary evaporator.

Yield: 3.1 mg (4.31 µmol, 69%), green powder, $C_{39}H_{37}N_5O_8S$ (735.81 g/mol).

R_f (silica gel RP-18, methanol:water 8:2 v/v): 0.55.

4.2.11. OB630

4.2.11.1 1-(6-Hydroxyhexyl)-2,3,3-trimethyl-3*H*-indolium Bromide

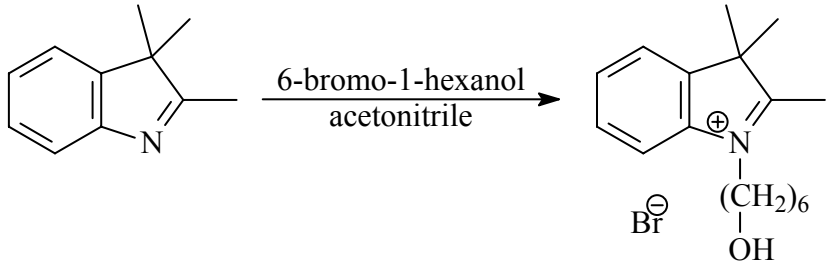

$C_{11}H_{13}N$
159.23

$C_{17}H_{26}BrNO$
340.30

700 µL (4.35 mmol) of 2,3,3-trimethyl-3*H*-indole and 856 µL (6.53 mmol) of 6-bromo-1-hexanol are dissolved in 9 mL of acetonitrile and refluxed for 20 h. After cooling to room temperature the solvent is removed on a rotary evaporator. The raw product is dissolved in water and extracted with ether. The aqueous phase is collected and water is removed on a rotary evaporator. The product is dried in a desiccator over P_2O_5.

Yield: 605 mg (1.78 mmol, 41%), faintly violett powder, $C_{17}H_{26}BrNO$ (340.30 g/mol).

R_f (silica gel RP-18, methanol): 0.61.

^{1}H-NMR (methanol, TMS): δ 7.87 (m, 1H), 7.77 (m, 1H), 7.67 (m, 2H), 4.51 (t, 2H), 3.56 (t, 2H), 1.97 (m, 2H), 1.61 (s, 6H), 1.50 (m, 6H).

4.2.11.2. 3-Butoxy-4-(1,3,3-trimethyl-1,3-dihydro-indol-2-ylidenemethyl)-cyclobut-3-ene-1,2-dione

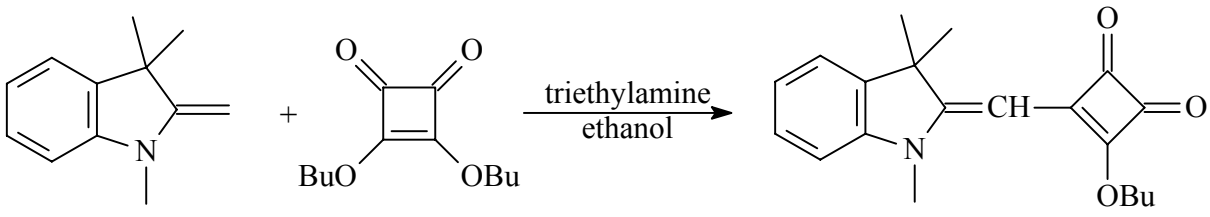

$C_{12}H_{15}N$
173.26

$C_{12}H_{18}O_4$
226.27

$C_{20}H_{23}NO_3$
325.41

2.16 mL (10.0 mmol) of 3,4-dibutoxy-3-cyclobutene-1,2-dione and 2 mL of triethylamine are dissolved in 15 mL of ethanol and heated to 70 °C. 2.66 mL (15.7 mmol) of 2-methylene-1,3,3-trimethylindoline are added, and the reaction mixture is refluxed for one hour. After cooling to room temperature the solvents are removed on a rotary evaporator, and a brown liquid remains. The residue is triturated with 15 mL of diethylether and is allowd to stand 1-2 hours at 4 °C whereupon the liquid crystallizes in yellow needles. Diethylether is decanted and the crystalls are washed with small amounts of cold ether and dried in a desiccator over P_2O_5.

Yield: 1.57 g (4.82 mmol, 48%), yellow crystalls, $C_{20}H_{23}NO_3$ (325.41 g/mol).
R_f (silica gel, chloroform: methanol 97:3 v/v): 0.87.

4.2.11.3. 3-Hydroxy-4-(1,3,3-trimethyl-1,3-dihydro-indol-2-ylidenemethyl)-cyclobut-3-ene-1,2-dione

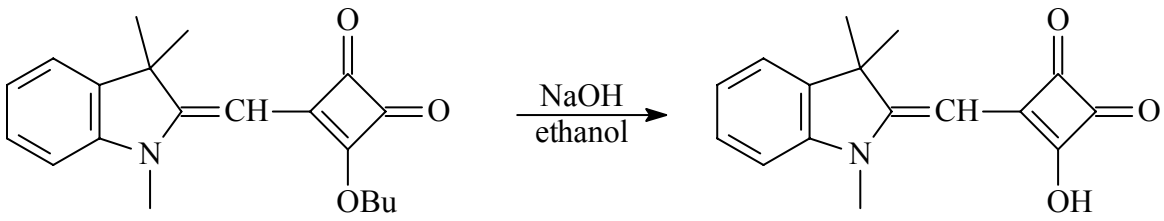

$C_{20}H_{23}NO_3$
325.41

$C_{16}H_{15}NO_3$
269.30

1.57 g (4.82 mmol) of 3-butoxy-4-(1,3,3-trimethyl-1,3-dihydro-indol-2-ylidenemethyl)-cyclobut-3-ene-1,2-dione are suspended in 10 mL of ethanol and heated to 70 °C. 500 µL of a 50% (w/w) NaOH solution in water are added whereupon the reaction mixture turns to a brown solution which is refluxed for 10 min. After cooling yellow crystalls precipitate. 7 mL of 2 N HCl are added and the product is sucked off.

Yield: 1.10 g (4.08 mmol, 85%), yellow crystalls, $C_{16}H_{15}NO_3$ (269.30 g/mol).
R_f (silica gel, chloroform: methanol 97:3 v/v): 0.78.
^{1}H-NMR (d_1-chloroform/TMS): δ 7.28 (m, 2H), 7.07 (t, 1H), 6.89 (d, 1H), 5.36 (s, 1H), 3.39 (s, 3H), 1.62 (s, 6H).

4.2.11.4. OB630-OH

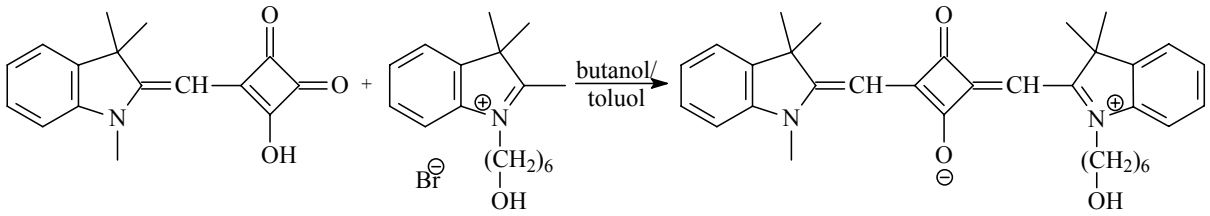

$C_{16}H_{15}NO_3$ 269.30 | $C_{17}H_{26}BrNO$ 340.30 | $C_{33}H_{38}N_2O_3$ 510.68

310 mg (1.15 mmol) of 3-hydroxy-4-(1,3,3-trimethyl-1,3-dihydro-indol-2-ylidenemethyl)-cyclobut-3-ene-1,2-dione and 391 mg (1.15 mmol) of 1-(6-hydroxyhexyl)-2,3,3-trimethyl-3*H*-indolium bromide are dissolved in 30 mL of a butanol/toluene mixture (1/1, v/v) and refluxed for 24 h. After cooling the solvents are removed on a rotary evaporator and the product is purified by chromatography using silica gel 60 (40-63 µm) as the stationary phase and a chloroform/methanol mixture (97/3, v/v) as the eluent. The second blue fraction is collected which contains the unsymmetrical dye.

Yield: 138 mg (0.27 mmol, 23%), blue crystalls, $C_{33}H_{38}N_2O_3$ (510.68 g/mol).

R_f (silica gel, chloroform: methanol 9:1 v/v): 0.54.

R_f (silica gel RP 18, chloroform: methanol 95:5 v/v): 0.51.

^{1}H-NMR (d_1-chloroform, TMS): δ 7.37 (m, 4H), 7.21 (m, 2H), 7.06 (d, 2H), 6.41 (s, 1H), 6.22 (s, 1H), 4.13 (t, 2H), 4.09 (m, 2H), 3.69 (t, 2H), 3.65 (s, 3H), 1.86 (m, 2H), 1.76 (s, 6H), 1.74 (s, 6H), 1.62 (m, 2H), 1.56 (m, 2H), 1.37 (m, 2H).

4.2.11.5. OB630-PAM

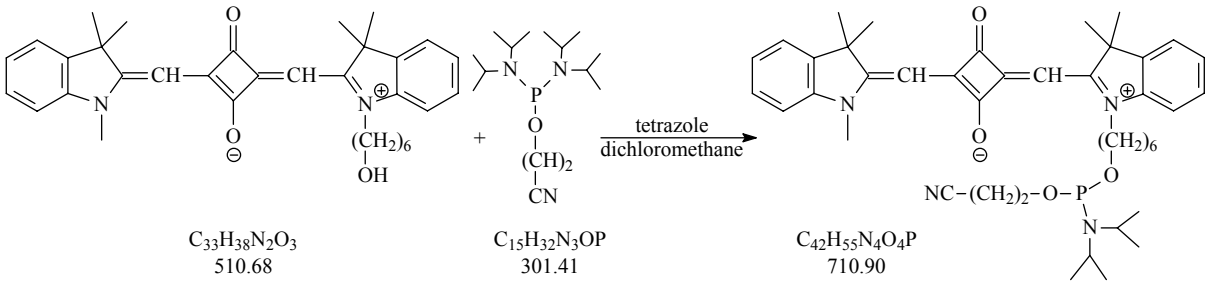

$C_{33}H_{38}N_2O_3$ 510.68 | $C_{15}H_{32}N_3OP$ 301.41 | $C_{42}H_{55}N_4O_4P$ 710.90

50 mg (97.9 µmol) of OB630-OH are dissolved in 3 mL of dry dichloromethane under argon. 47.5 µL (166 µmol) of 2-cyanoethyl-N,N,N',N',-tetraisopropyl-phosphordiamidite and 330 µL

of a saturated tetrazole solution in acetonitrile are added under stirring. The solution is stirred for 1 h at room temperature, and then extracted twice with 5 mL of a 5% $NaHCO_3$ solution in water and once with 10 mL of a saturated aqueous NaCl solution. The organic phase is dried over Na_2SO_4. The product is purified by two successive column chromatographies using LiChroprep RP-18 (40-63 µm) as the stationary phase and first dichloromethane as the eluent and second an acetonitrile/dichloromethane mixture (95:5 v/v) as the eluent.

Yield: 30 mg (42.2 mmol, 43%), blue crystalls, $C_{43}H_{55}N_4O_4P$ (710.90 g/mol).
R_f (silica gel RP 18, chloroform:methanol 95:5 v/v): 0.57.
^{1}H-NMR (d_6-acetone): δ 7.48 (m, 2H), 7.33 (m, 2H), 7.28 (m, 2H), 7.17 (m, 2H), 5.94 (s, 1H), 5.86 (s, 1H), 4.16 (t, 2H), 3.85 (m, 2H), 3.70-3.58 (m, 7H), 2.74 (t, 2H), 1.87 (m, 2H), 1.77 (s, 6H), 1.76 (s, 6H), 1.63 (m, 2H), 1.52 (m, 4H), 1.16 (dd, 12H). ^{31}P{^{1}H}-NMR (d_6-acetone, H_3PO_4 external): δ 148.56.

4.2.12. OG670

4.2.12.1. 2-[3-Butoxy-4-oxo-2-(1,3,3-trimethyl-1,3-dihydro-indol-2-ylidenemethyl)-cyclobut-2-enyl]malonodinitrile

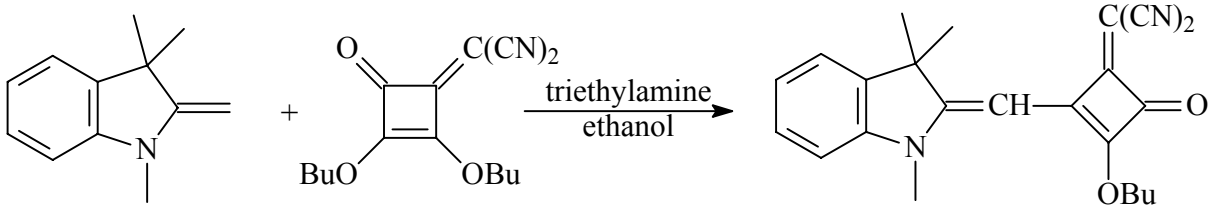

$C_{12}H_{15}N$ 173.26 | $C_{15}H_{18}N_2O_3$ 274.32 | $C_{23}H_{23}N_3O_2$ 373.45

2.11 g (7.68 mmol) of 2-(2,3-dibutoxy-4-oxo-2-cyclobutenyliden)malonodinitrile and 6.79 mL of triethylamine are dissolved in 100 mL of ethanol and heated to 60 °C. 1.36 mL (7.68 mmol) of 2-methylene-1,3,3-trimethylindoline are added and the reaction mixture is kept at 60 °C for 6 h. After cooling to room temperature the solvents are removed on a rotary evaporator and a brown oil remains. The raw product can be used without further purification.

4.2.12.2. OG670-OH

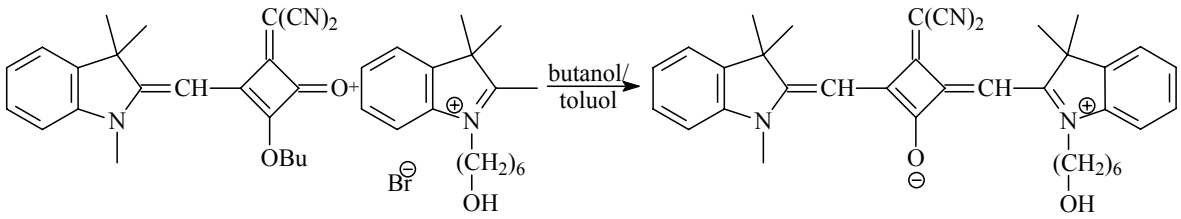

$C_{23}H_{23}N_3O_2$ 373.45 | $C_{17}H_{26}BrNO$ 340.30 | $C_{36}H_{38}N_4O_2$ 558.72

3.29 g of raw 2-[3-butoxy-4-oxo-2-(1,3,3-trimethyl-1,3-dihydro-indol-2-ylidenemethyl)-cyclobut-2-enyl]malonodinitrile and 1.80 g (5.29 mmol) of 1-(6-hydroxyhexyl)-2,3,3-trimethyl-3*H*-indolium bromide are dissolved in 200 mL of a butanol/toluene mixture (1/1, v/v) and refluxed for 24 h. After cooling to room temperature the solvents are removed on a rotary evaporator and the product is purified by chromatography using silica gel 60 (40-63 µm) as the stationary phase and a chloroform/methanol mixture (95/5, v/v) as the eluent. The second green fraction is collected which contains the unsymmetrical dye.

Yield: 532 mg (0.95 mmol, 18%), green crystalls, $C_{36}H_{38}N_4O_2$ (558.72 g/mol).
R_f (silica gel RP 18, acetonitrile: chloroform 95:5 v/v): 0.38.

4.2.12.3. OG670-PAM

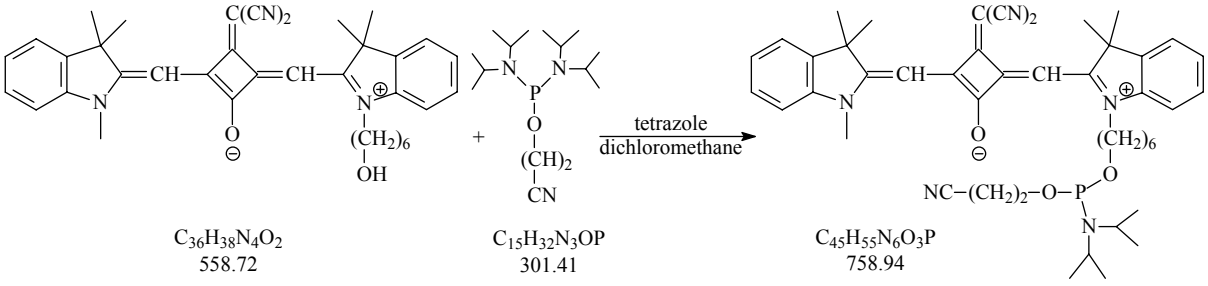

$C_{36}H_{38}N_4O_2$ 558.72 | $C_{15}H_{32}N_3OP$ 301.41 | $C_{45}H_{55}N_6O_3P$ 758.94

150 mg (268 µmol) of OG670-OH are dissolved in 10 mL of dry dichloromethane under argon. 225 µL (795 µmol) of 2-cyanoethyl-N,N,N',N',-tetraisopropyl-phosphordiamidite and 750 µL of a saturated tetrazole solution in acetonitrile are added under stirring. The solution is stirred for 1 h at room temperature, and then extracted twice with 10 mL of a 5% $NaHCO_3$ solution in water and once with 20 mL of a saturated aqueous NaCl solution. The organic phase is dried with Na_2SO_4. The product is purified by two successive column chromatographies using LiChroprep RP-18 (40-63 µm) as the stationary phase and first

dichloromethane as the eluent, second an acetonitrile/dichloromethane mixture (95:5 v/v) as the eluent.

Yield: 105 mg (138 mmol, 52%), green crystalls, $C_{45}H_{55}N_6O_3P$ (758.94 g/mol).
R_f (silica gel RP 18, acetonitrile: chloroform 95:5 v/v): 0.46.
^{1}H-NMR (d_6-acetone): δ 7.54 (m, 2H), 7.40 (m, 4H), 7.26 (m, 2H), 6.52 (s, 1H), 6.48 (s, 1H), 4.12 (t, 2H), 3.83 (m, 2H), 3.68 (s, 3H), 3.67-3.58 (m, 4H), 2.72 (t, 2H), 1.88 (m, 2H), 1.78 (s, 6H), 1.76 (s, 6H), 1.62 (m, 2H), 1.50 (m, 4H), 1.17 (dd, 12H). $^{31}P\{^1H\}$-NMR (d_6-acetone, H_3PO_4 external): δ 148.65.

4.3. General Labeling Procedures

4.3.1. General Procedure for Labeling Proteins and Determination of Dye-to-Protein Ratios

Protein labeling was carried out in a 50 mM bicarbonate buffer (BCBS) of pH 9.0. 2 mg of protein (HSA or anti-HSA) are dissolved in 1 mL of BCBS. Different amounts of OSI ester (0.01-0.25 mg) are added to give different dye-to-protein ratios (DPR = 0.4-7). The mixtures are gently stirred for 1 h at room temperature in the dark. Unconjugated label is separated from the labeled proteins using gel permeation chromatography with Sephadex G-25 and a 22 mM phosphate buffer of pH 7.2 as the eluent. The first colored band containes the dye-protein conjugate, while the colored band with a much longer retention time containes the separated free dye [9-11].

The dye-to-protein ratio (DPR) can be determined with the help of the following formula, which is derived from the Lambert-Beer law:

$$\frac{D}{P} = \frac{A^{max} \cdot \varepsilon_P^{280\ nm}}{A^{280\ nm} \cdot \varepsilon_F^{max} - A^{max} \cdot \varepsilon_F^{280\ nm}}$$

with $\varepsilon_P^{280\ nm}$ = molar absorption coefficient of the protein at 280 nm,
$\varepsilon_F^{280\ nm}$ = molar absorption coefficient of the dye at 280 nm,
ε_F^{max} = molar absorption coefficient of the free dye at its maximum,
A^{max} = absorbance of the dye-protein solution at its maximum,
$A^{280\ nm}$ = absorbance of the dye-protein solution at 280 nm.

This formula is valid assuming that at long-wavelengths only the label absorbs and that there are no spectral differences between the free and the covalently bound dye.

4.3.2. General Procedure for Labeling Amino Acids

30 mmol of amino acid (L-valine or L-aspartic acid) are dissolved in 500 µL of BCBS (50 mM, pH 9.0). A solution of 10 mmol of dye OSI ester in 50 µL of DMF is added. The solution is stirred at room temperature for 30 h. The conjugate is purified by HPLC using a Hibar pre-packed column RT (250 x 4 mm) packed with LiChrosorb RP 18 (10 µm) as the stationary phase and a methanol/water mixture (50:50, v/v) as the eluent.

FO546-valine: ^{1}H-NMR (d_4-methanol): δ 8.54 (t, 1H), 7.53 (m, 2H), 7.47-7.27 (m, 6H), 6.48 (dd, 2H), 4.30 (m, 2H), 4.22 (d, 1H), 4.17 (t, 2H), 3.96 (quin, 2H), 2.23 (m, 2H), 2.11 (m, 1H), 2.01 (m, 2H), 1.84 (m, 2H), 1.76 (s, 12H), 1.60 (m, 2H), 1.47-1.32 (m, 6H), 1.26 (t, 3H), 0.87 (dd, 6H).

FO546-aspartic acid: ^{1}H-NMR (d_4-methanol): δ 8.54 (t, 1H), 7.53 (m, 2H), 7.47-7.27 (m, 6H), 6.48 (dd, 2H), 4.48 (t, 1H), 4.30 (m, 2H), 4.17 (t, 2H), 3.96 (quin, 2H), 2.65 (d, 1H), 2.20 (t, 2H), 2.01 (m, 2H), 1.83 (m, 2H), 1.76 (s, 12H), 1.60 (m, 2H), 1.47-1.37 (m, 6H), 1.26 (t, 3H).

FR642-valine: ^{1}H-NMR (d_4-methanol): δ 8.23 (dt, 2H), 7.47 (t, 2H), 7.42-7.22 (m, 6H), 6.64 (t, 1H), 6.32 (dd, 2H), 4.25 (m, 2H), 4.22 (d, 1H), 4.13 (t, 2H), 3.97 (quin, 2H), 2.27 (t, 2H), 2.13 (m, 1H), 1.98 (m, 2H), 1.84 (t, 2H), 1.72 (s, 6H), 1.71 (s, 6H), 1.64 (m, 2H), 1.47 (m, 2H), 1.28 (t, 3H), 0.97 (dd, 6H).

FR642-aspartic acid: ^{1}H-NMR (d_4-methanol): δ 8.22 (m, 2H), 7.49-7.21 (m, 8H), 6.64 (t, 1H), 6.31 (dd, 2H), 4.50 (m, 1H), 4.24 (m, 2H), 4.13 (t, 2H), 3.97 (quin, 2H), 2.66 (t, 2H), 2.24 (t, 2H), 1.98 (m, 2H), 1.81 (m, 2H), 1.72 (s, 6H), 1.71 (s, 6H), 1.49 (m, 2H), 0.32 (m, 2H), 1.28 (t, 3H).

4.3.3. General Procedure for Labeling Oligonucleotides

0.30 µmol of amino modified 15-mer oligonucleotide are dissolved in 500 µL of BCBS (50 mM, pH 9.0). 2 mg of dye OSI ester dissolved in 50 µL of DMF are added and the solution is allowed to stand for 15 h in the dark. 1.5 mL of ice-cold ethanol are added. The solution is mixed well and placed at -18 °C for 1-2 h. The solution is centrifuged at 15,000 RPM for 10 min. The supernatant containing unreacted dye is removed carefully and the pellet containing labeled and unlabeled oligonucleotide is rinsed twice with cold ethanol.

Labeled oligonucleotides are purified by HPLC using a Hibar pre-packed column RT (250 x 4 mm) packed with LiChrosorb RP 18 (10 µm). The pellet is dissolved in 0.1 M triethylammonium acetate (TEAA) of pH 7.1. The dissolved pellet is loaded onto the column in 0.1 M TEAA and a linear 10-65% acetonitrile gradient is run over 30 min. In all cases, the

unlabeled oligonucleotide migrates fastest, followed by the labeled oligonucleotide, and finally the free dye-acid, and the OSI ester [12]. The solvent of the HPLC fraction is removed on a rotary evaporator.

The residue is dissolved in 100 µL of water. 1 mL of ice-cold ethanol is added. The solution is mixed well and and placed at -18 °C for 1-2 h. The solution is centrifuged at 15,000 RPM for 10 min. The supernatant is removed carefully and the pellet containing the labeled oligonucleotide can either be stored at 4 °C or be dissolved in 22 mM PBS for further experiments.

4.3.3. General Procedure for Labeling dUTP

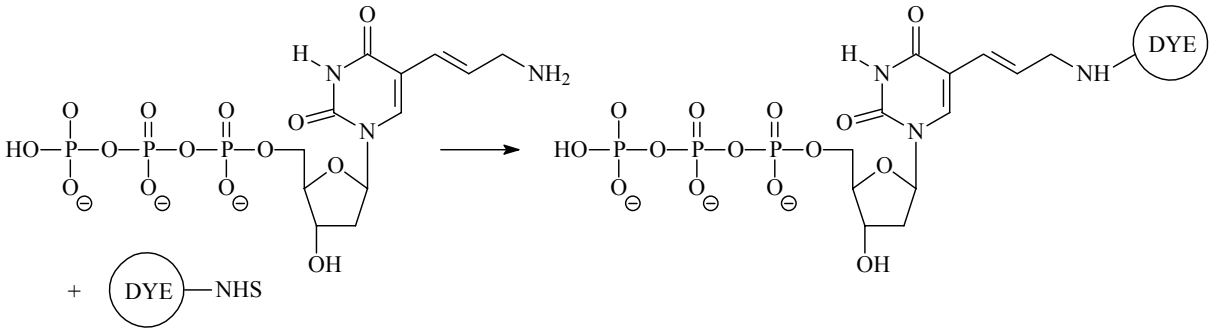

1 mg (1.91 µmol) of amino allyl dUTP is dissolved in 500 µL of BCBS (50 mM, pH 9.0). A solution of 2.9 µmol of dye OSI ester in 100 µL of DMF is added. The solution is stirred for 4 h at room temperature. Labeled dUTP is separated from the non labeled dUTP and the non reacted dye using gel permeation chromatography with Sephadex G-10 as the stationare phase and doubly destilled water as the eluent. The first colored band which containes the conjugate is lyophilized.

The labeled dUTP was used in fluorescence in situ hybridization (FISH) studies. PCR and FISH was carried out by Chrombios GmbH (Martinsried, Germany).

4.4. Determination of Quantum Yields [13]

The quantum yields ϕ of the dyes and the dye conjugates, respectively, were measured in phosphate buffer (22 mM, pH 7.2) relative to a reference fluorophor with a known quantum yield. These references were Cy5 (Amersham) with a quantum yield of 0.28 in PBS [14] for dyes absorbing from 630 to 670 nm, and Rhodamine 6G (Aldrich) with a quantum yield of 0.95 in ethanol [13] for dyes absorbing from 530 to 550 nm. The quantum yields ϕ_x of the dyes and the dye conjugates were determined using the following formula:

$$\phi_X = \phi_R \frac{A_R \cdot I_X \cdot n_X^{\,2}}{A_X \cdot I_R \cdot n_R^{\,2}}$$

where ϕ_R is the quantum yield of the reference, A_R and A_X are the absorbances of the reference and the dye, respectively, at the excitation wavelength, I_R and I_X are the integrated areas of the corrected emission spectra of the reference and the dye, respectively, and n_R and n_X are the refractive indices of the solvent of the reference and the dye, respectively.

4.5. Determination of Dissociation Constants K_D^*

Dissociation constants K_D^* of non-reactive dyes and HSA were determined as follows. The values y_1 and y_2 were determined graphically as shown in figure 4.1. y_3 was calculated according to the following formula:

$$y_3 = y_1 + \frac{y_2 - y_1}{2}$$

The corresponding x value to y_3 gives K_D^* which is the concentration of HSA needed to bind half of the non-reactive dye.

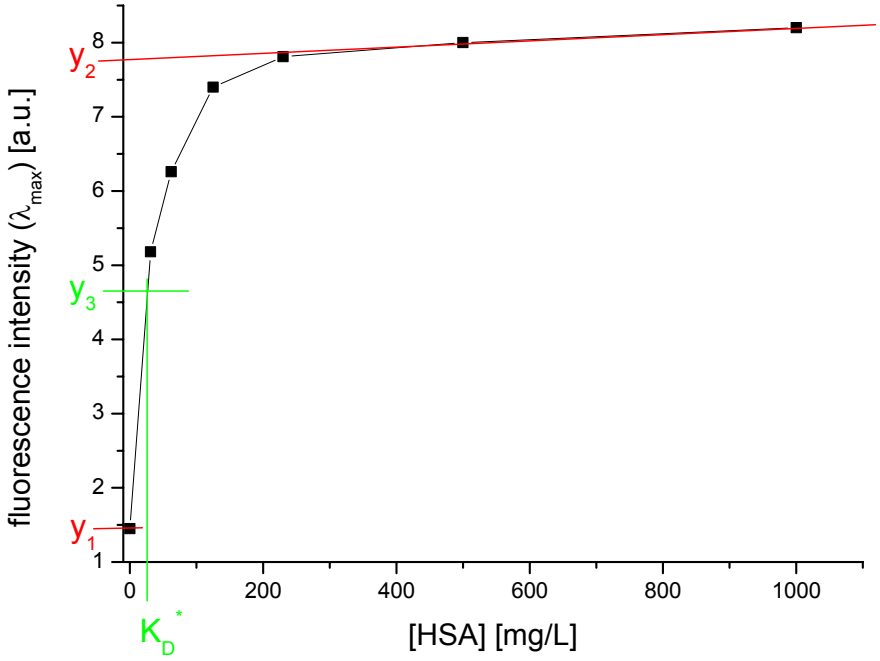

Figure 4.1. Plot of the fluorescence intensities the free dye at the emission maximum versus the concentration of added HSA.

4.6. General Procedures for Energy Transfer Measurements

4.6.1. Immunostudies and Hybridization Studies

Varying quantities (typically 25-400 µL) of acceptor solution of a certain concentration (typically 10^{-6}-10^{-7} mol/L) were diluted with 22 mM PBS of pH 7.2 to a final volume of 400 µL. 100 µL of donor solution with the same concentration were added. After incubation of 20 min at room temperature fluorescence was measured at 20 °C.

4.6.2. Competitive Assays

Varying quantities (typically 25-400 µL) of a solution of the non labeled probe (protein or oligonucleotide) were diluted with 22 mM PBS of pH 7.2 to a final volume of 400 µL. Then, 100 µL of donor solution and 100 µL of acceptor solution were added in this order. All three solutions had the same concentration (typically 10^{-6}-10^{-7} mol/L). After incubation of 20 min at room temperature fluorescence was measured at 20 °C.

4.7. Flow-Cytometry

For flow-cytometric measurements "Development COOH Microspheres" of 5.6 µm diameter ($1.25 \cdot 10^7$ beads/mL) from Luminex (Austin, Texas) were used. The following solutions were needed: activation buffer (AB), 0.1 M PBS, pH 6.1; sulfo-NHS solution, 10 mg sulfo-NHS in 200 mL of AB; EDC solution, 5 mg EDC in 1 mL of AB; coupling buffer (CB), 25 mM PBS, 150 mM NaCl, pH 7.3; washing buffer (WB), 10 mL CB + 5 µL Tween 20; blocking buffer (BB), 0.1 M TRIS-HCl, pH 7.3.

The microsphere stock was dispersed with sonification and vortexed for 1 min. 40 µL of the stock were taken and centrifuged for 2 min at 13,000 rpm. The supernatant was aspirated and the pellet was resuspended in 40 µL of AB. The suspension was vortexed and centrifuged for 1 min at 13,000 rpm. Again the supernatant was aspirated and the pellet was resuspended in 16 µL of AB. 2 µL of freshly prepared sulfo-NHS solution and 2 µL of freshly prepared EDC solution were added. The suspension was mixed and allowed to stand for 20 min in the dark at room temperature. 30 µL of AB were added. The suspension was mixed and centrifuged for 2 min at 13,000 rpm. The supernatant was aspirated and the pellet was resuspended in 50 µL of CB. Again, the suspension was centrifuged for 2 min at 13,000 rpm. The supernatant was aspirated and the pellet was resuspended in 50 µL of CB.

Six cups were prepared containing 5µL of the activated particles. 5 µL of different amounts of HSA dissolved in CB (0, 31, 63, 125, 250, and 500 µg/mL) were added to the particle suspensions, respectively. The 6 suspensions were mixed and allowed to stand for 60

min in the dark at room temperature. 40 µL of CB were added. The suspensions were mixed and centrifuged for 2 min at 13,000 rpm. The supernatant was aspirated and the pellets were resuspended in 50 µL of WB. Again, the suspensions were centrifuged for 2 min at 13,000 rpm. The supernatant was aspirated and the pellets were resuspended in 50 µL of WB. After a second washing step the pellets were resuspended in 50 µL of BB and allowed to stand for 30 min in the dark at room temperature. The particles were washed twice with 50 µL of WB and the pellets were dispersed in 50 µL of WB.

Each of the six cups was divided into four cups with 8 µL of microsphere suspension each. 8 µL of different amounts of FO548 labeled anti-HSA (DPR=2.1) dissolved in CB (0, 8, 33, and 131 µg/mL) were added to the particle suspensions, respectively. The 24 suspensions were mixed and allowed to stand for 2 h in the dark at 37 °C. After two washing steps the microsphere suspensions were measured on a Luminex 100 Flow Cytometer at Multimetrix (Regensburg).

4.8. References

[1] *Organikum,* 19. Aufl., Dt. Verl. der Wiss., Leipzig, 1993.

[2] H. E. Fierz-David, L. Blangley (Eds.) (1943), Grundlegende Operationen der Farbenchemie, 5. Aufl., 123.

[3] B. Oswald (2000) New Long-Wavelength Fluorescent Labels for Bioassays, *Dissertation*, University of Regensburg (Germany).

[4] R. B. Mujumdar, L. A. Ernst, S. R. Mujumdar, C. J. Lewis, A. S. Waggoner (1993) Cyanine Dye Labeling Reagents: Sulfoindocyanine Succinimidyl Esters. *Bioconjugate Chem.* **4**, 105 - 111.

[5] B. Wetzl (2002) New Rhodamines and Squarylium Dyes for Biological Applications, *Diploma Thesis,* University of Regensburg (Germany).

[6] M. Probst (1999) Synthese und Charakterisierung von reaktiven diodenlaserkompatiblen Fluoreszenzfarbstoffen, *Diploma Thesis,* University of Regensburg (Germany).

[7] B. Gerecht, T. Kämpchen, K. Köhler, W. Massa, G. Offermann, R. E. Schmidt, G. Seitz, R. Sutrisno, *Chem. Ber. 117*, **1984**, 2714 - 2729.

[8] T. Kämpchen, G. Seitz, R. Sutrisno, *Chem. Ber. 114*, **1981**, 3448 - 3455.

[9] D. B. Craig, N. J. Dovichi, *Anal. Chem. 70*, **1998**, 2493 - 2494.

[10] A. J. Sophianopoulos, J. Lipowski, N. Narayanan, G. Patonay, *Appl. Spectrosc. 51*, **1997**, 1511 - 1515.

[11] M. Brinkley, *Bioconjugate Chem. 3*, **1992**, 2 - 13.

[12] Oligonucleotide Phosphate Labeling Protocol, Molecular Probes (Eugene, Oregon), http://www.probes.com/handbook/sections/0802.html

[13] J. N. Demas, G. A. Crosby, *J. Phys. Chem. 75*, **1971**, 991 – 1024.

[14] Fluoro Link Cy5, Product Description, Cat. No. PA25001, Amersham Life Science, Inc. (IL, USA).

5. Summary

The aim of this work was the synthesis and spectral and analytical characterization of new long-wavelength fluorescent labels which can be coupled to biomolecules and be used as markers in biological applications.

The dyes belong to either the class of the cyanine dyes or to the squaraines. They were characterized by their absorption and emission spectra, their molar absorbance and their fluorescence quantum yields. Having absorption maxima in the range of 545 nm to 668 nm and emission maxima between 562 nm and 687 nm, the markers cover the longwave part of the visible spectrum. The labels exhibit molar absorbances between 86,000 L/(mol·cm) and as high as 220,000 L/(mol·cm).

The labels contain either amine-reactive oxysuccinimidyl (OSI) esters or saccharide-reactive phosphoramidite (PAM) moieties. All labels contain solely one reactive group to avoid crosslinking. Several biomolecules were labeled. These include amino acids (L-valine, L-aspartic acid), proteins (HSA, anti-HSA), nucleotides (dUTP), and synthetic oligonucleotises (with and without amino-modification). In general, the quantum yield of the free dye in aqueous solution is low compared to the quantum yield of the dye covalently attached to a biomolecule (except for amino acids). In the case of proteins, the extent of the increase is dependent on the dye-to-protein ratio (DPR). The highest quantum yields are achieved at DPR values between 1 and 2, because at higher DPRs the dyes undergo self-quenching, and fluorescence quantum yields decrease.

Immunostudies were carried out on the system HSA/anti-HSA. Binding studies were performed as well as homogenous competitive immunoassays. These systems can be used for the determination of HSA concentrations in the range of $2 \cdot 10^{-9}$ - $2.5 \cdot 10^{-7}$ mol/L. A cytometric measurement was performed to show the applicability of the dyes in flow cytometry. The introduced systems can be used for the determination of HSA concentrations in the range of 10 - 120 µg/mL ($1.5 \cdot 10^{-7}$ - $1.8 \cdot 10^{-6}$ mol/L).

Fluorescently labeled DNA oligonucleotides were applied in hybridization binding studies and homogenous competitive hybridization assays. The binding studies enable the determination of donor-to-acceptor distances. The presented competitive assays show that it is possible to determine oligonucleotide concentrations in the range of $4 \cdot 10^{-8}$ to $6 \cdot 10^{-6}$ mol/L. In addition, these measurements enable the distinction of oligonucleotides without, with a single, or with a double mismatch in their sequence. Fluorescence in situ hybridization has been performed. It was possible to clearly visualize under a fluorescence microscope that the labeled probe hybridized to a mouse Y-chromosome.

6. Acronyms, Definitions, and Nomenclature of the Dyes

6.1. Acronyms

anti-HSA	polyclonal anti-human serum albumin
BCBS	bicarbonate buffer solution
DCC	dicyclohexylcarbodiimide
DMF	dimethylformamide
DMSO	dimethylsulfoxide
DPR	dye-to–protein ratio
EDC	ethyl(dimethylaminopropyl)carbodiimide
ESI	electro-spray ionization
FAB	fast-atom bombardment
FRET	fluorescence resonanz energy transfer
HSA	human serum albumin
m.p.	melting point
NHS	N-hydroxysuccinimide
OSI	oxysuccinimidyl
PAM	phosphoramidite
PBS	phosphate buffered saline
TEAA	triethylammonium acetate
TMS	tetramethylsilane
sulfo-NHS	3-sulfo-N-hydroxysuccinimide

6.2. Definitions

fluorophore	part of the dye that causes fluorescence
label	reactive dye
conjugate	biomolecule with covalently attached dye

6.3. Nomenclature of the Dyes

FO544-acid: 2-[3[1-(3-carboxypropyl)-1,3-dihydro-3,3-dimethyl-2H-indol-2-ylidene]trienyl]-1-[2-(ethoxyhydroxyphosphoryl)ethyl]-3,3-dimethyl-indole

FO545-acid: 2-[3[1-(5-carboxypentyl)-1,3-dihydro-3,3-dimethyl-2H-indol-2-ylidene]trienyl]-1-[2-(ethoxyhydroxyphosphoryl)ethyl]-3,3-dimethyl-indole

FO546-acid: 2-[3[1-(7-carboxyheptyl)-1,3-dihydro-3,3-dimethyl-2H-indol-2-ylidene]trienyl]-1-[2-(ethoxyhydroxyphosphoryl)ethyl]-3,3-dimethyl-indole

FO548-acid: 2-[3[1-(5-carboxypentyl)-5-hydroxysulfonyl-1,3-dihydro-3,3-dimethyl-2H-indol-2-ylidene]trienyl]-1-[2-(ethoxyhydroxyphosphoryl)ethyl]-3,3-dimethyl-indole

FR626-acid: 2-{[1-(5-carboxypentyl)-3,3-dimethyl-2,3-dihydro-1H-2-indolyliden]methyl}-4-{[1-ethyl-5-hydroxsulfonyl-3,3-dimethyl-3H-2-indoliumyl]methylidene}-3-oxo-1-cyclobuten-1-olate

FR642-acid: 2-[5[1-(5-carboxypentyl)-1,3-dihydro-3,3-dimethyl-2H-indol-2-ylidene]-1,3-pentadienyl]-1-[2-(ethoxyhydroxyphosphoryl)ethyl]-3,3-dimethyl-indole

FR646-acid: 2-[5[1-(5-carboxypentyl)-5-hydroxysulfonyl-1,3-dihydro-3,3-dimethyl-2H-indol-2-ylidene]-1,3-pentadienyl]-1-[2-(ethoxyhydroxyphosphoryl)ethyl]-3,3-dimethyl-indole

FR661-acid: 2-{[1-(2-(diethoxyphosphoryl)ethyl)-3,3-dimethyl-2,3-dihydro-1H-2-indolyliden]methyl}-4-{[1-(5-carboxypentyl)-1,4-dihydro-4-quinolinyl]methylidene}-3-oxo-1-cyclobuten-1-olate.

FR662-acid: 2-{[1-(5-Carboxypentyl)-5hydroxysulfonyl-3,3-dimethyl-2,3-dihydro-1H-2-indolyliden]methyl}-4-{[1-[2-(ethoxyhydroxyphosphoryl)ethyl]-3,3-dimethyl-3H-2-indoliumyl]methylidene}-3-dicyanomethylene-1-cyclobuten-1-olate

FR670-acid: 2-{[1-(3-Carboxypropyl)-3,3-dimethyl-2,3-dihydro-1H-2-indolyliden]methyl}-4-{[5-hydroxysulfonyl-1-ethyl-3,3-dimethyl-3H-2-indoliumyl]methylidene}-3-dicyanomethylene-1-cyclobuten-1-olate

OB630-OH: 2-{[1-(6-Hydroxyhexyl)-3,3-dimethyl-2,3-dihydro-1H-2-indolyliden]methyl}-4-{[1-methyl-3,3-dimethyl-3H-2-indoliumyl]methylidene}-3-oxo-1-cyclobuten-1-olate.

OG670-OH: 2-{[1-(6-Hydroxyhexyl)-3,3-dimethyl-2,3-dihydro-1H-2-indolyliden]methyl}-4-{[1-methyl-3,3-dimethyl-3H-2-indoliumyl]methylidene}-3-dicyanomethylene-1-cyclobuten-1-olate

7. Curriculum Vitae

Name:	Michaela Gruber, nee Arbter
Date of Birth:	22.04.1975
Place of Birth:	Landshut, Bavaria
Nationality:	German
Family Status:	Married
Address:	Flurstr. 62, 84030 Ergolding

Education:

09/1981 - 07/1985	Grundschule Kumhausen
09/1985 - 06/1994	Gymnasium der Cistercienserinnen Seligenthal in Landshut
06/1994	Abitur

Studies:

11/1994 – 03/1999	Chemistry (Diploma) at the University of Regensburg
05/1999 – 02/2000	Diploma Work at the Institute of Analytical Chemistry, Chemo- and Biosensors, supervisor: Prof. O. S. Wolfbeis Subject: "Diode Laser Compatible Cyanine and Squarylium Dyes"
03/2000	Academic degree of a Diplomchemikerin
since 04/2000	Ph.D. Work at the Institute of Analytical Chemistry, Chemo- and Biosensors (head: Prof. Wolfbeis) Subject: "FRET Compatible Long-Wavelength Labels and Their Application in Immunoassays and Hybridization Assays"

Employment

since 04/2002	employed at Chromeon GmbH, Regensburg

8. List of Papers Posters and Presentations

8.1. Papers Published, Submitted, or in Preparation

B. Oswald, M. Gruber, M. Böhmer, F. Lehmann, M. Probst, and O. S. Wolfbeis (2001) Novel Diode Laser-compatible Fluorophores and Their Application to Single Molecule Detection, Protein Labeling and Fluorescence Resonance Energy Immunoassay. *Photochem. Photobiol.* **74(2)**, 237-245.

O. S. Wolfbeis, M. Böhmer, A. Dürkop, J. Enderlein, M. Gruber, I. Klimant, C. Krause, J. Kürner, G. Liebsch, Z. Lin, B. Oswald, and M. Wu (2002) Advanced Luminescent Labels, Probes, and Beads, and Their Application to Luminescence Bioassay, and Imaging *in* Springer Series in Fluorescence, (Kraayenhof, R., Ed.), Springer Verlag, Berlin-Heidelberg.

B. Wetzl, M. Gruber, B. Oswald, A. Dürkop, B. Weidgans, M. Probst, and O. S. Wolfbeis (2002) Set of Fluorochromophores for Labeling Proteins and DNA in the Wavelength Range from 450 nm to 700 nm, *J. Chromatogr., Part A*, submitted (July 2002).

M. Gruber, B. Oswald, B. Wetzl, J. Enderlein and O. S. Wolfbeis (2002) New Long-Wavelength Absorbing Fluorophores and Their Application to Oligonucleotide Labeling and Fluorescence Resonance Energy Transfer (FRET) Hybridization Studies, *Nucl. Acid Res.,* (in prep.).

8.2.Patent

O. S. Wolfbeis, F. Lehmann, M. Arbter (2001) Verfahren zur Solubilisierung von optischen Markern, Deutsches Patent- und Markenamt, DE 199 54 934 A 1.

8.3. Posters and Presentations

Posters

M. Gruber, B. Oswald, O. S. Wolfbeis (2001) Long-wavelength Fluorescent Labels for Bioanalytical Applications. 7th *International Conference on Methods and Applications of Fluorescence Spectroscopy (MAFS),* September 16-19, Amsterdam, Netherlands.

B. Oswald, A. Dürkop, M. Gruber, Ch. Krause, M. Kroder, J. Kürner, E. Pringsheim, M. Probst, E. Simo, and O. S. Wolfbeis (2001) Novel Fluorescent Beads and Novel Cytometric Immunoassays. *14th Heidelberg Cytometry Symposium,* October 18-20, Heidelberg, Germany.

Presentation

M. Gruber (2001) Diodenlaser-gestützte Immun- und Gentests auf der Grundlage des Fluoreszenz-Resonanz-Energietransfers. *Bayer-Workshop,* Regensburg, Germany.

Erklärung

Hiermit versichere ich, dass ich die vorliegende Arbeit selbst verfaßt und keine anderen als die angegebenen Quellen und Hilfsmittel verwendet habe.

Landshut, 24.07.2002

Michaela Gruber